THE MIDDLE ATLANTIC BIGHT:

A CLIMATOLOGICAL ATLAS OF OCEANOGRAPHIC PROPERTIES

Alan F. Blumberg

George L. Mellor

Sydney Levitus*

Geophysical Fluid Dynamics Program
Princeton University, Princeton, N.J. 08540

PRINCETON UNIVERSITY

THE MIDDLE ATLANTIC BIGHT:

A CLIMATOLOGICAL ATLAS OF OCEANOGRAPHIC PROPERTIES

Alan F. Blumberg

George L. Mellor

Sydney Levitus*

Geophysical Fluid Dynamics Program
Princeton University, Princeton, N.J. 08540

*Geophysical Fluid Dynamics Laboratory/NOAA
Princeton University, Princeton, N.J. 08540

This work is a result of research sponsored by NOAA office of Sea Grant, Department of Commerce, under Sea Grants 04-6-158-44076 and 04-7-158-44042

August, 1977

New Jersey Marine Sciences Consortium, Fort Hancock, N.J. 07732

Report No. NJ/P-SG-01-8-77

Abstract

An atlas of the climatological temperature, salinity, oxygen, density and geostrophic velocity distributions is presented for the Middle Atlantic Bight. The source of the data is 484,118 temperature, 40,339 salinity and 18,340 oxygen measurements on file at the National Oceanographic Data Center (NODC) collected in the field up to June, 1973. The major features of the various distributions are briefly discussed.

Table of Contents

I. Introduction

In recent years man has become acutely aware of the need to maintain the quality of our coastal waters. The Middle Atlantic Bight (MAB) is one of the coastal regions receiving a great deal of attention because of man's ever-increasing utilization of its resources. The conflicting uses of the MAB require skillful management, a prerequisite of which is a knowledge of the physical processes governing water quality. Toward this end, this atlas has been prepared to present a quantitative description of the climatological physical oceanographic properties prevailing in the MAB.

The MAB will be defined here as the oceanic region bounded by the shoreline between Cape Cod, Massachusetts and Cape Hatteras, North Carolina and extending eastward to 69°W and southward to 35°N, as shown in Figure 1. The term climatological implies a long-term mean. However, since the observations are randomly distributed in time and space, the results can only be considered approximations to climatological means.

II. Data Source and Analysis

The source of the data used in this study is temperature, salinity and oxygen data on file at the National Oceanographic Data Center (NODC) collected in the field up to June 1973. Some of the data extend back to 1897. From this data Levitus and Oort (1977) have produced global fields on a one-degree latitude-longitude grid at standard analysis levels between the surface and 5000m depth. The mean and the standard deviation of the various data were determined for each month of the year for each Marsden square (10° square) and for each level. Then a second data set was obtained

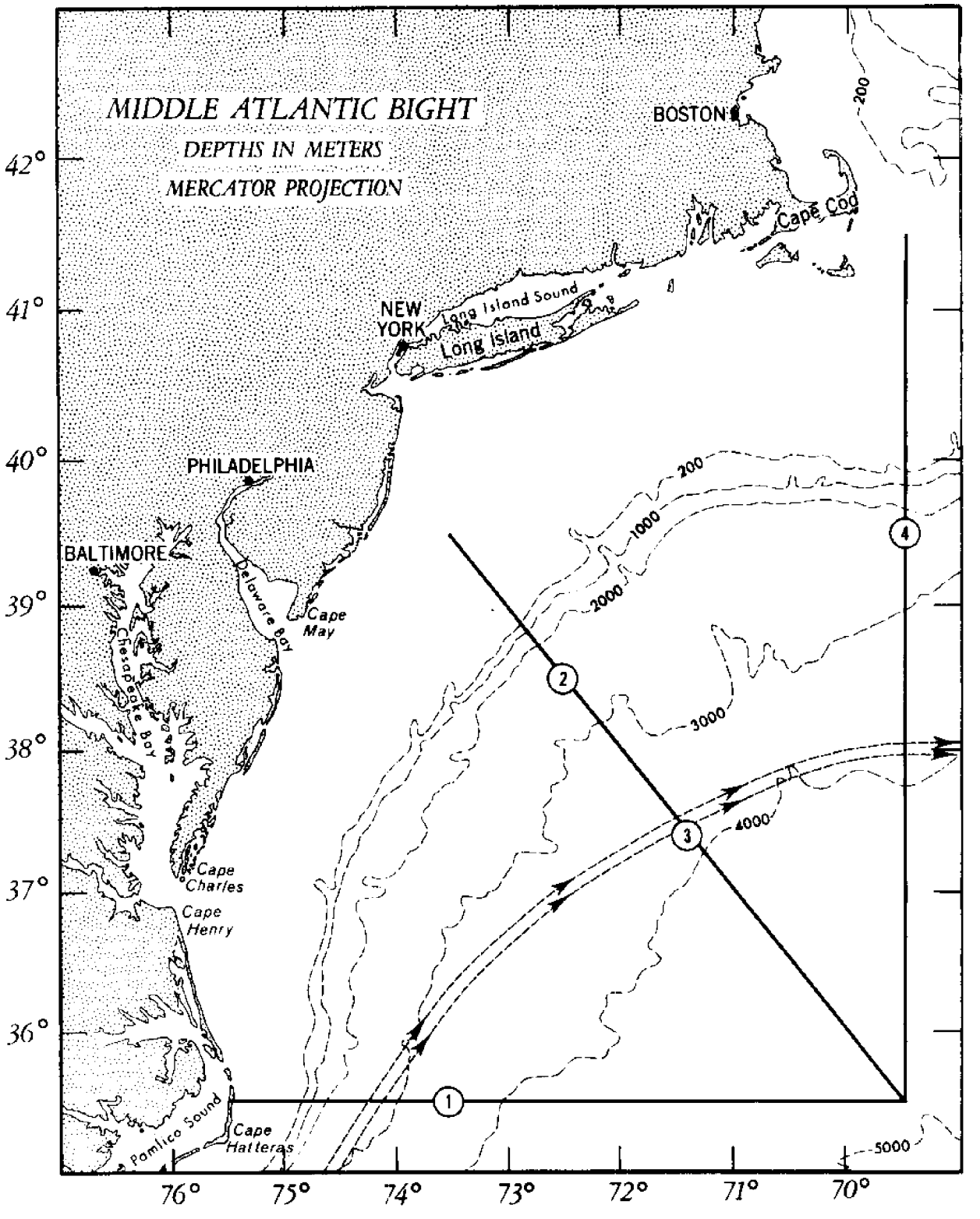

Figure 1. Map of Middle Atlantic Bight. The axis of the climatological Gulf Stream is denoted by heavy dashed lines. The solid lines indicate the tracks used for the vertical section diagrams and the circled numbers are the locations of the stations referenced in Figure 2.

by eliminating all observations in each one-degree square that differed from the mean by more than five standard deviations; this eliminated less than 0.5% of the data.

For the present study, a subset of the second data set* was used for this atlas on a 7 by 7 grid representing the area of the MAB. Simple averages of all data at a given grid point, depth, and month of the year were obtained. A further control on the data was then exercised; that is, where there were less than 5 (2 for salinity) observations at a particular grid point and depth, the data were discarded and mean values were obtained by interpolation such that

$$\phi_{i,j} = \frac{1}{4}\left[\phi_{i+1,j} + \phi_{i-1,j} + \phi_{i,j+1} + \phi_{i,j-1}\right] \qquad (1)$$

where $\phi_{i,j}$ is the missing datum. If several contiguous data were missing, the requisite set of algebraic equations is solved by a relaxation technique. The process is identical to that of solving Laplace's equation for the interpolated points implying, then, that the interpolated points can have no maxima or minima.

The MAB data set contains monthly horizontal distributions of temperature and salinity at nineteen levels between the surface and 1000m. Annual distrubtions from 1000 to 4000m at eleven different levels were found to be adequate since the temperature and salinity fields exhibited little monthly variation. The relative scarcity of oxygen observations permitted only annual distributions at all thirty levels. The total number of temperature, salinity and oxygen observations along with the percentage of mean points which had to be interpolated and the number of one-degree squares of ocean are summarized in Table I as a function of depth. It is of interest to mention that

*In continuing their global analysis, Levitus and Oort by necessity further smoothed the fields such that detail in the MAB was lost.

Table I: Distribution with respect to depth of the number of one-degree squares of ocean (NOS), the total number of temperature, salinity and oxygen observations (NO), and the percentage of mean values interpolated (PI). The dashed line indicates the depth below which only annual mean values are computed.

			Temperature		Salinity		Oxygen	
Level	Depth(m)	NOS	NO	PI	NO	PI	NO	PI
1	0	39	55,364	0.0	4,186	14.1	1,669	0.0
2	10	39	54,684	0.0	3,732	14.7	1,694	0.0
3	20	39	51,867	0.0	3,385	15.8	1,532	0.0
4	30	39	47,489	0.0	2,966	16.5	1,341	0.0
5	50	38	43,486	0.4	2,265	23.2	1,064	5.3
6	75	36	38,549	1.4	1,925	25.5	902	2.8
7	100	30	35,915	0.0	1,755	18.3	852	0.0
8	125	30	34,350	0.3	1,677	19.2	806	0.0
9	150	27	31,745	0.0	1,606	19.1	778	0.0
10	200	27	29,913	0.0	1,463	20.1	715	0.0
11	250	27	25,689	0.0	1.400	21.3	655	0.0
12	300	27	9,764	0.9	1,345	21.6	567	0.0
13	400	27	8,751	1.5	1,241	22.5	523	0.0
14	500	27	3,030	13.0	1,145	25.0	484	3.7
15	600	27	2,750	13.9	1,095	25.9	475	0.0
16	700	27	1,976	16.4	1,029	28.4	429	0.0
17	800	25	1,079	24.7	979	26.3	421	0.0
18	900	25	1,027	26.3	932	28.0	407	0.0
19	1000	24	929	29.2	859	30.2	387	0.0
20	1100	24	865	0.0	800	0.0	369	0.0
21	1200	24	824	0.0	765	0.0	355	0.0
22	1300	24	801	0.0	737	0.0	337	0.0
23	1400	24	781	0.0	724	0.0	326	0.0
24	1500	23	753	0.0	702	0.0	324	0.0
25	1750	23	594	0.0	557	0.0	301	0.0
26	2000	22	519	0.0	486	0.0	273	0.0
27	2500	18	328	0.0	318	0.0	192	0.0
28	3000	14	166	0.0	155	0.0	96	0.0
29	3500	13	74	23.1	60	30.8	37	30.8
30	4000	8	56	0.0	50	12.5	29	12.5
			484,118		40,339		18,340	

the month of August has the most complete spatial coverage.

In the Introduction it was noted that the data cannot be considered true climatological averages since in any one-degree square there may be data from certain years while another nearby square may contain only data from other years. If there are long-term trends or significant inter-annual variations present, the data cannot be expected to represent the long-term mean. An additional climatic bias arises if many observations are taken in studying transient phenomena, such as mesoscale eddies and Gulf Stream meanders.

III. Data Presentation

The various oceanographic properties used in this atlas are the temperature (T,°C), the salinity (S,°/$_{oo}$) and the oxygen (O_2,ml/l). The density of the water is computed from the temperature and salinity distributions and the result is presented in the form of σ_t, defined as

$$\sigma_t = (\text{Density} - 1)10^3 \ . \tag{2}$$

The σ_t parameter represents the density of a water parcel when the total pressure on it has been reduced to atmospheric while using the in situ temperature and salinity. A geostrophic velocity distribution, computed from the density fields, provides an additional characterization of the MAB. The geostrophic velocity is found by vertically integrating the "thermal" wind equations which are

$$u(z) = \frac{g}{f\rho_o} \int_{-h}^{0} \frac{\partial \rho}{\partial y} \, dz + u(-h)$$

$$v(z) = -\frac{g}{f\rho_o} \int_{-h}^{0} \frac{\partial \rho}{\partial x} \, dz + v(-h) \tag{3}$$

where x,y are the eastward, northward coordinates and u,v are the corresponding velocity components whose units are cm/sec. The other symbols in equation (3) are z, the vertical coordinate increasing upwards; g, the gravitational acceleration; f, the Coriolis parameter; ρ , the density; ρ_o , the reference density; and h, the depth of the reference level. A level of no motion at h=2000m is assumed. The geostrophic velocity is only a portion of the total mean velocity and does not account for the effects of acceleration or Reynolds stresses. In particular, near the surface, changes in the wind stress can produce a large deviation from geostrophic balance. The concept of the depth of the level of no motion is another source of uncertainty.

Two types of diagrams have been chosen to illustrate the properties of the MAB. Vertical sections (Figure 1) are used to show the depth dependence of a property along three tracks: an East-West track along 35°30'N, a Diagonal track from 40°N,74°W to 35°N,69°W and a North-South track along 69°30'W. The vertical exaggeration of the sections is 770:1 in the upper 1000m and 154:1 below 1000m. A second type of diagram displays horizontal distributions of various properties at selected depths.

IV. Discussion of Oceanographic Properties

The climatological oceanographic properties of the MAB are here characterized by distributions of temperature, salinity, oxygen and geostrophic velocity and their variability in space and time. For the purposes of this atlas, it suffices to briefly discuss some of the more general features of the various distributions.

1. Variability of the Data

The variability of oceanographic properties provides a useful measure of the persistence of mean values. Many sources of variability exist. The meandering of the Gulf Stream produces variability and very large changes in the properties occur when meanders grow to sufficient amplitude that they break away in the form of closed eddies moving through the MAB. Interannual variations of the annual temperature cycle and the existence of meso-scale eddies and internal waves all contribute to natural variability. Moreover, large salinity variations near the coast arise because of an annual variation in river runoff. Inaccuracies in the oceanographic data collecting instruments also introduce some variability, although much smaller than the physical variability. In this study the variability is defined by the standard deviation of the various types of observations.

The annual cycles of standard deviation of temperature at four grid stations (see Figure 1 for locations) on four different levels are shown in Figure 2. At the surface, the variability is between 1 and 5°C with the smallest values occurring from mid-June to September. Below the surface, the variability decreases with depth and ranges from 1 to 4°C. The summertime minimum has vanished before a depth of 50m is reached. Also, the variability of the station (at 38°30'N, 72°30'W) outside of the Gulf Stream region is somewhat less than that of the stations within the region.

Horizontal distributions of the temperature, salinity and oxygen variability (not shown) depict a region having a larger variability than other areas of the MAB. This region is approximately 250km wide and is

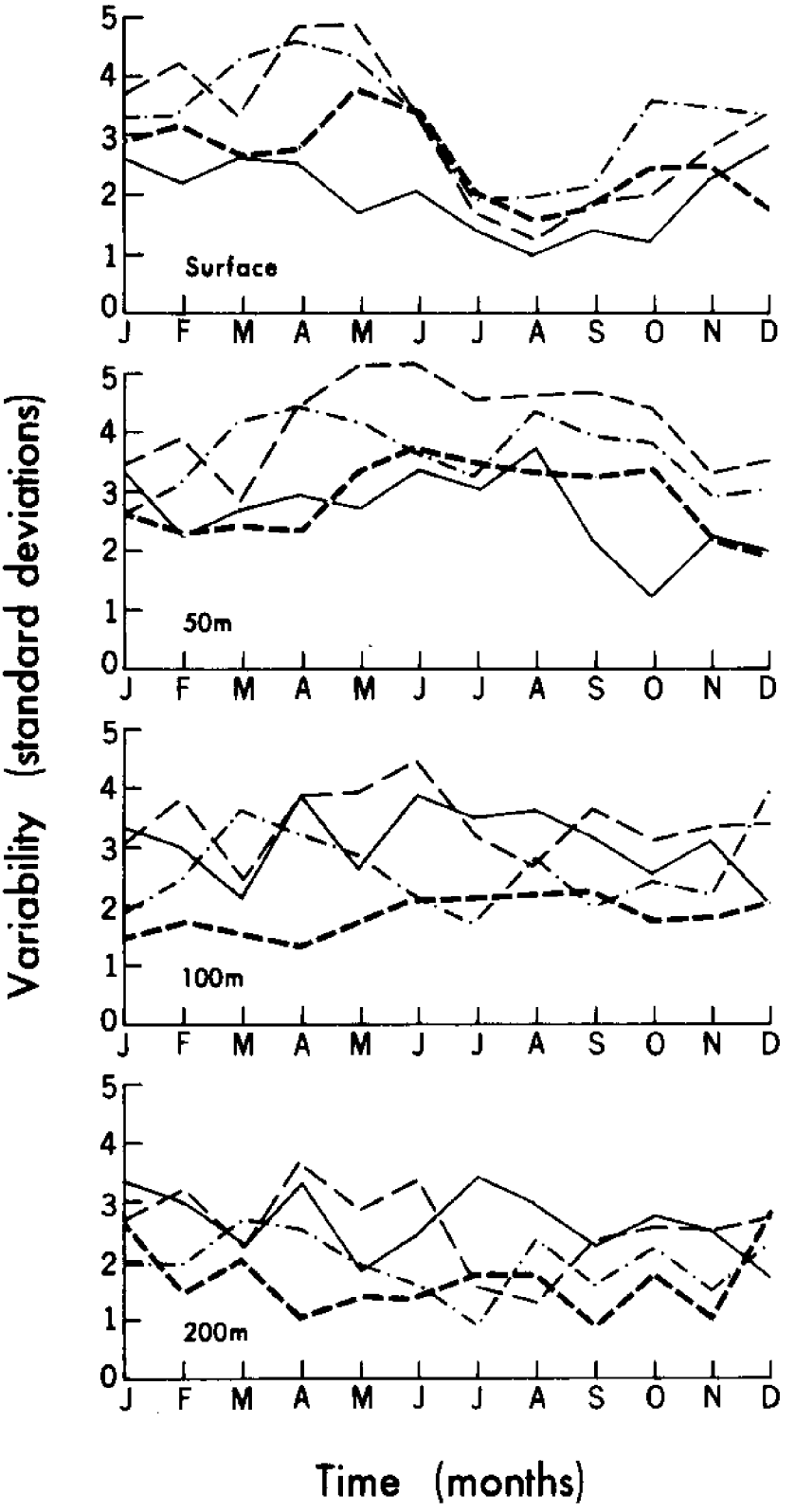

Figure 2. The annual cycles of standard deviation of temperature at four stations on four different levels. The stations are located at ① 35°30'N, 73°30'W (——), ② 38°30'N, 72°30'W (– – –), ③ 37°30'N, 71°30'W (– – –), and ④ 39°30'N, 69°30'W (– · –).

centered on the axis of the climatological Gulf Stream (Figure 1). Within the high variability region, the variabilities are 2-5°C for temperature, 0.25-0.50°/$_{oo}$ for salinity and 0.5-1.0ml/l for oxygen. The variabilities of temperature and salinity are about 50% lower in the other regions of the MAB. Near the coast, however, the spring river run-off produces a salinity variability of 3-5°/$_{oo}$. East of the Gulf Stream the oxygen variability is lowest, about 0.25ml/l, while coastal values are similar to those in the Gulf Stream. All the parameters exhibit variabilities that decrease with depth.

2. Distributions of Temperature, Salinity and Density

The annual range of surface temperature is about 7°C in the open ocean and about 18°C near the coast. The months of February and March have the lowest temperatures while July and August have the highest. The annual variation in surface salinity is from 0.5 to 1.0°/$_{oo}$ and is much smaller on a percentage basis than that variation displayed by temperature. Near the coast, the spring run-off produces changes of about 5°/$_{oo}$. In the figures presented here the influence of the run-off is somewhat exaggerated. The one-degree resolution makes contours of the low isohalines extend too far out (~1°) over the continental shelf. The greatest large scale horizontal gradients of temperature occur in the winter months, while the spring months have the largest salinity gradients. Another surface feature is that the isotherms and isohalines are parallel to each other, follow the axis of the climatological Gulf Stream and increase seaward. The mixed layer depths of temperature and salinity extend to approximately 350m in winter and less than 20m in summer. Both the temperature and salinity decrease with

depth, although there are numerous weak inversions. The annual ranges of both properties decrease with depth. At 1000m the annual range in temperature is 1°C and for salinity 0.10°/$_{oo}$. The properties also become more horizontally homogeneous with depth.

The density distributions show more horizontal structure than the temperature and salinity distributions. The density is smallest near the coast and increases seaward. The vertical density distrubution, with isopycnals ascending near the coast, closely parallels that of temperature. A large horizontal density gradient persists through 1200m depth. The few regions where the density does not increase with depth are probably not physical features, but arise from using climatological temperatures and salinities in the density computation.

3. Distribution of Geostrophic Velocity

The most significant feature of the MAB is the presence of the Gulf Stream. In this study, the Gulf Stream is spread out and weakened because of the use of climatological data and one-degree resolution. It meanders on a month to month basis about the main axis with largest surface velocities (~70cm/sec) in March and November and smallest velocities (~35cm/sec) in April. With the exception of the Gulf Stream, the velocities of the MAB are approximately 10cm/sec. At 1000m depth, the velocities everywhere are an order of magnitude lower than at the surface. These deep velocities show a much smaller annual variation. The velocity distributions also show that subsurface maxima exist. On the eastern side of the Gulf Stream there is often a southward flow of water which sometimes extends downward to 800m depth. The month of November has the largest amount of this return flow.

The transport of the Gulf Stream between 36°30'N, 70°30'W and 38°30'N, 72°30'W and the surface and 2000m depth has also been calculated. Small amounts of transport occur from April to July with June having the minimum of $22.4 \times 10^6 m^3/sec$. The remaining eight months have a larger transport with a maximum of $36.5 \times 10^6 m^3/s$ occurring in September. These transports are roughly 60% lower than other transports calculated using synoptic density distributions.

4. Distribution of Oxygen

In the MAB, the dissolved oxygen distributions tend to decrease seaward with the largest values found in the northeast portion at all depths. The isopleths of oxygen are almost perpendicular to the coast in shallow water, while they run parallel to the Gulf Stream in deeper water. The oxygen content decreases with depth from values near saturation at the surface to minimum values near 800m depth. Below this level, the oxygen increases downward to a maximum near the bottom. A secondary minimum appears off the shelf break at 200-300m depth. The two minima appear to be separated by the Gulf Stream.

V. Conclusions

As a result of this work, an atlas of the climatological temperature, salinity, oxygen, density and geostrophic velocity distributions is available for the Middle Atlantic Bight. The major features of the various distributions have been pointed out and they agree with previously published studies. Deficiencies in the distributions clearly exist. An atlas based upon 1/4° to 1/2° resolution would be desirable, but until the data base is expanded tremendously, this fine resolution cannot be attained.

Acknowledgments

The authors wish to acknowledge Dr. Abraham Oort for his interest in the project. This atlas would not have been completed were it not for the efforts of many members of the staff of the Geophysical Fluid Dynamics Laboratory/NOAA. In particular we thank Tom Reek and Jim Haines for their aid in producing contour plots of the various distributions, and John Connor for his photographic services. The excellent draftsmanship of Mike Zadworney, Phil Tunison and Bill Ellis was a key element in the production of this atlas.

References

Levitus, S. and A.H. Oort, 1977: Global Analysis of Oceanographic Data. To be published by Bull. of Am. Met. Soc.

Distributions of Temperature, Salinity, Density and Geostrophic Velocity

Surface Distribution, January

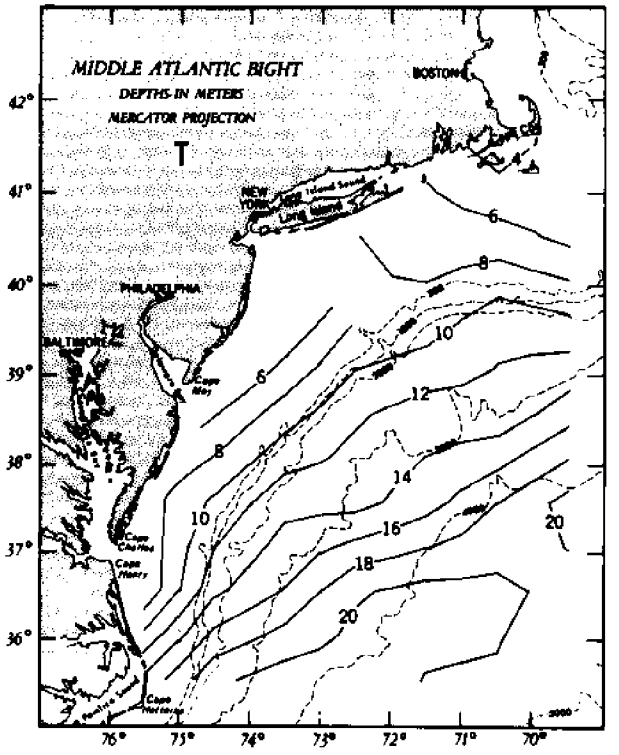

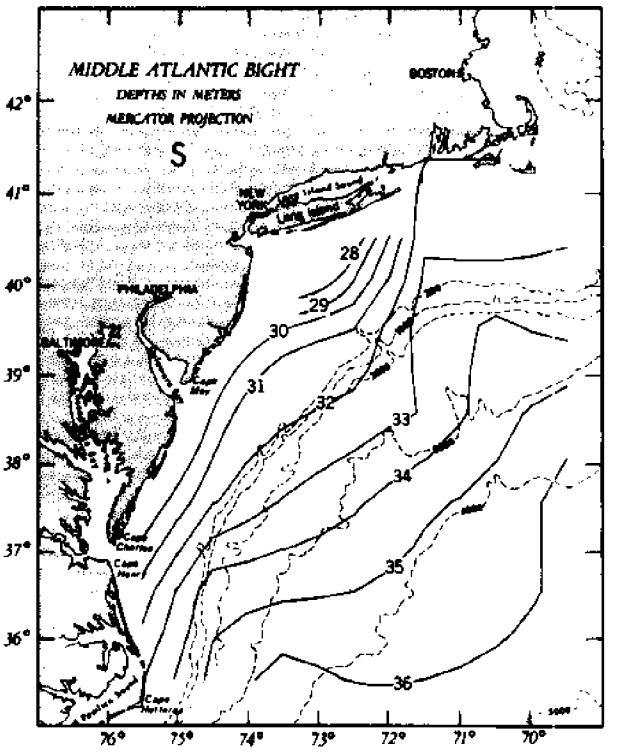

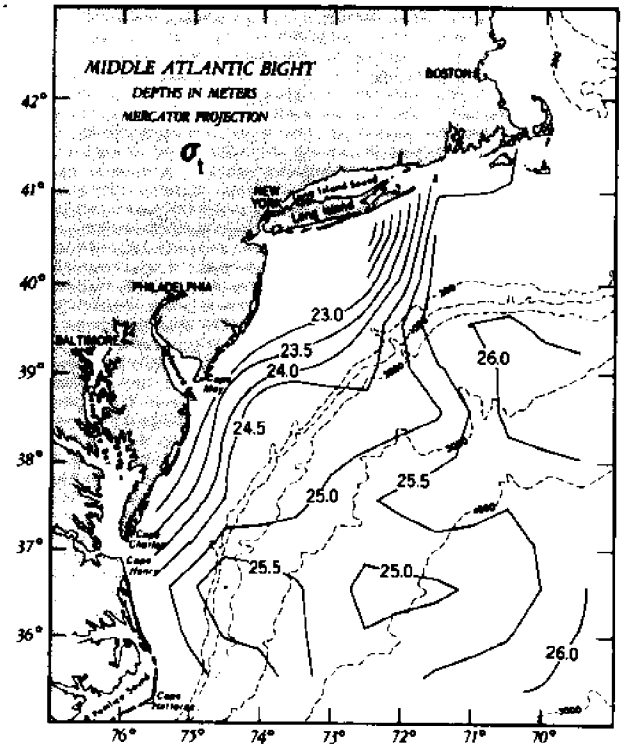

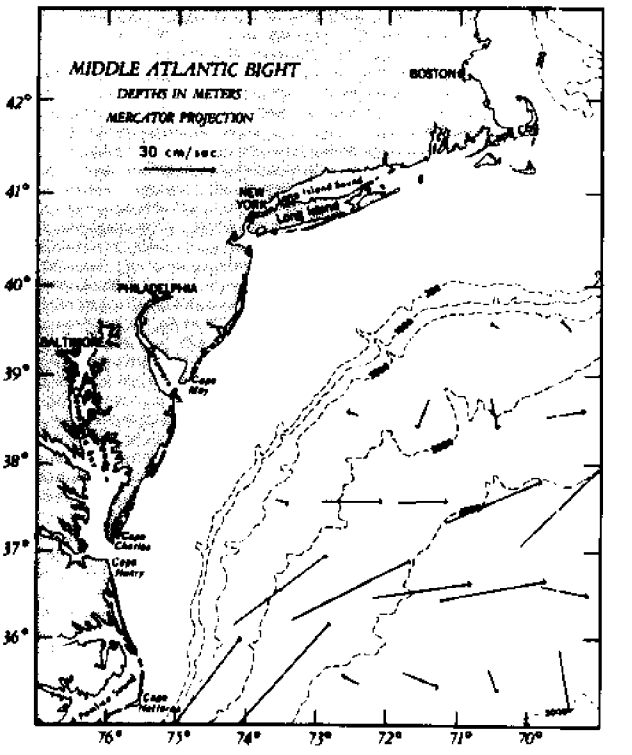

Surface Distribution, February

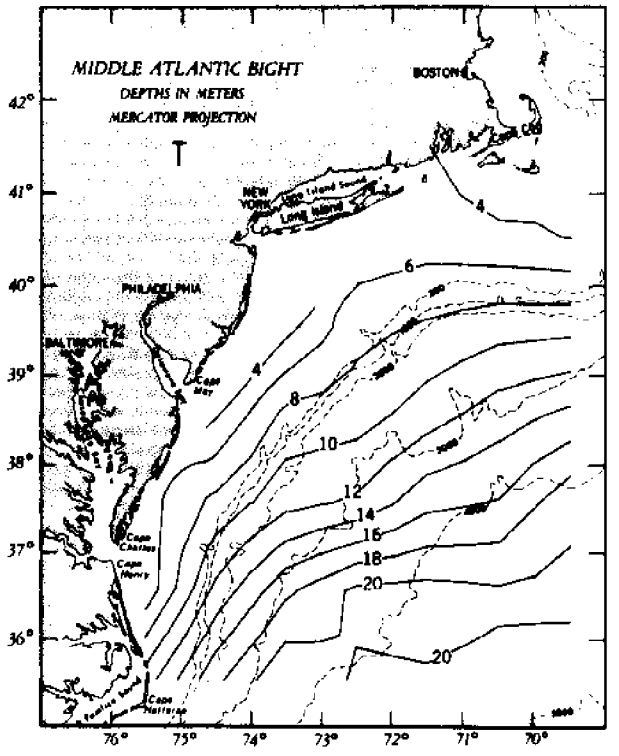

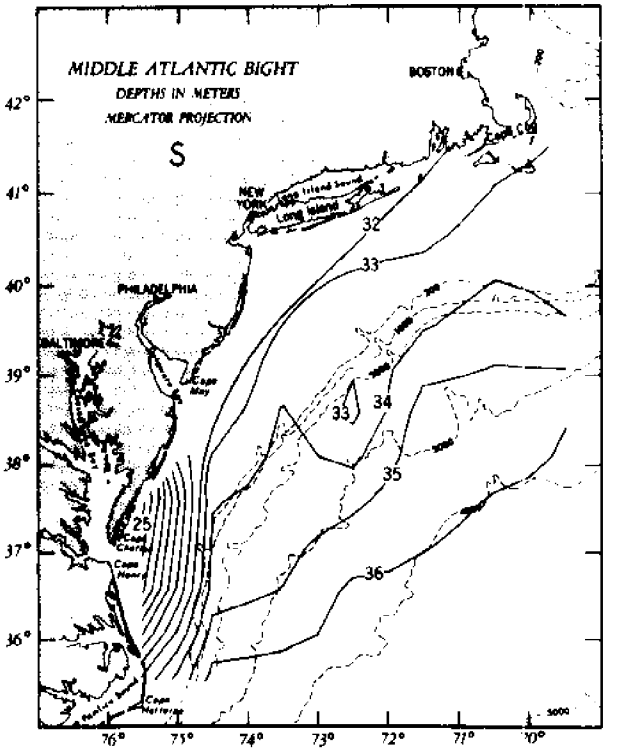

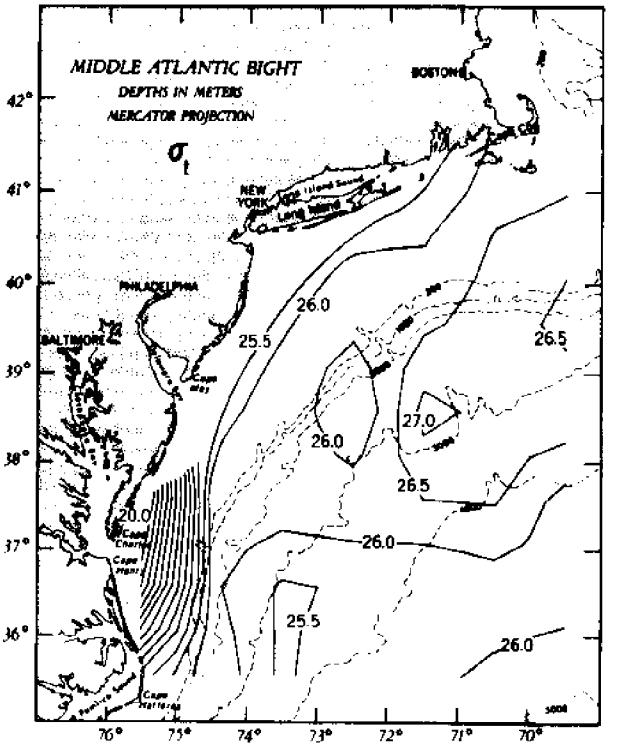

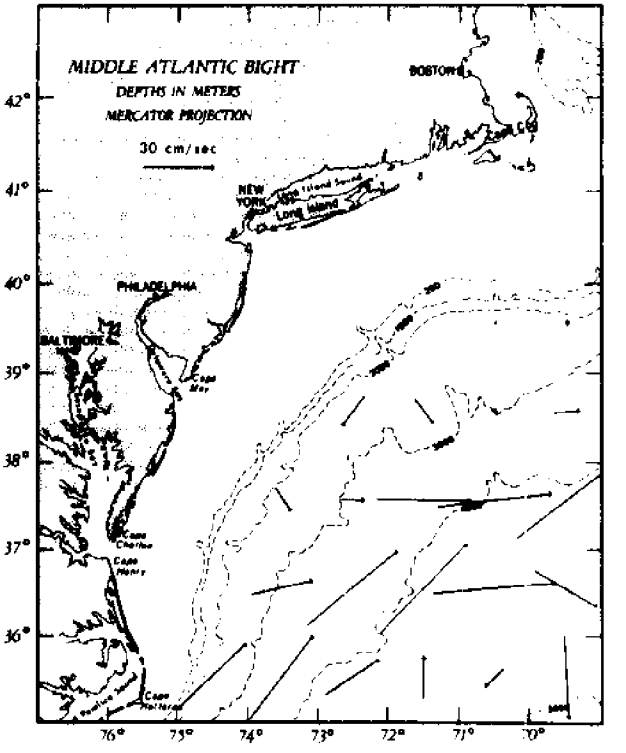

Surface Distribution, March

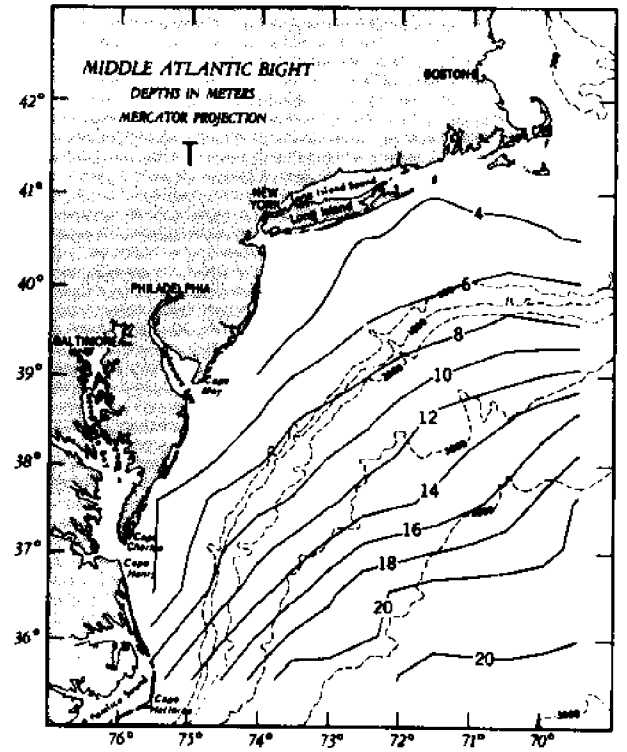

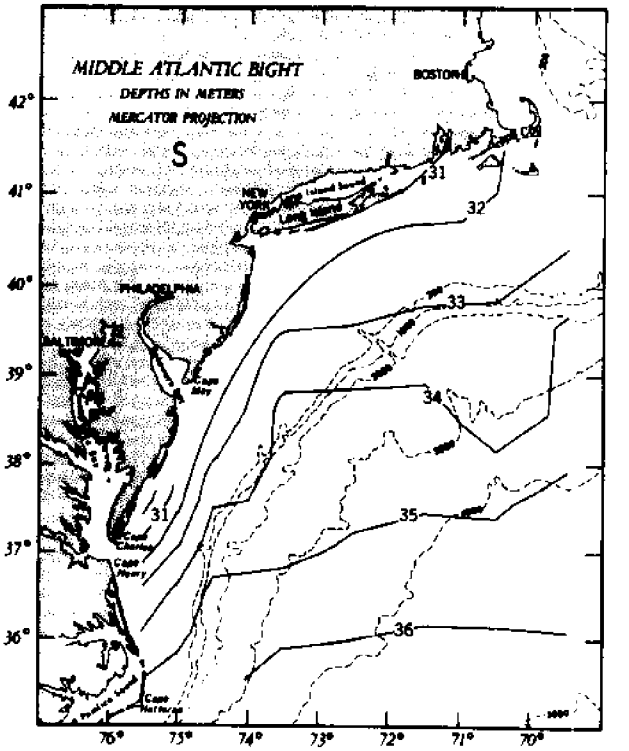

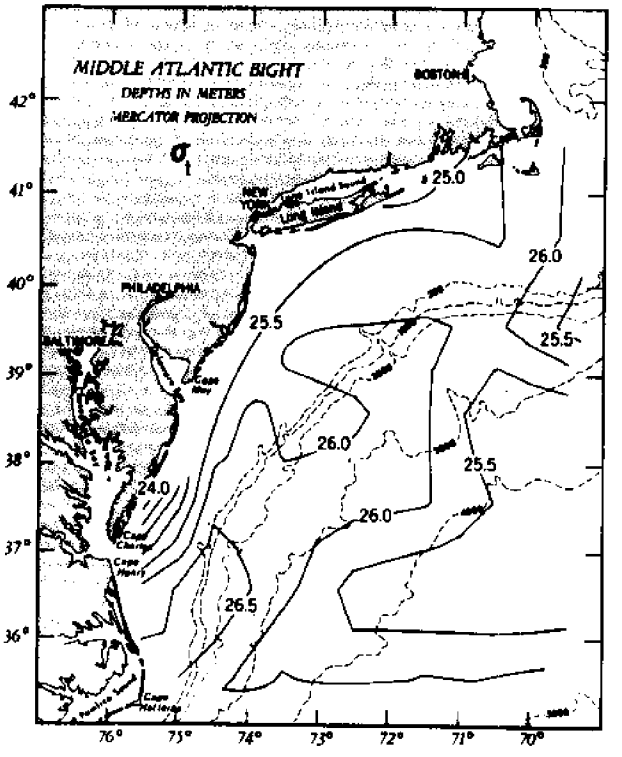

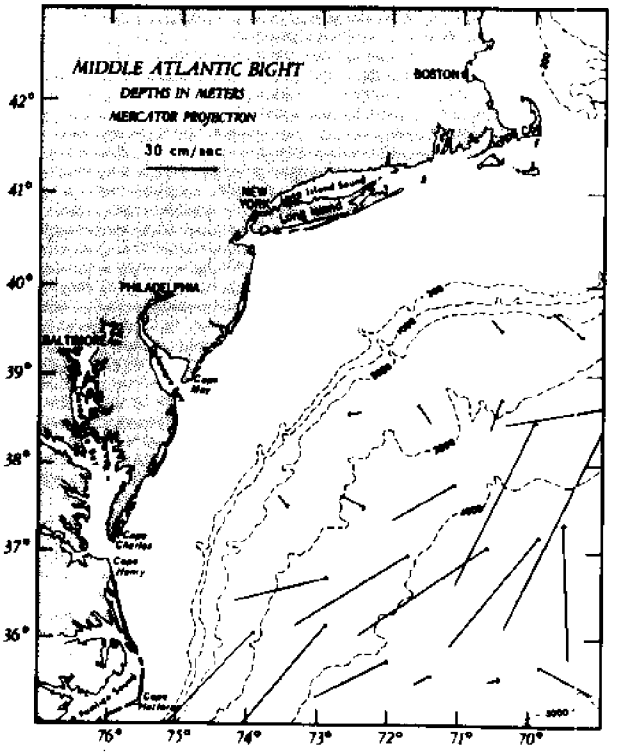

Surface Distribution, April

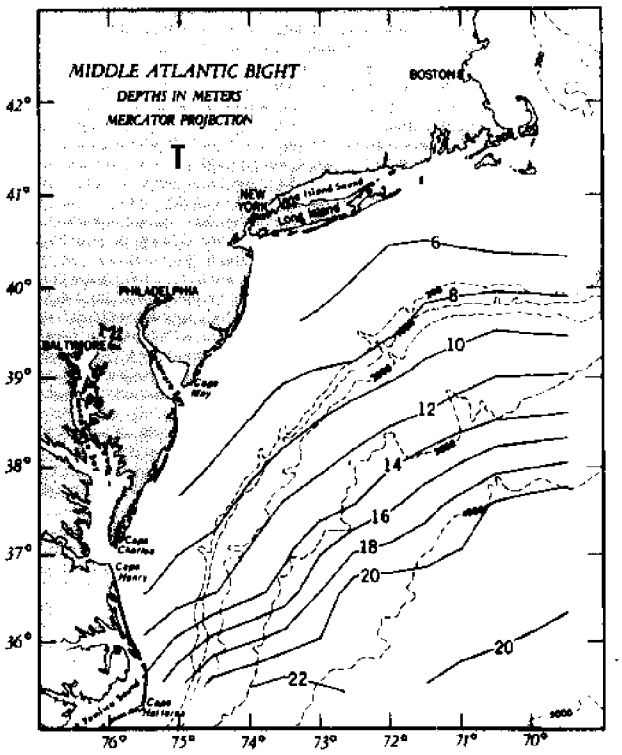

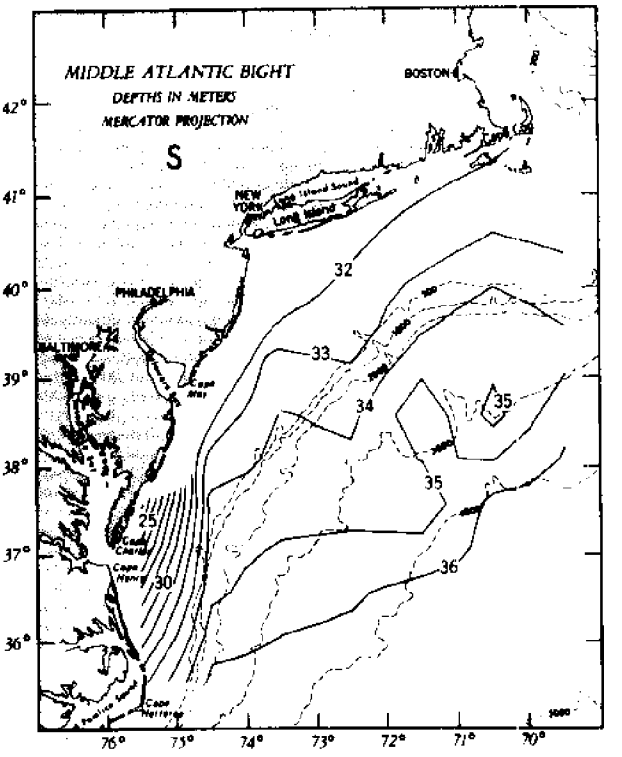

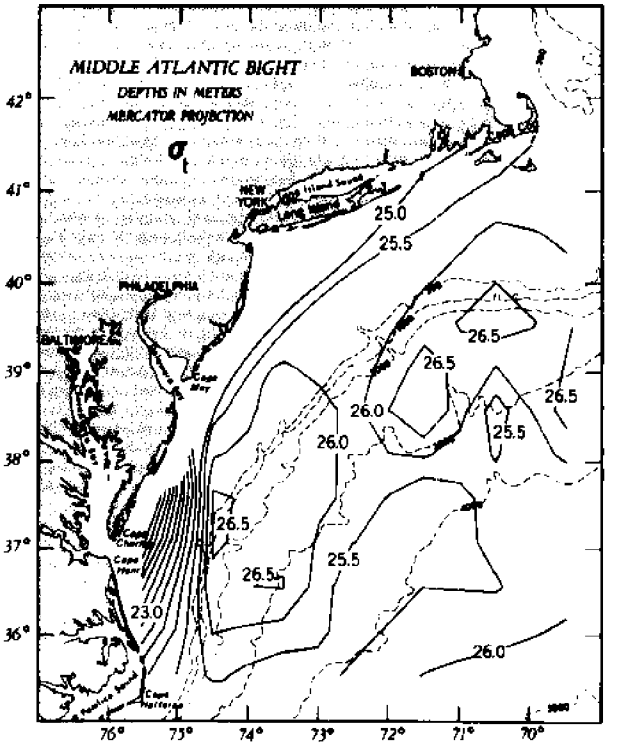

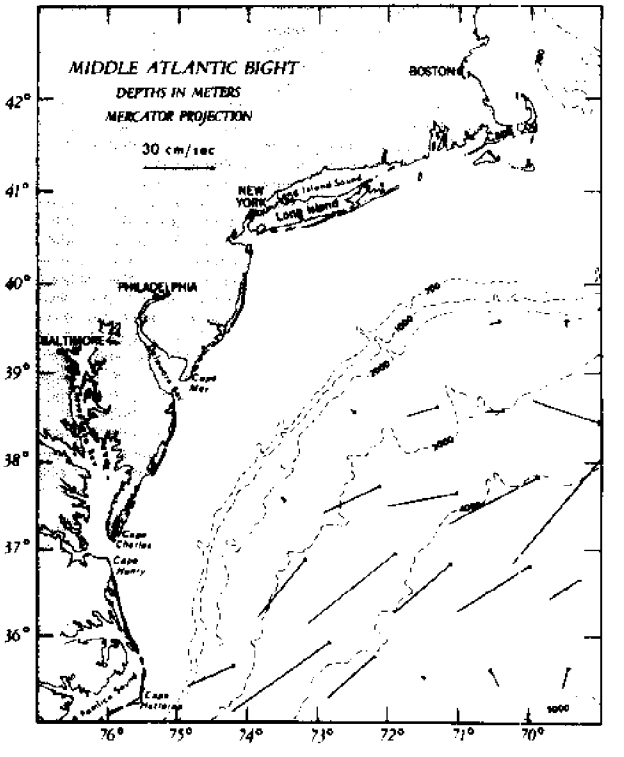

Surface Distribution, May

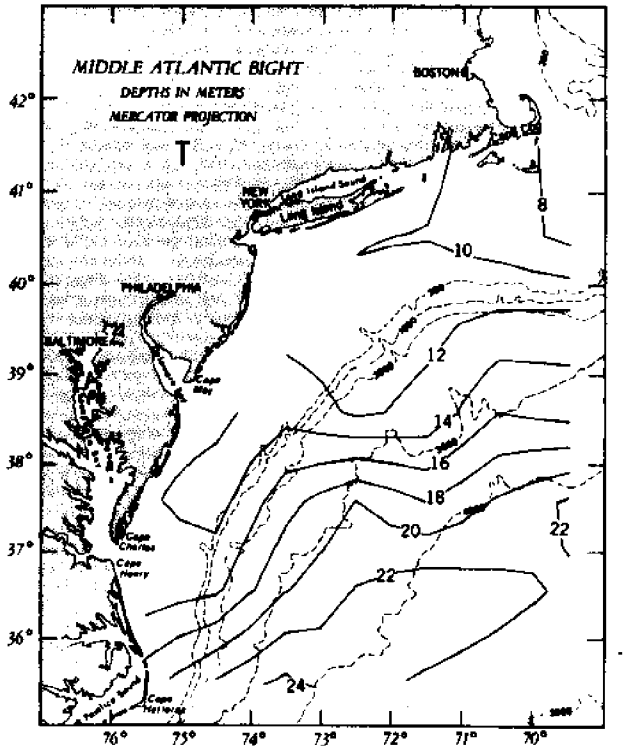

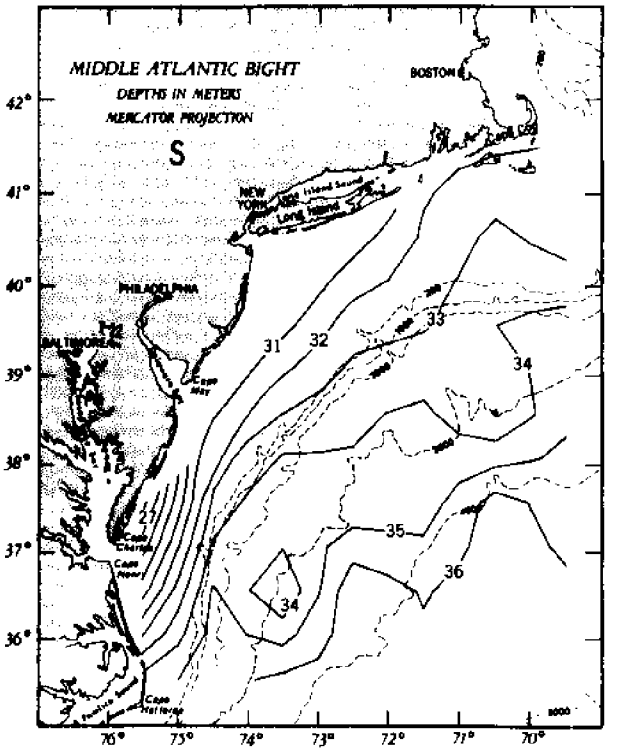

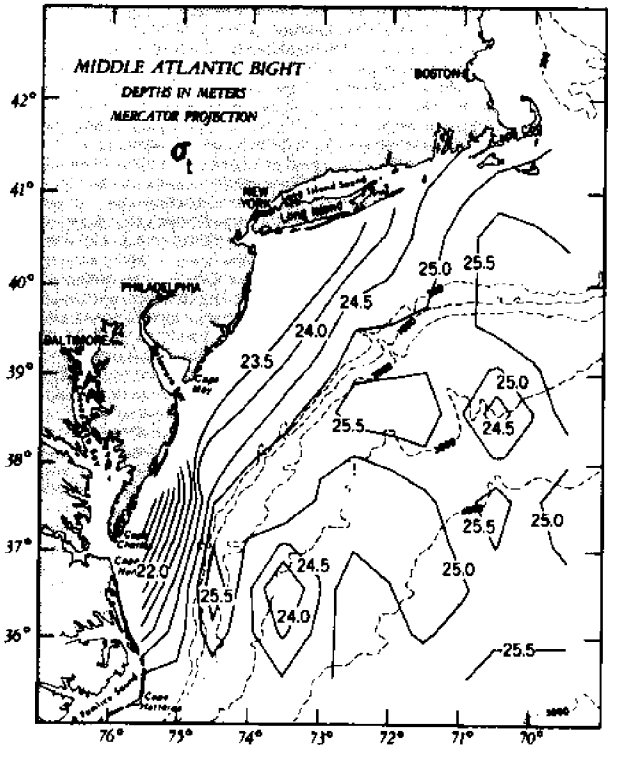

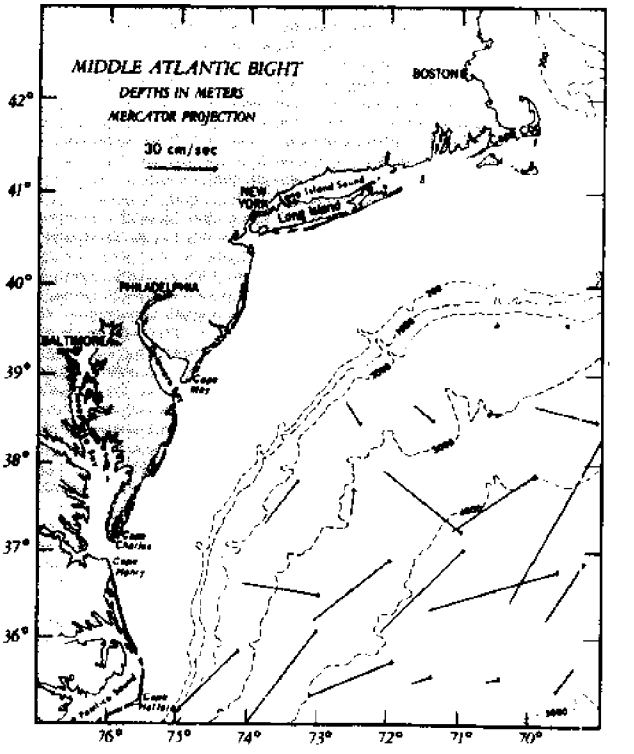

Surface Distribution, June

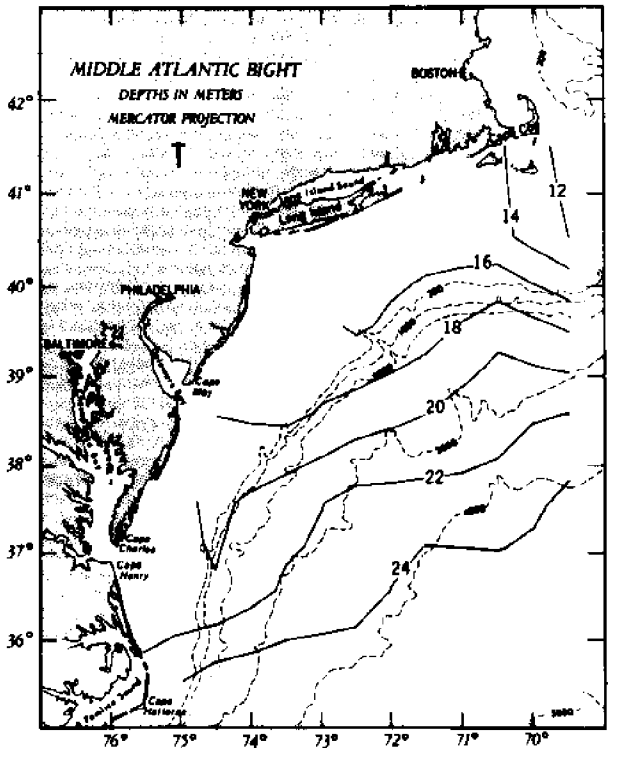

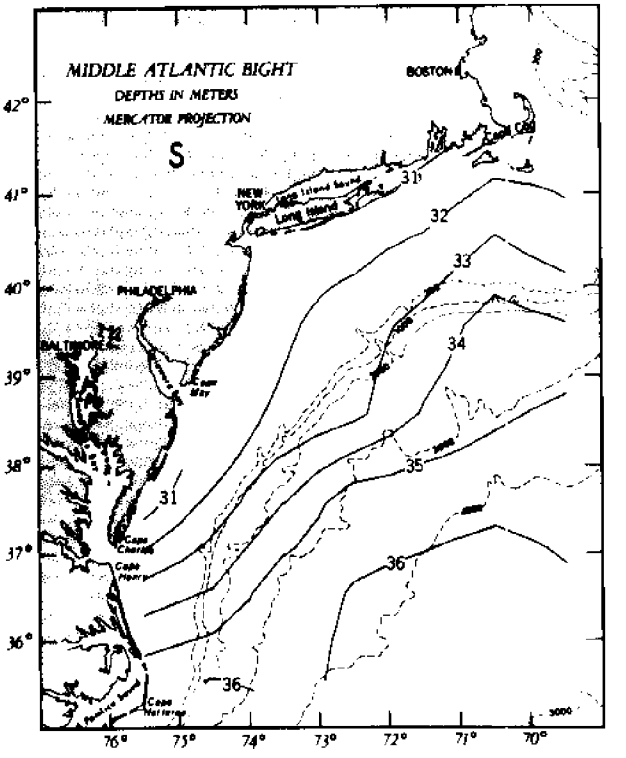

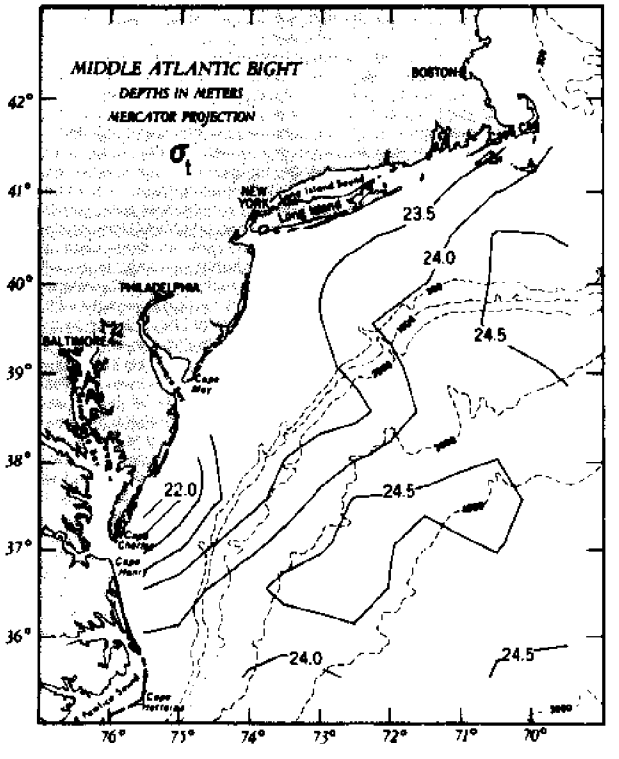

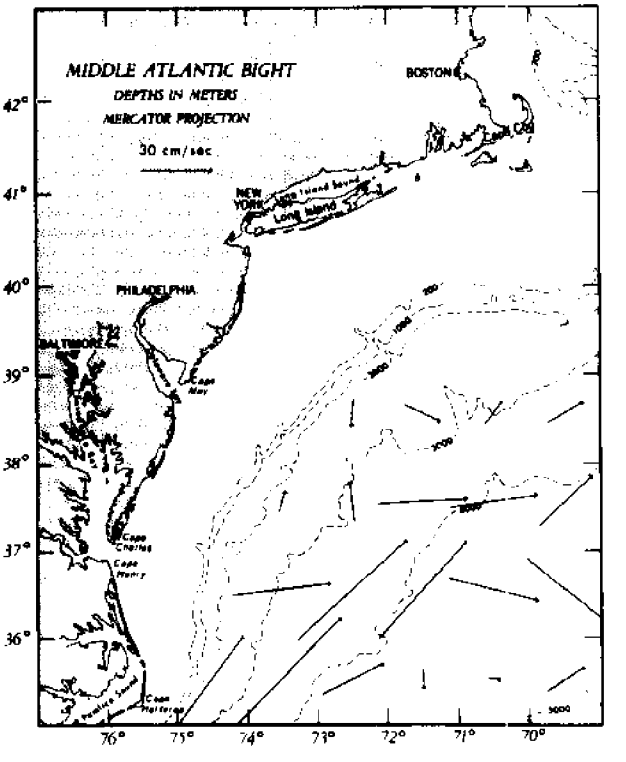

Surface Distribution, July

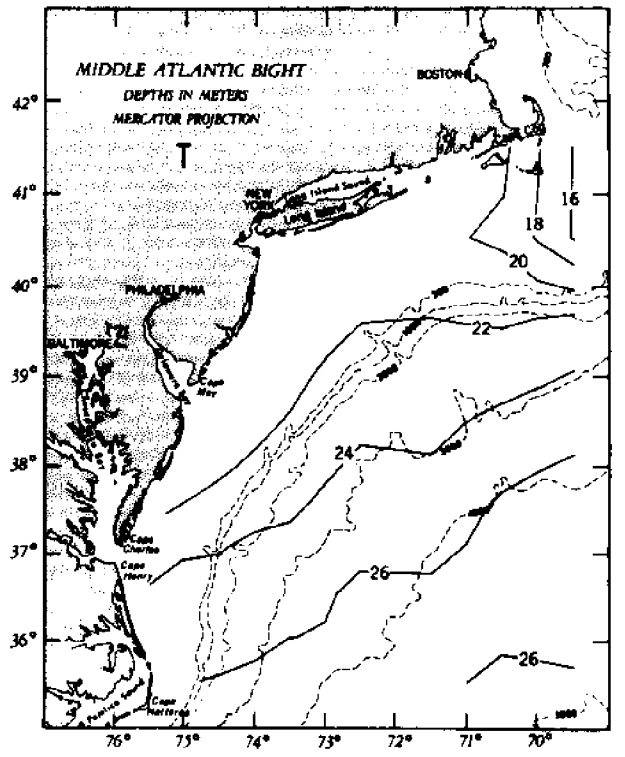

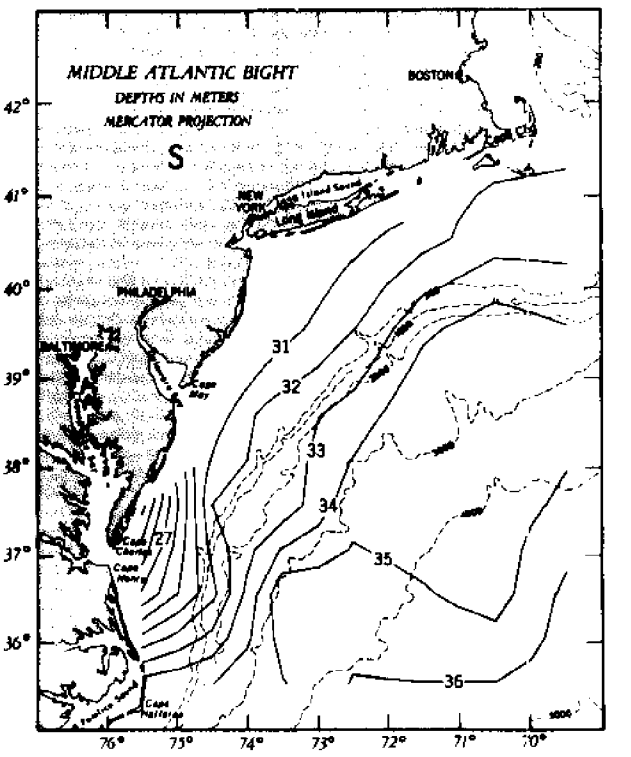

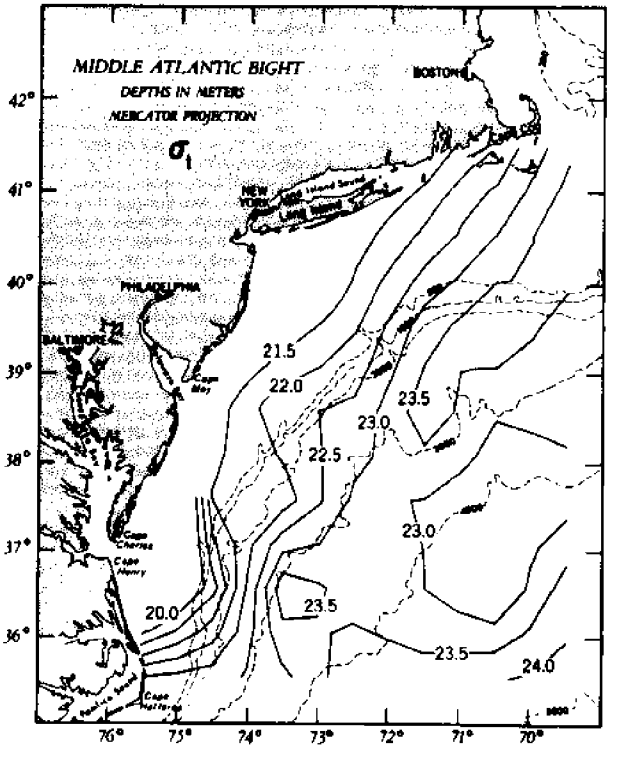

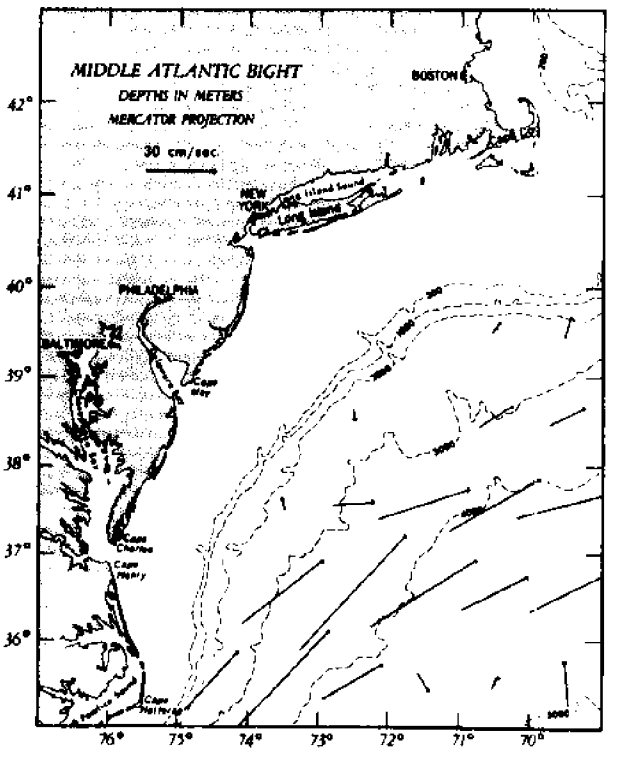

Surface Distribution, August

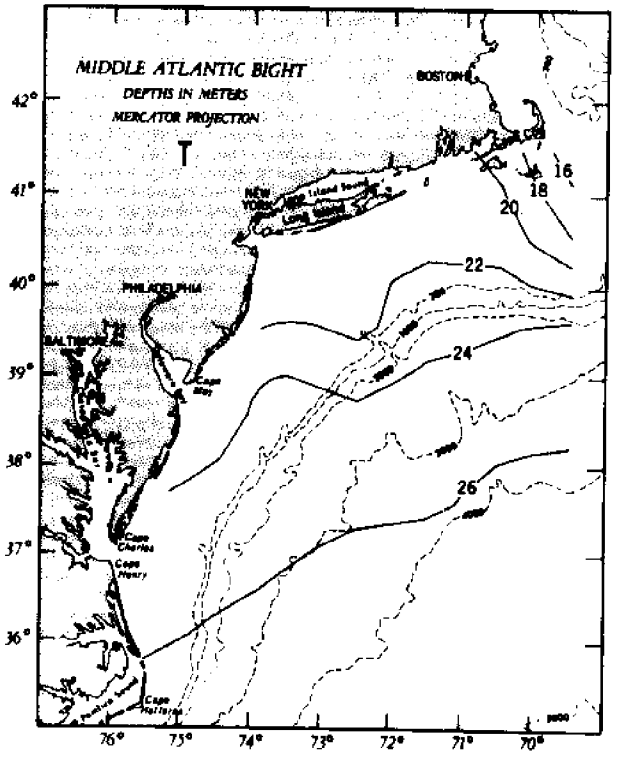

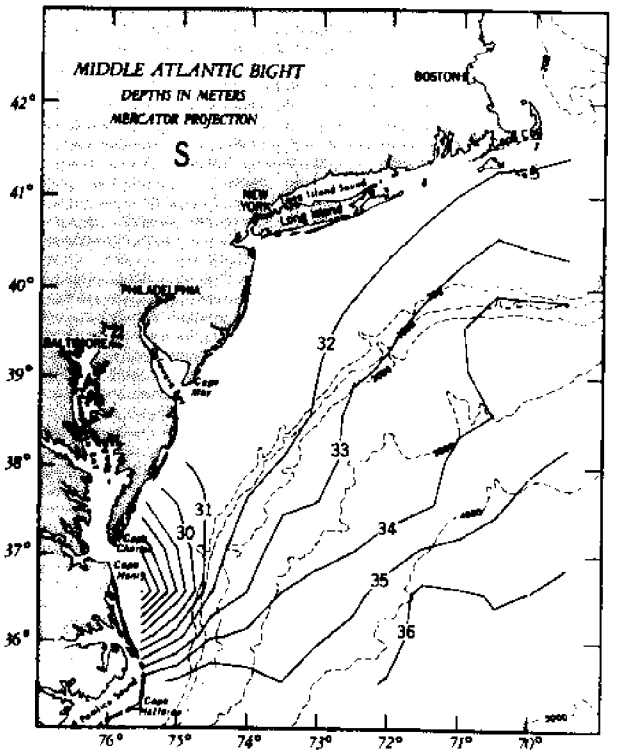

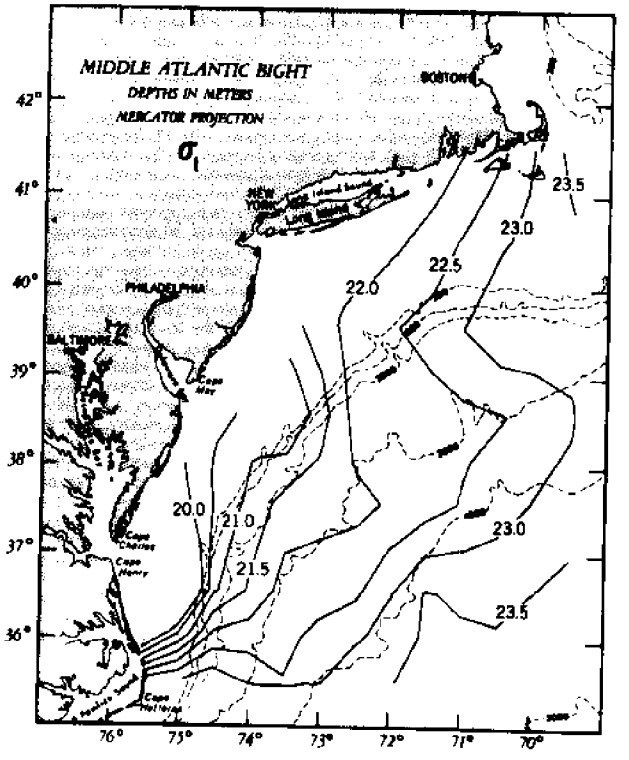

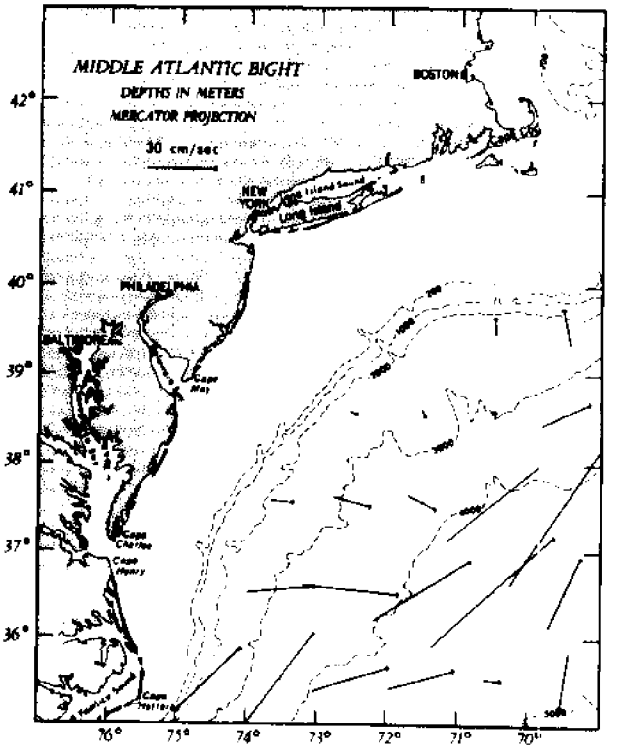

Surface Distribution, September

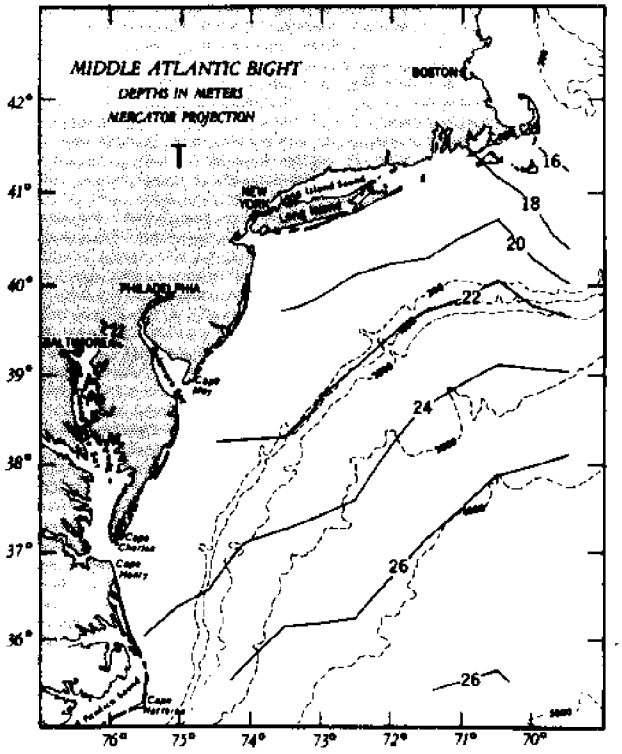

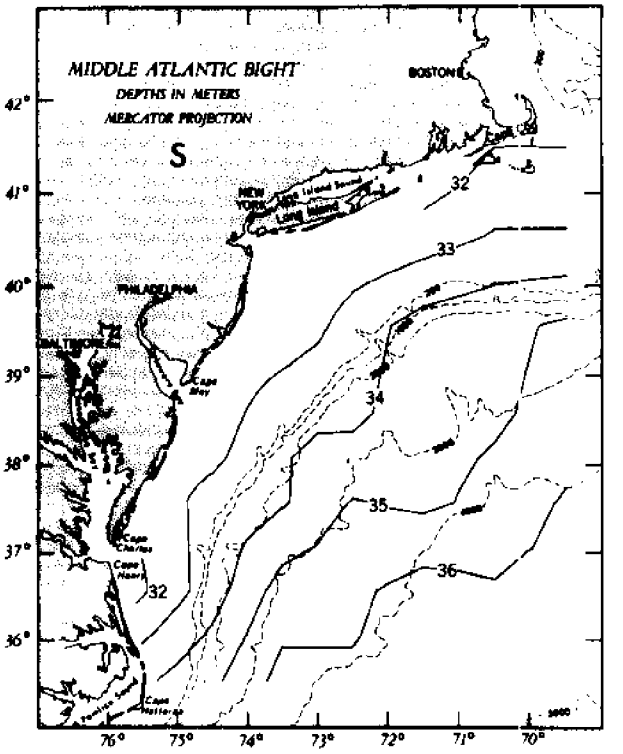

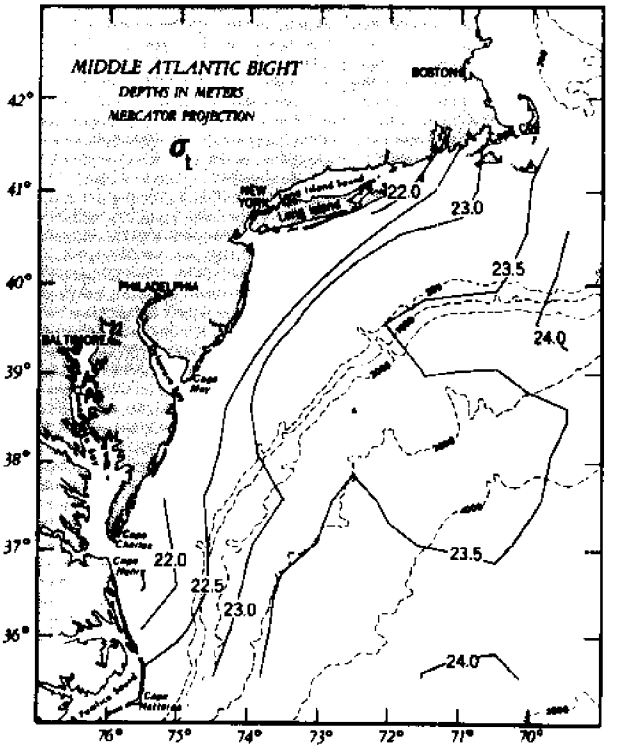

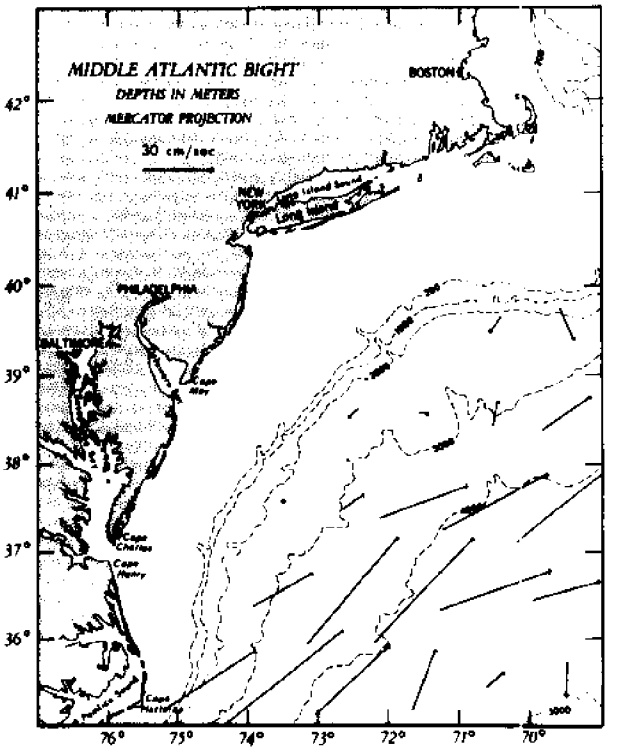

Surface Distribution, October

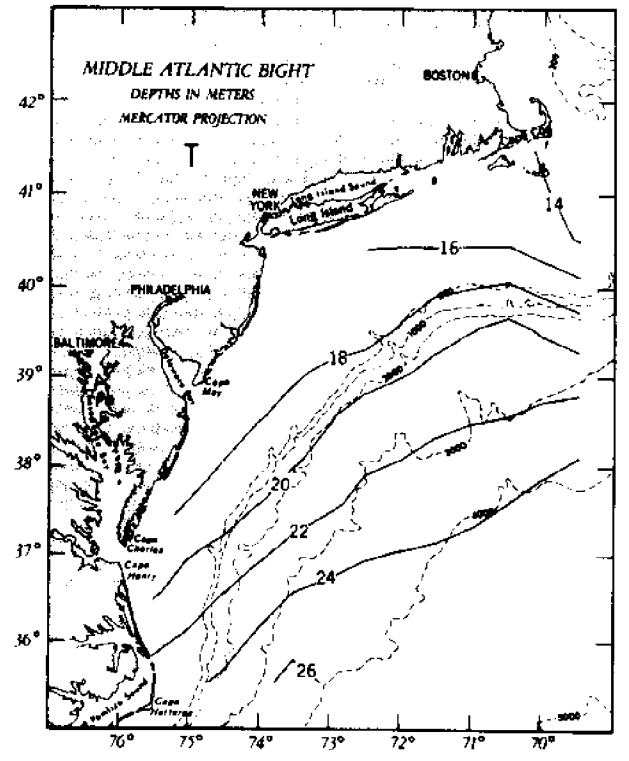

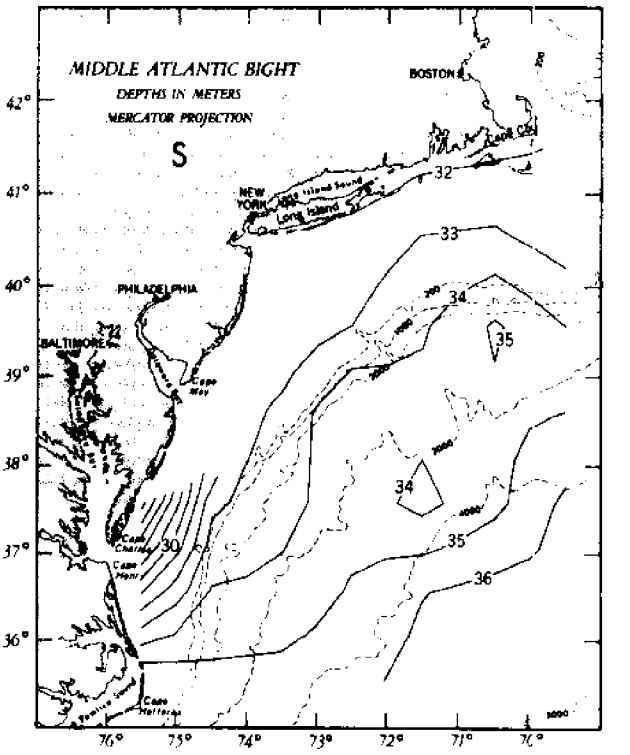

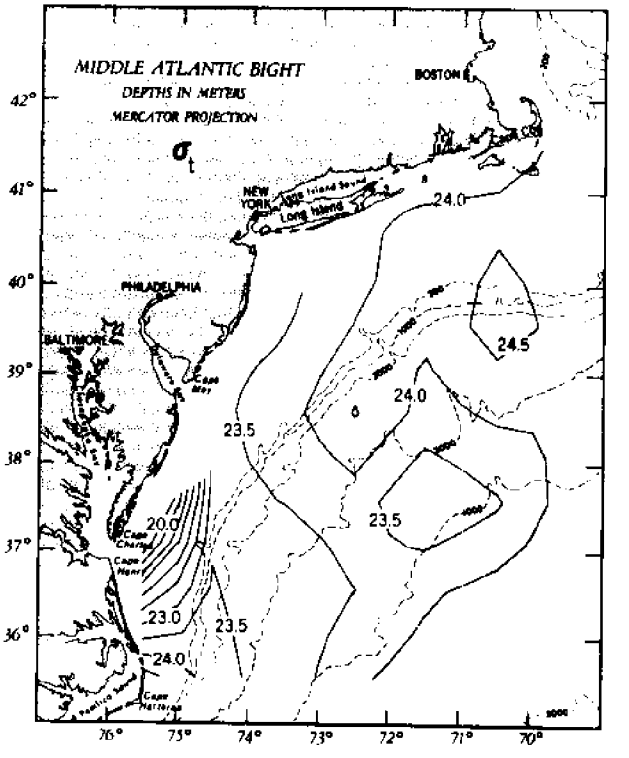

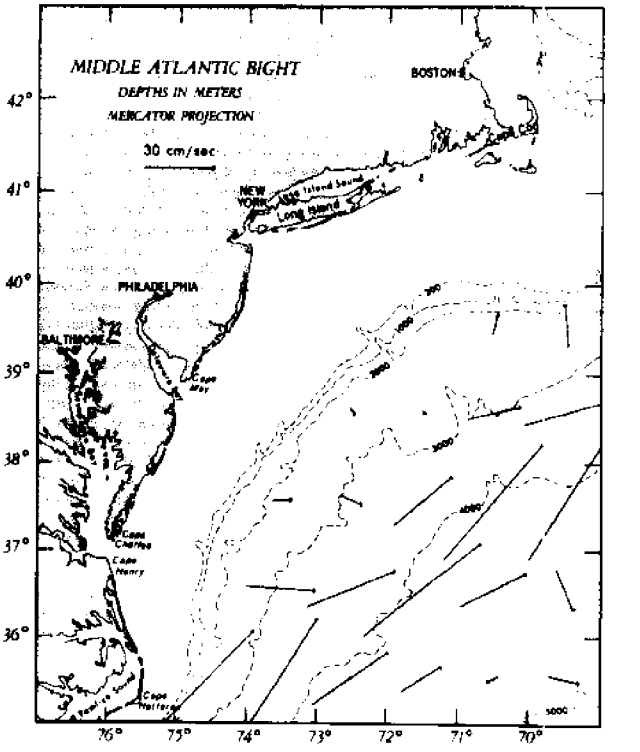

Surface Distribution, November

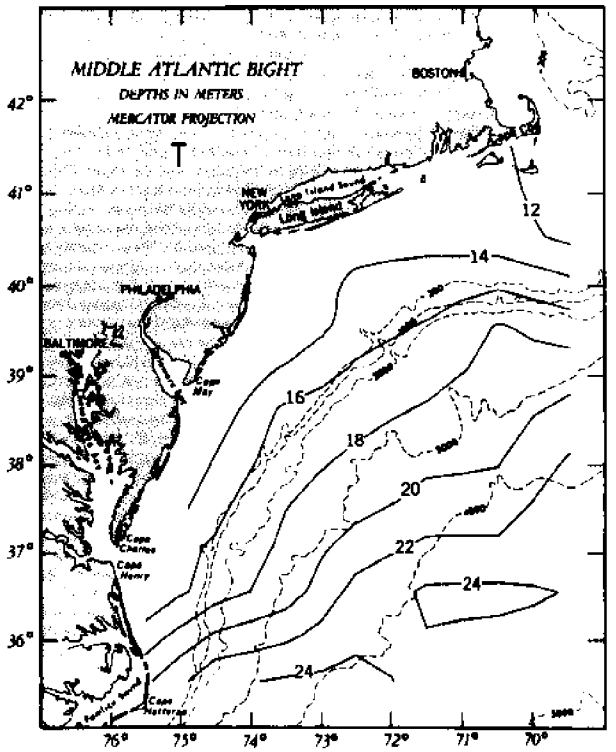

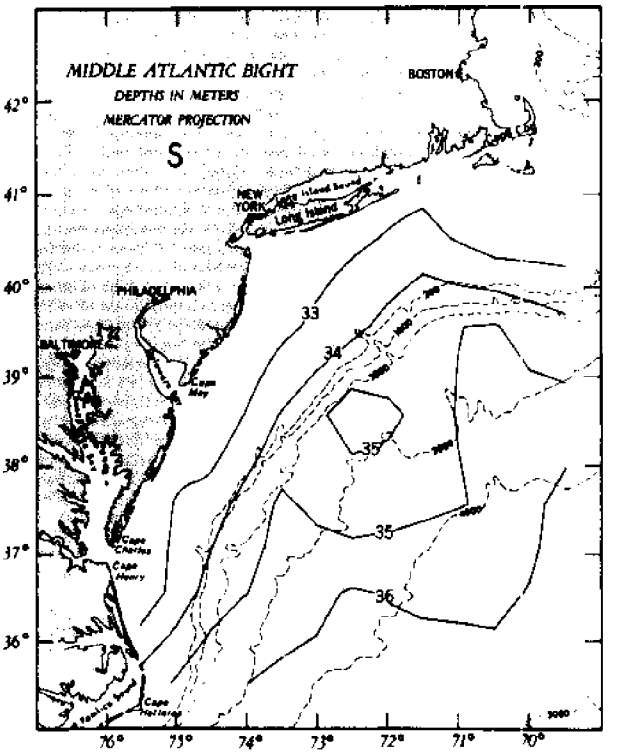

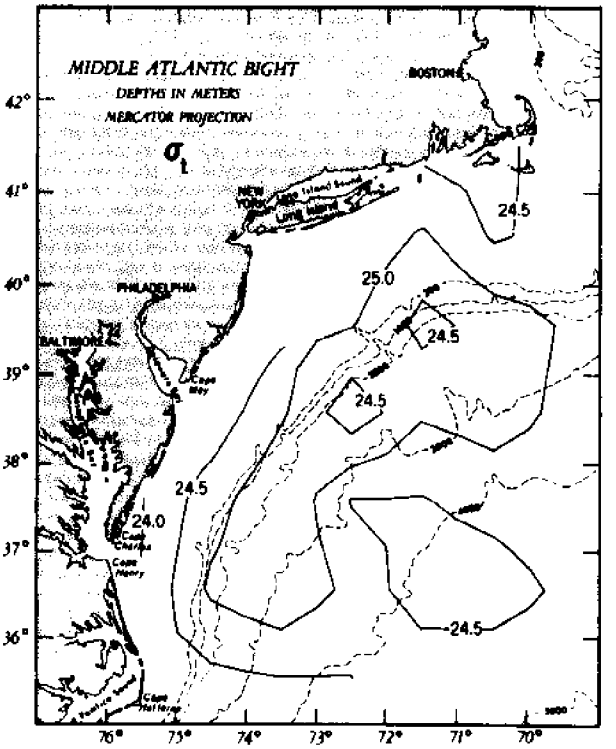

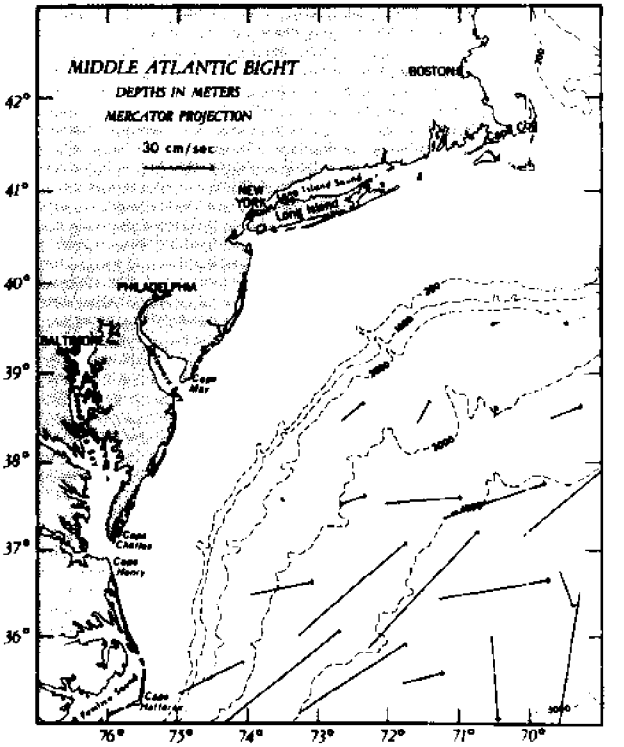

Surface Distribution, December

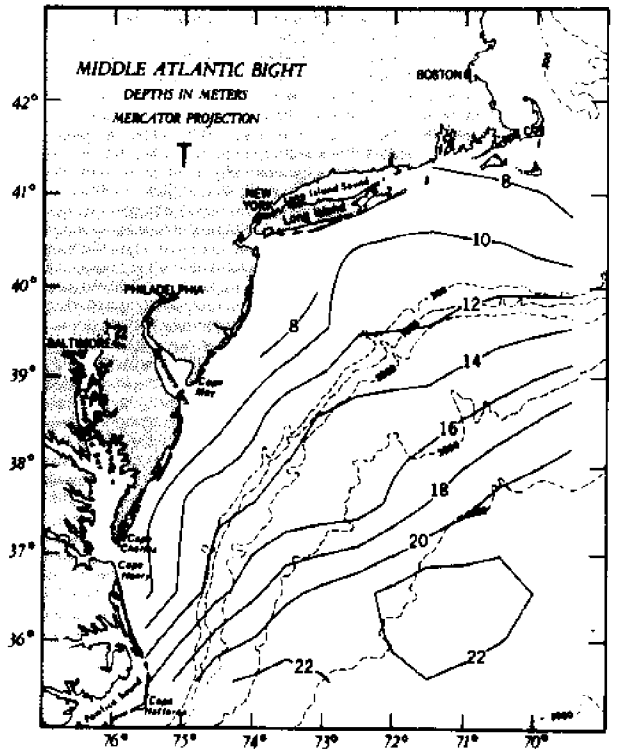

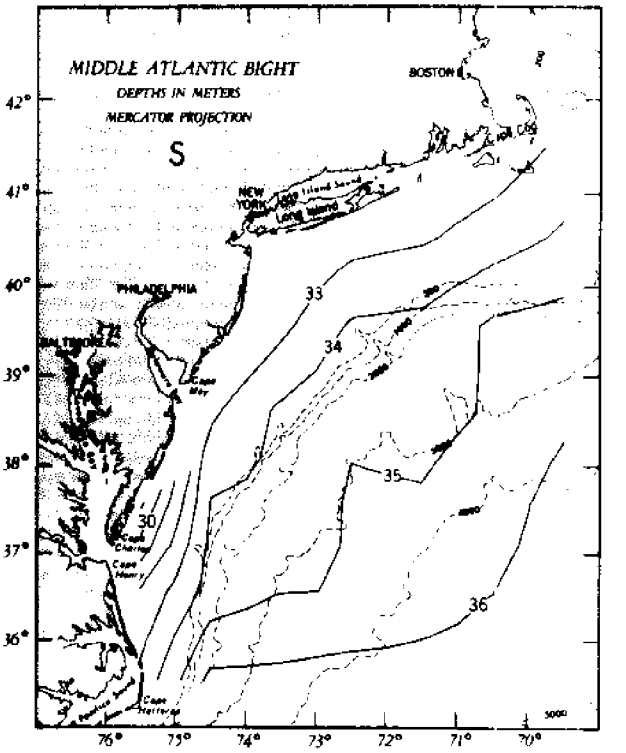

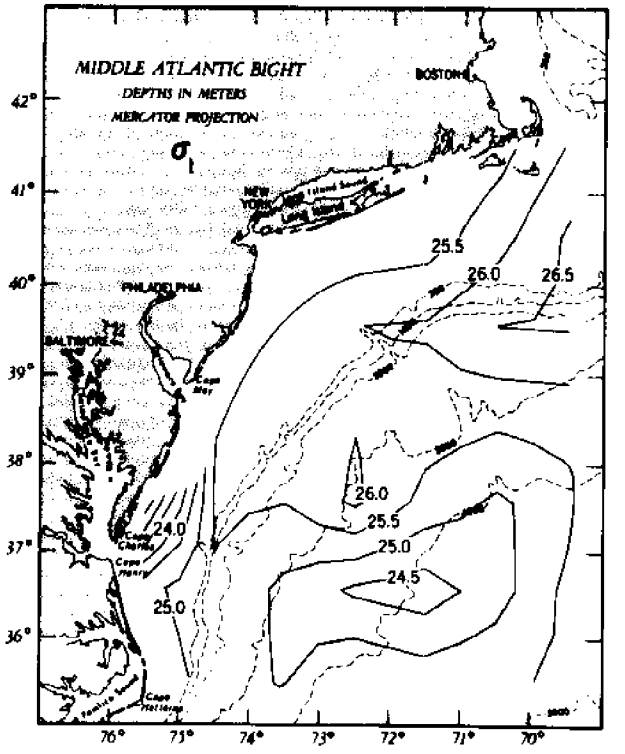

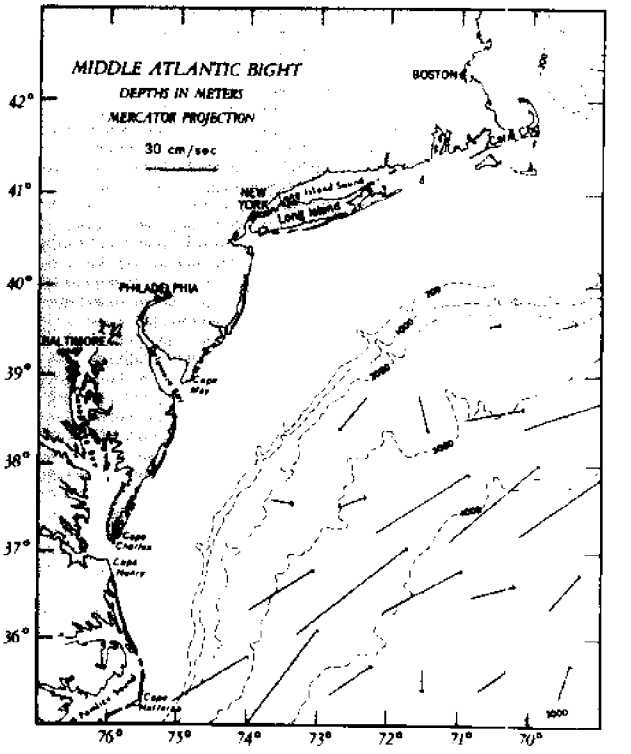

1000m Distribution, January

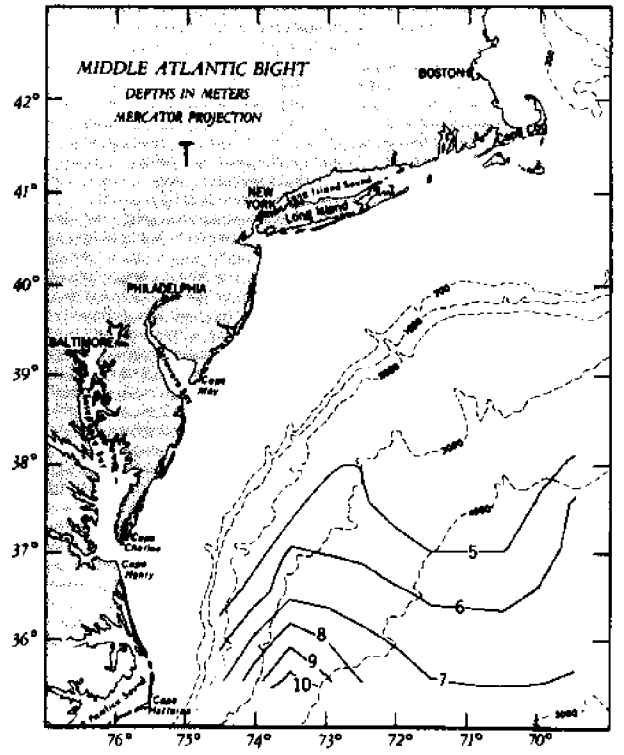

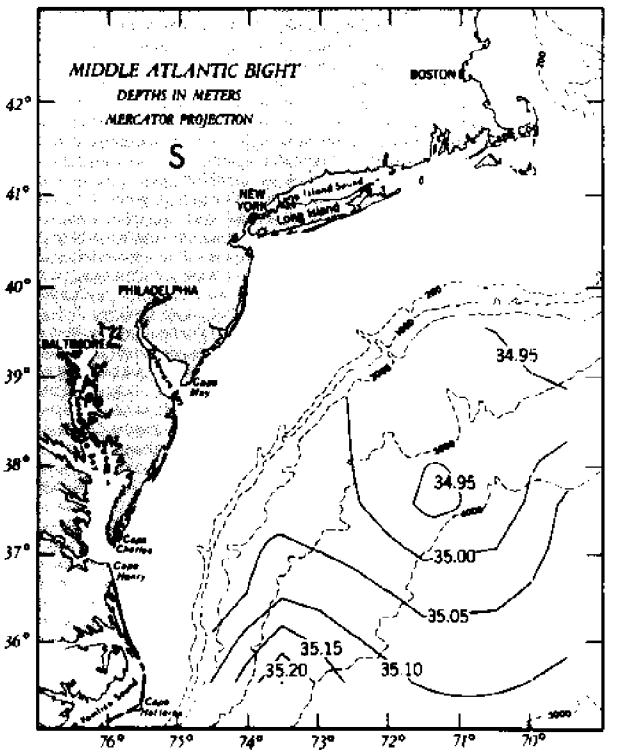

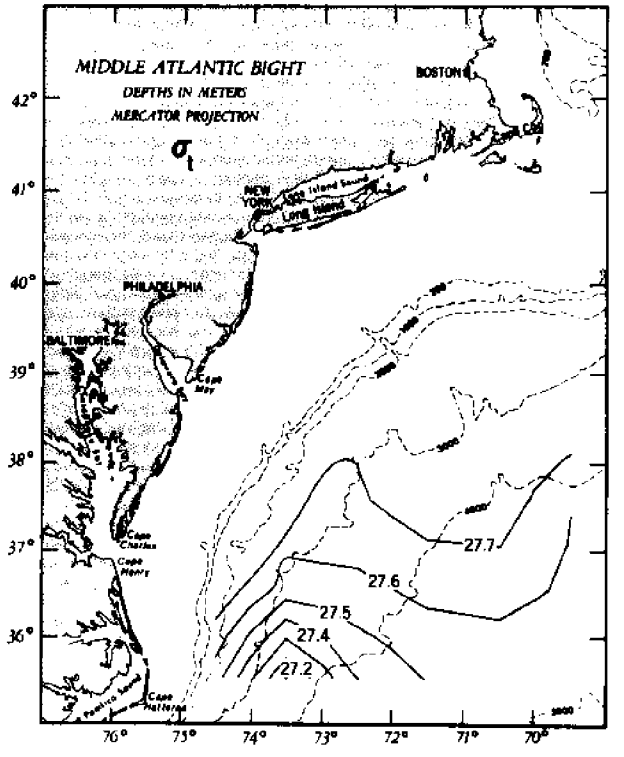

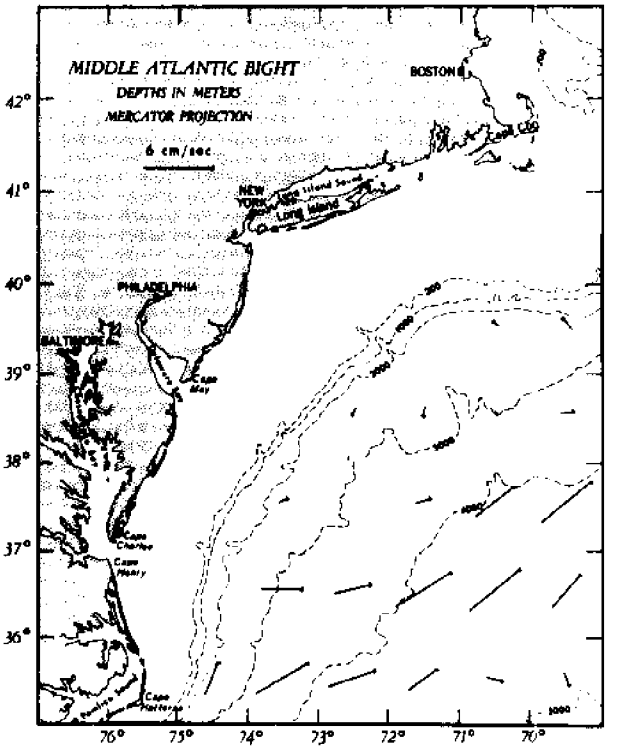

1000m Distribution, February

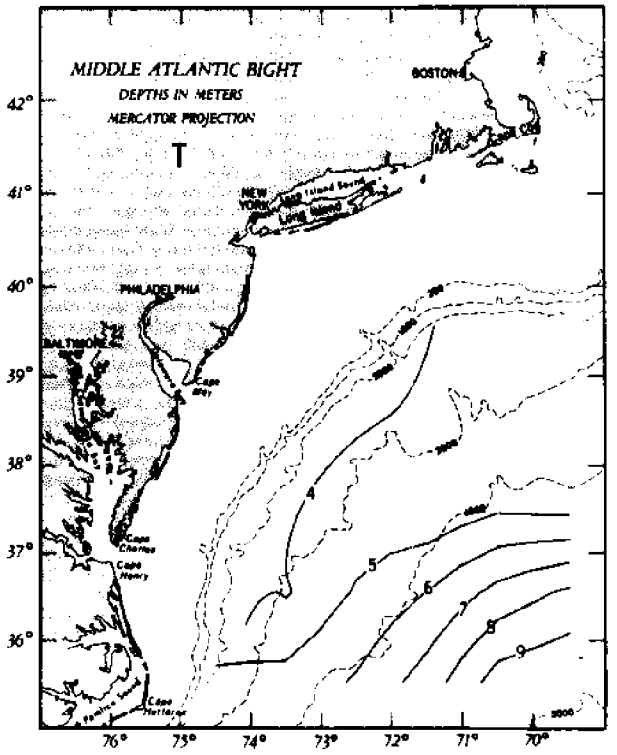

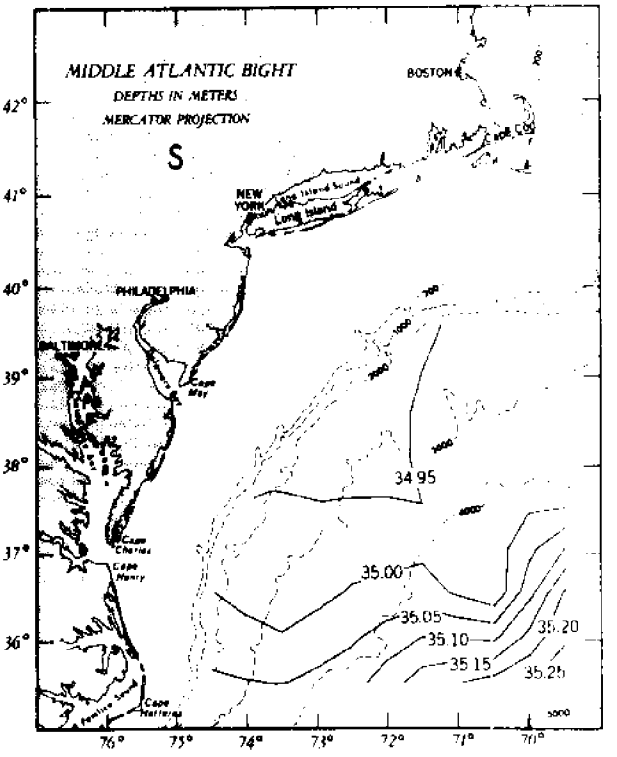

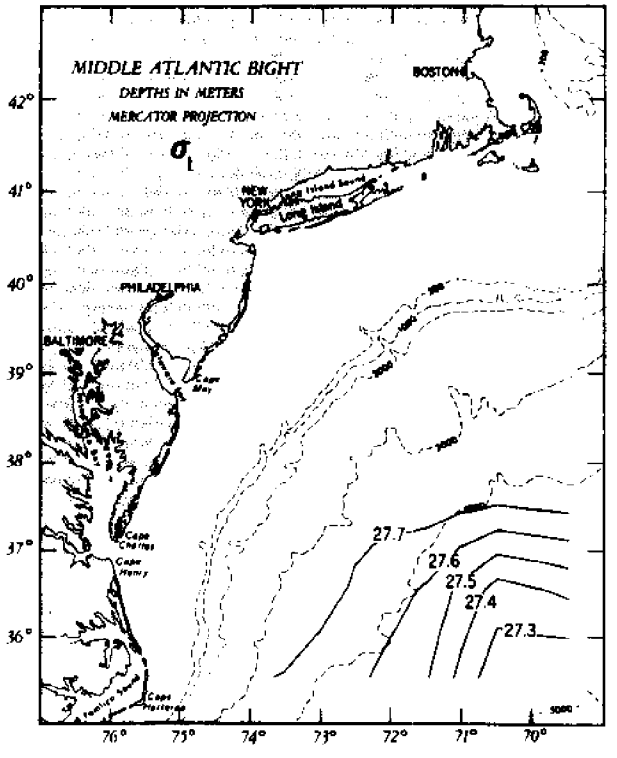

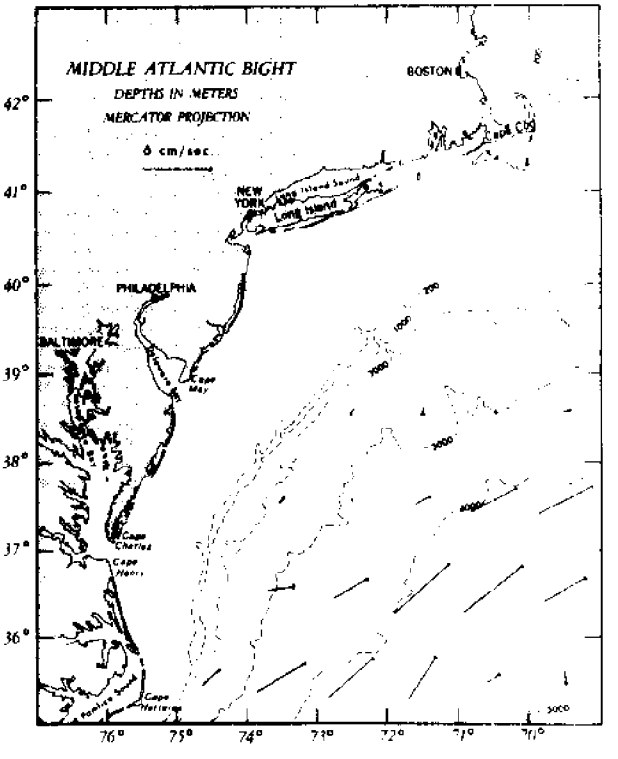

1000m Distribution, March

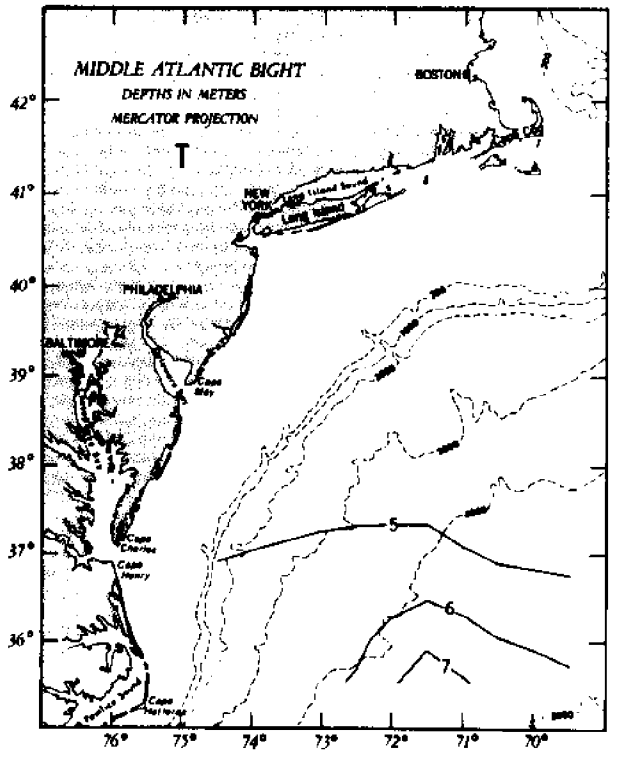

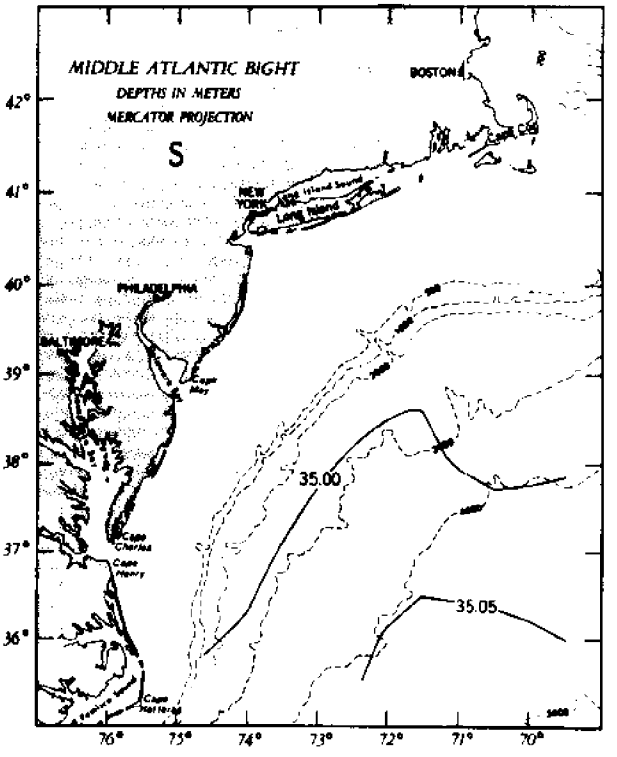

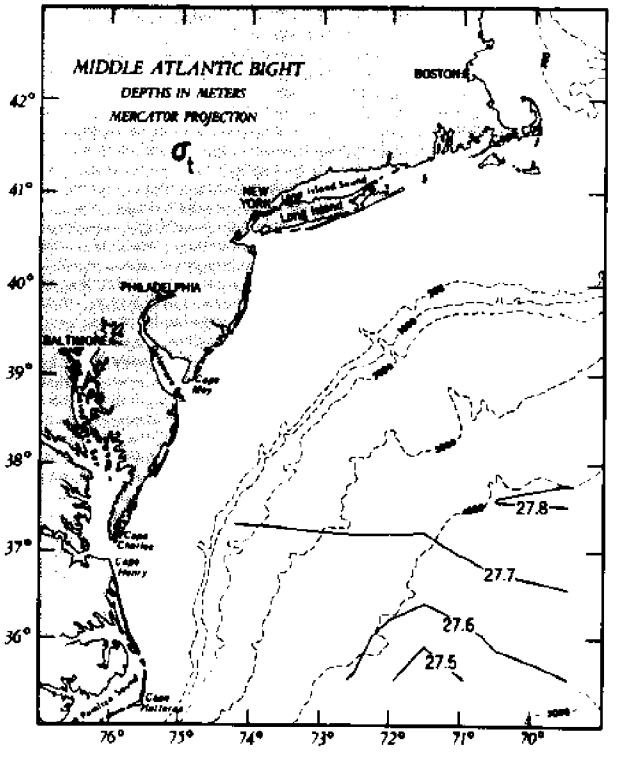

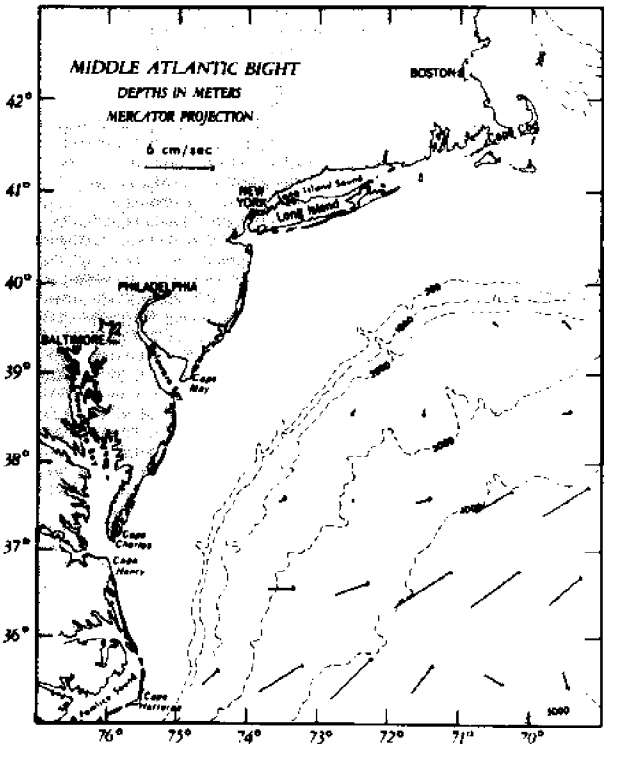

1000m Distribution, April

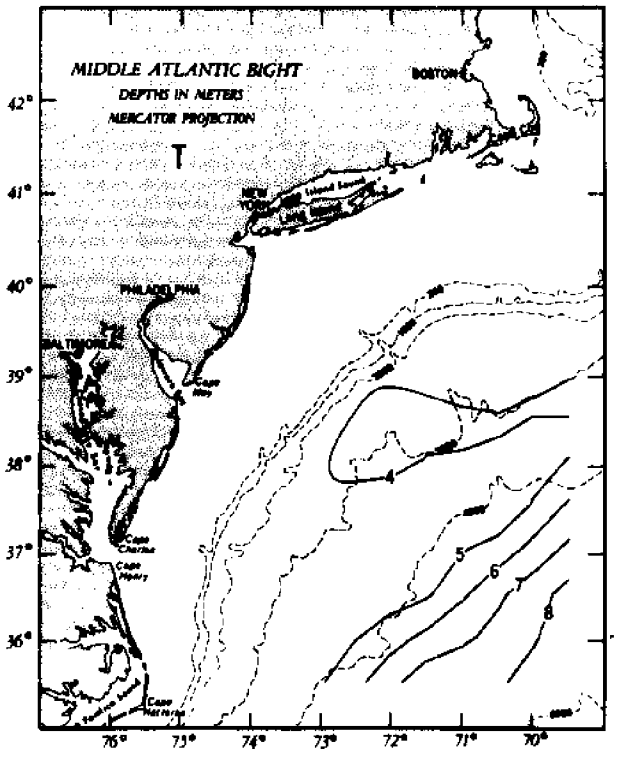

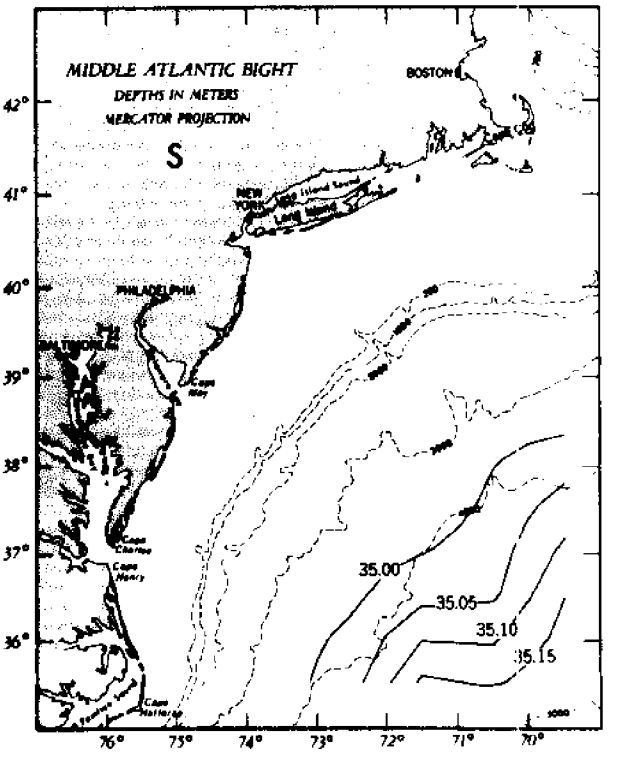

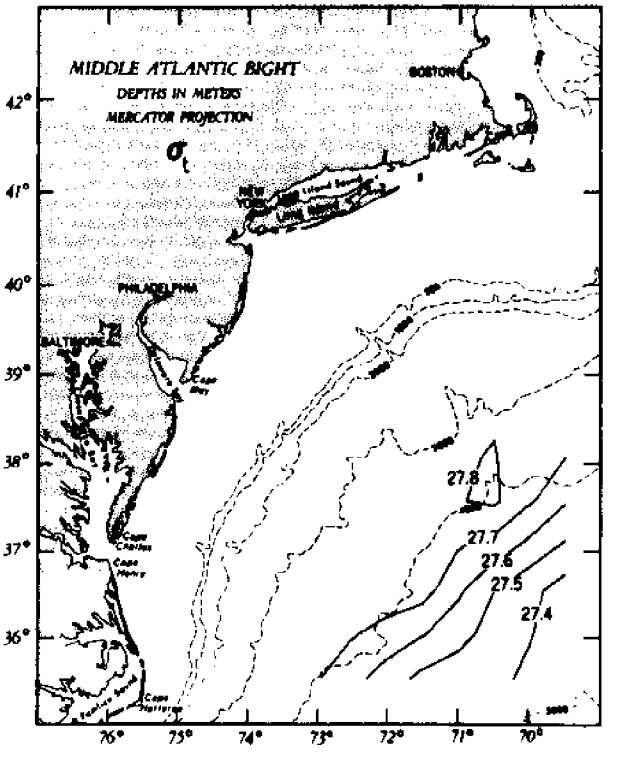

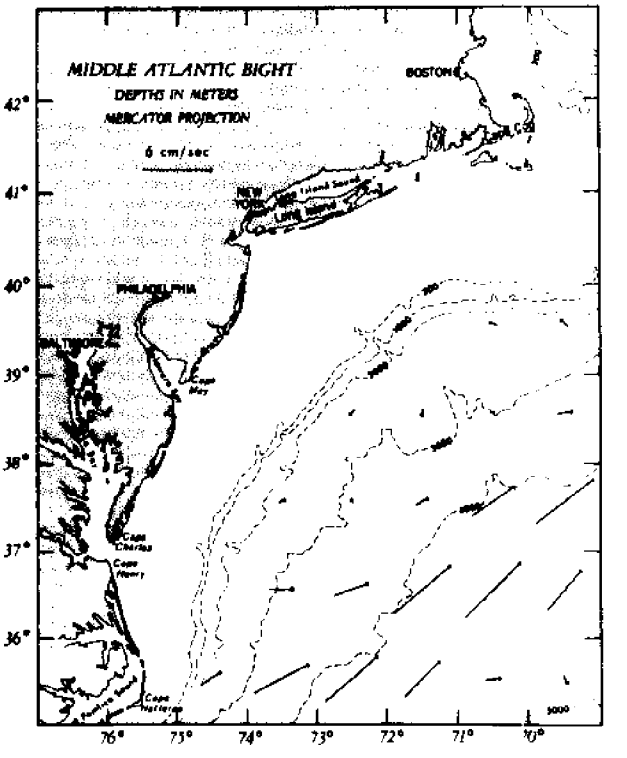

1000m Distribution, May

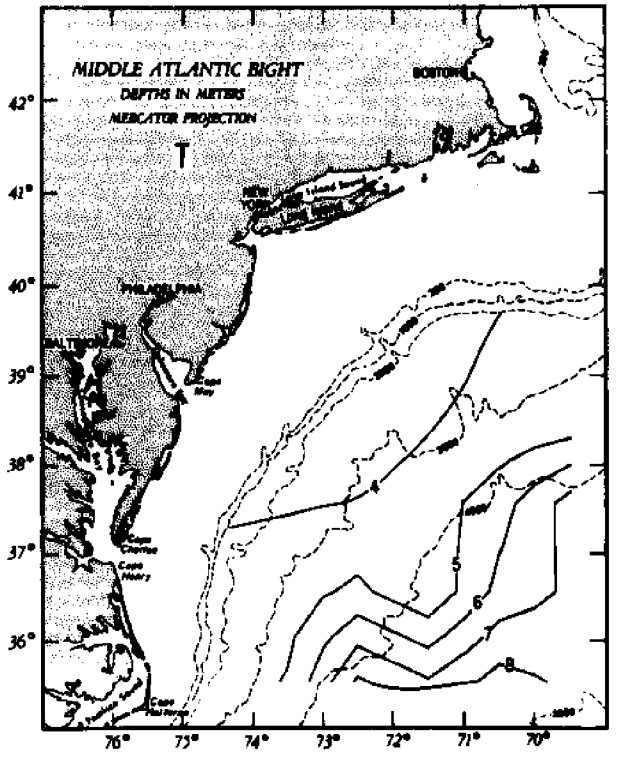

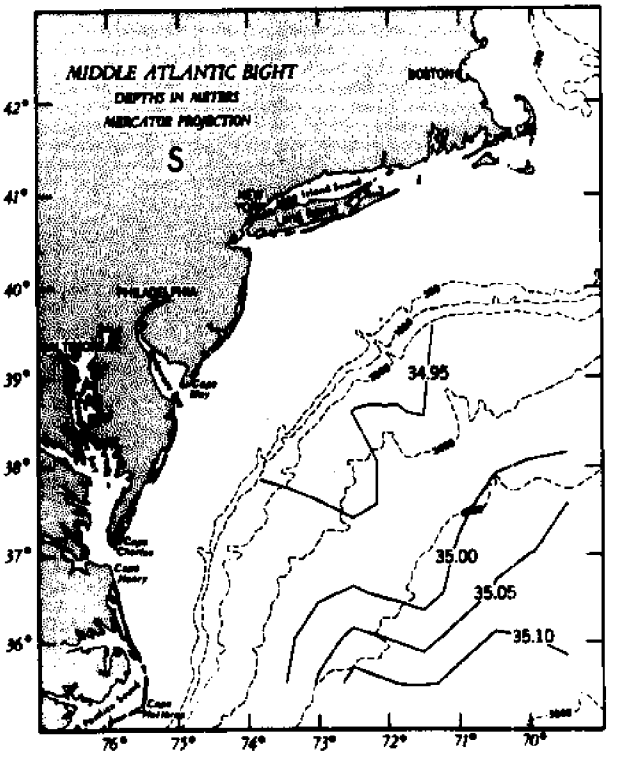

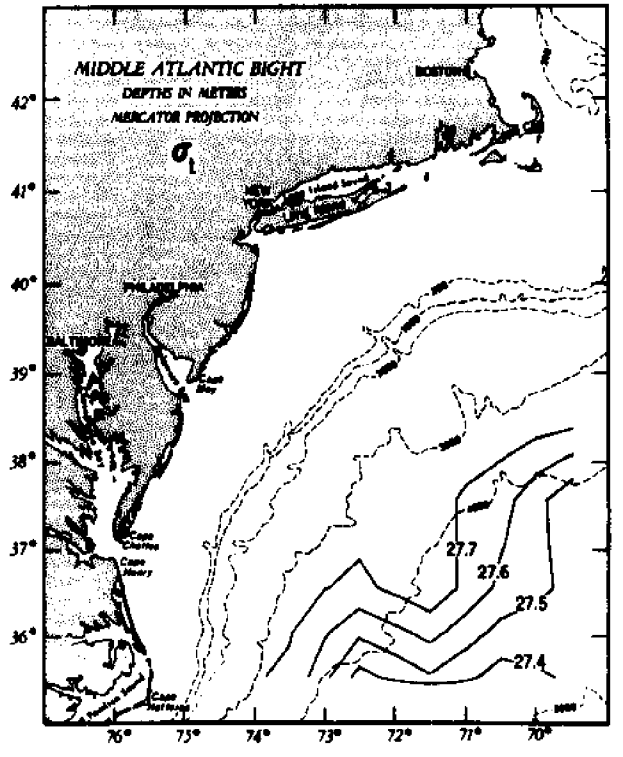

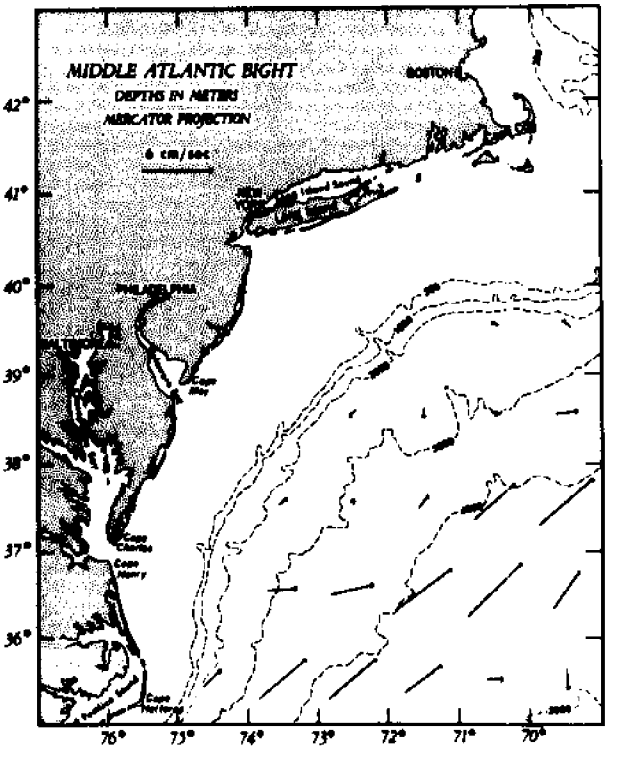

1000m Distribution, June

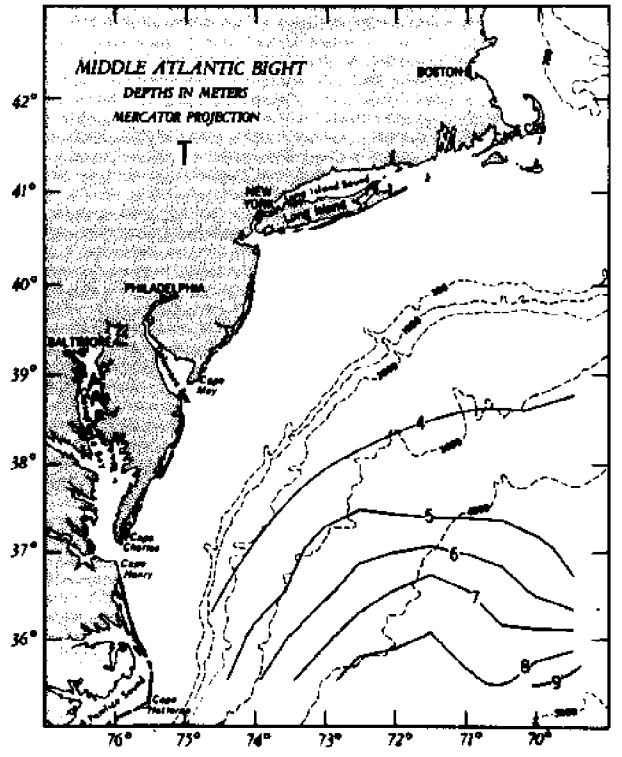

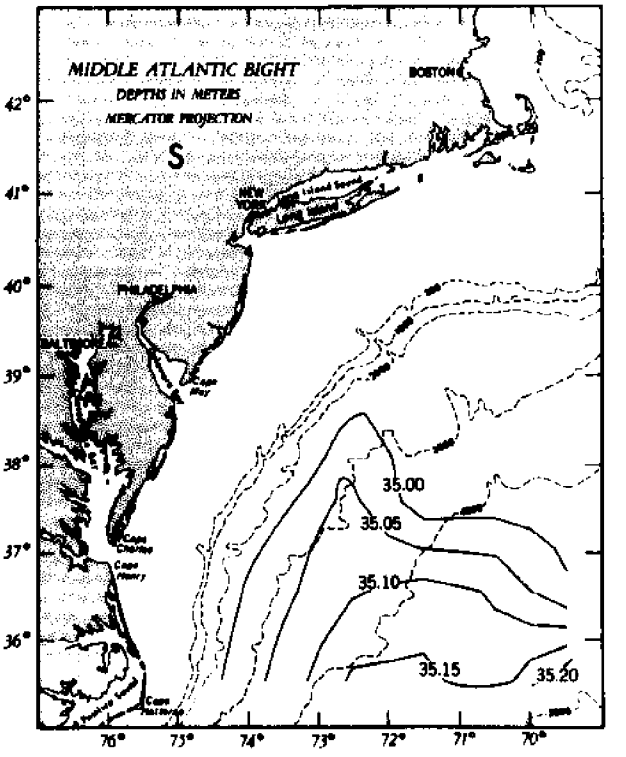

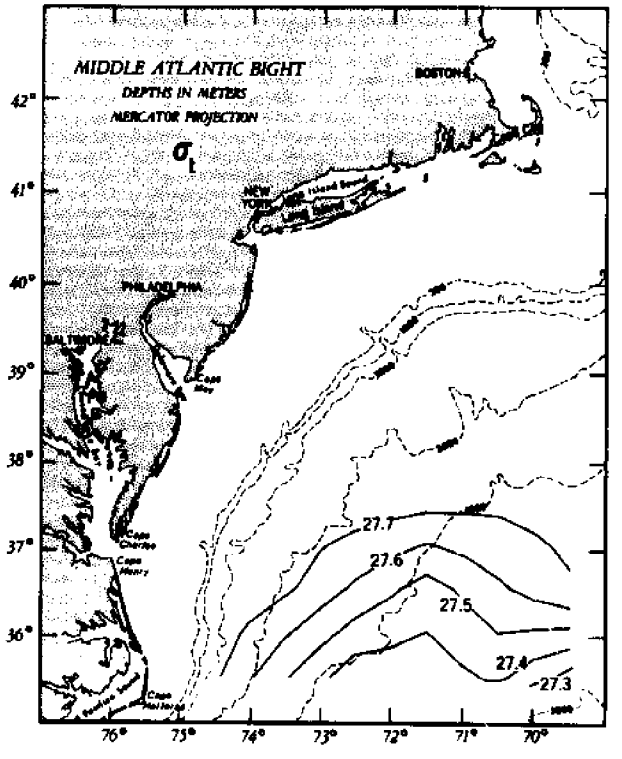

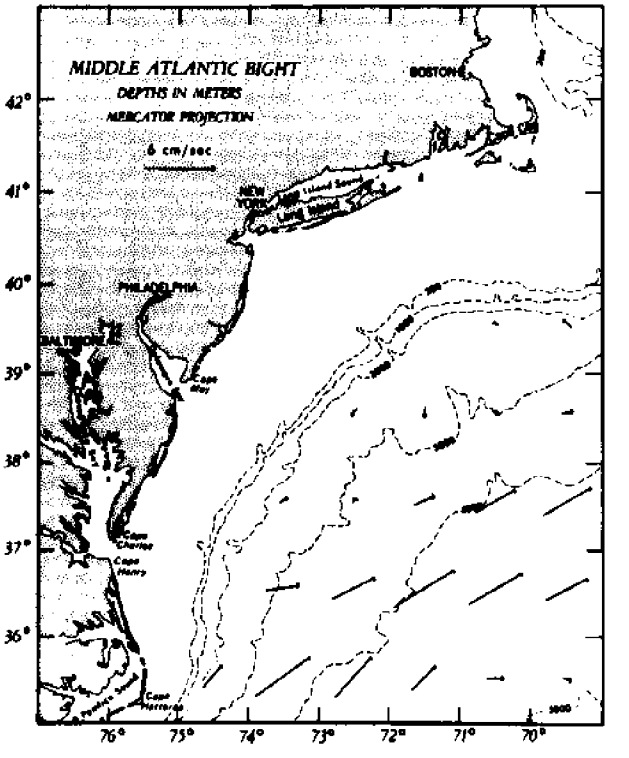

1000m Distribution, July

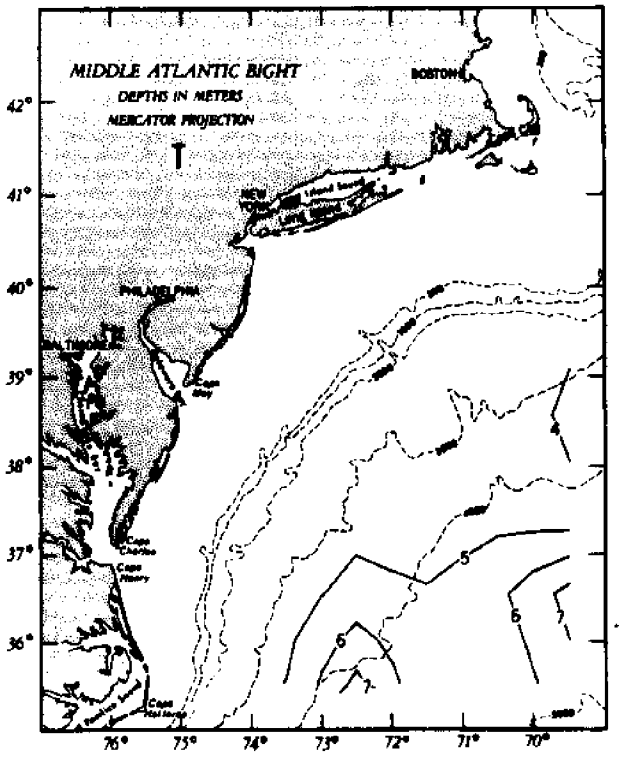

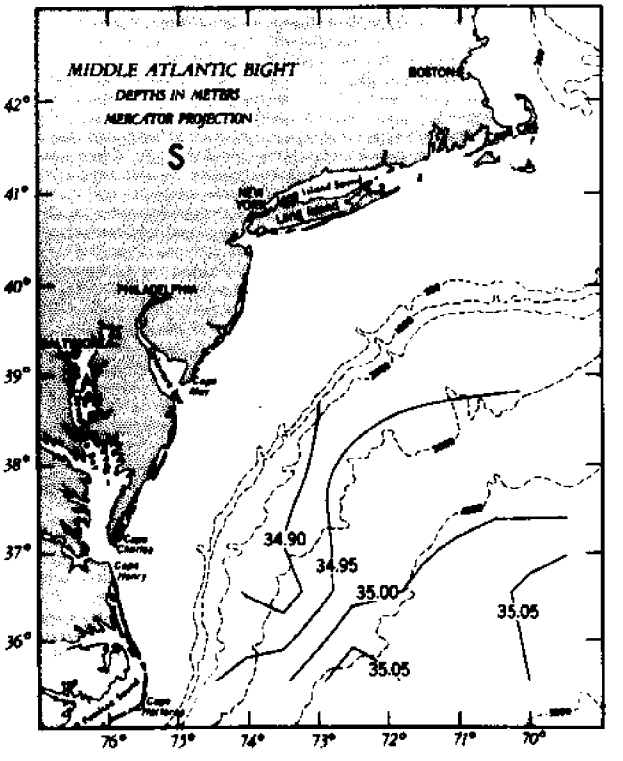

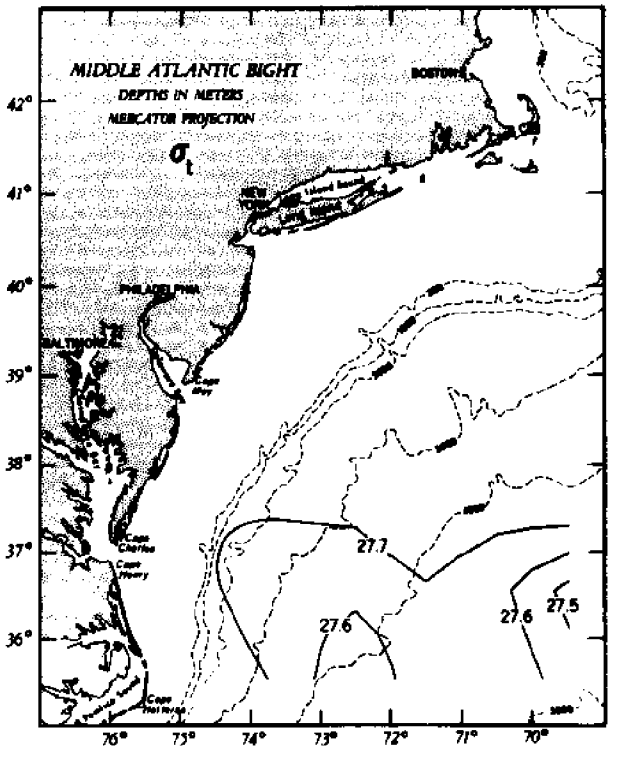

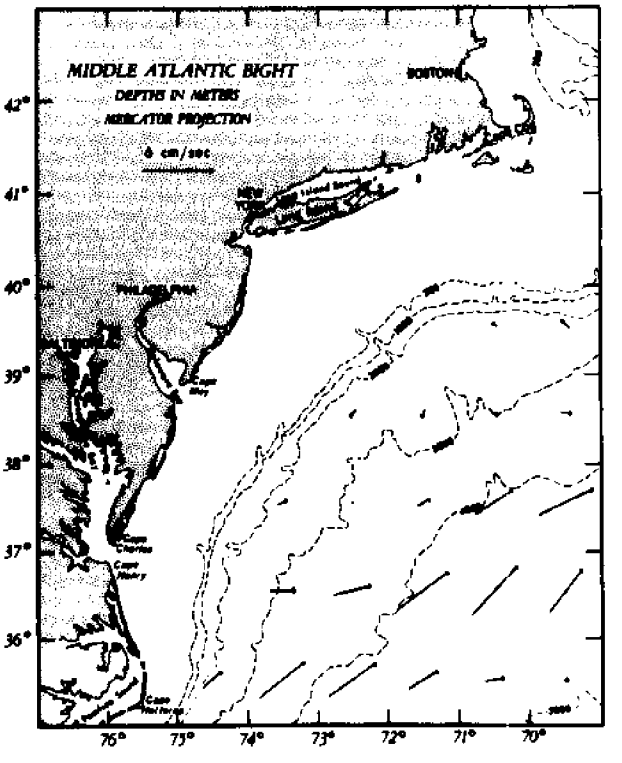

1000m Distribution, August

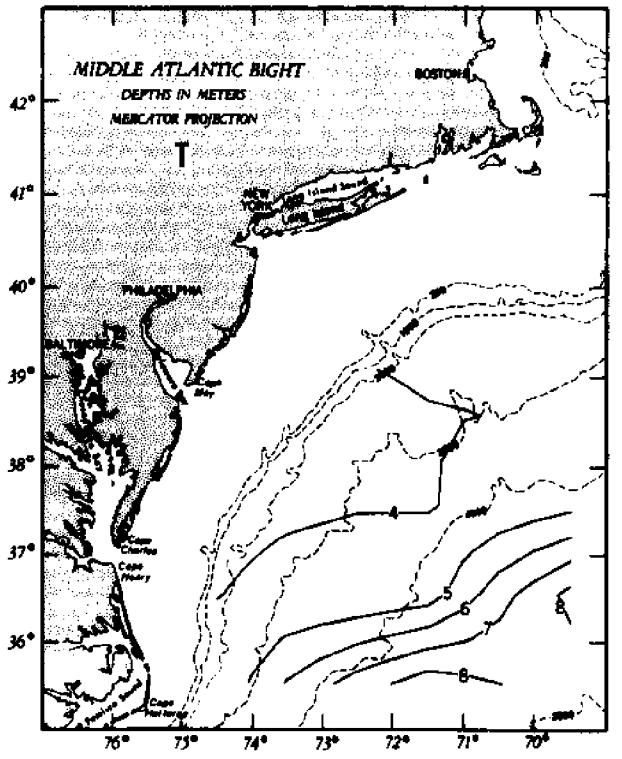

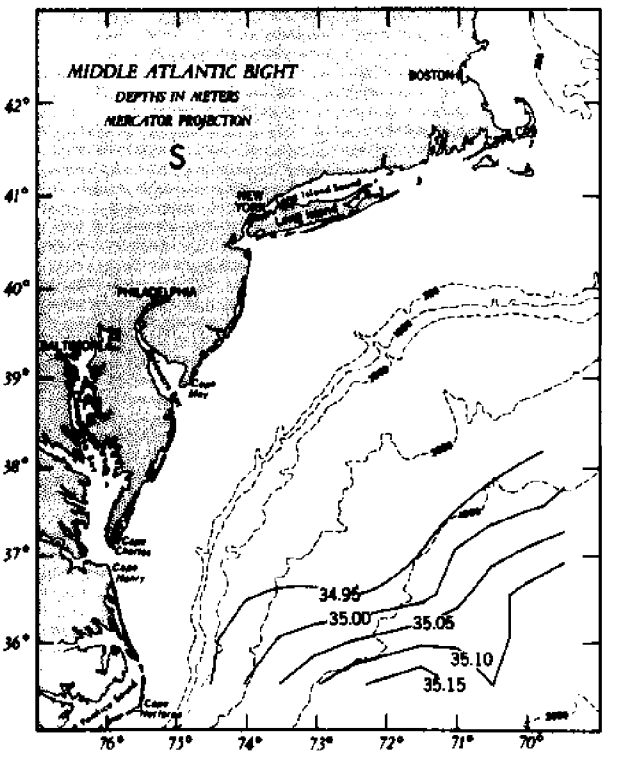

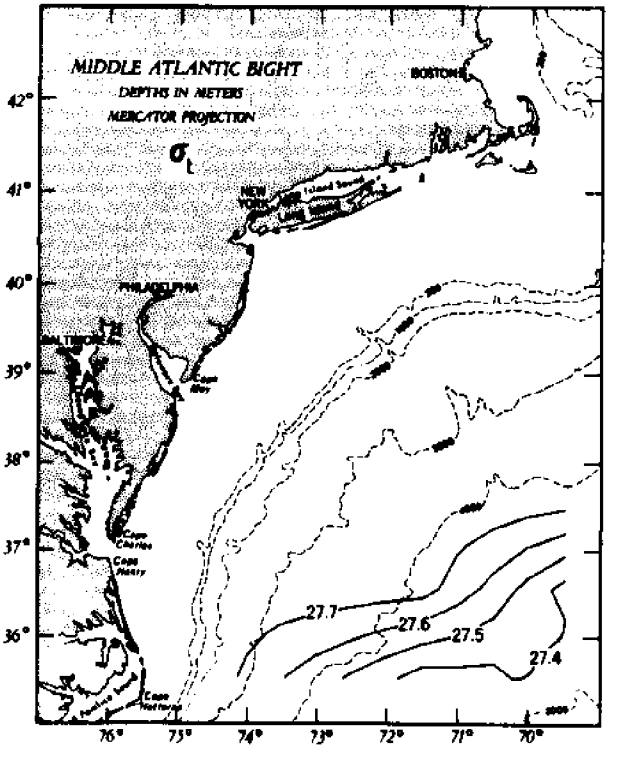

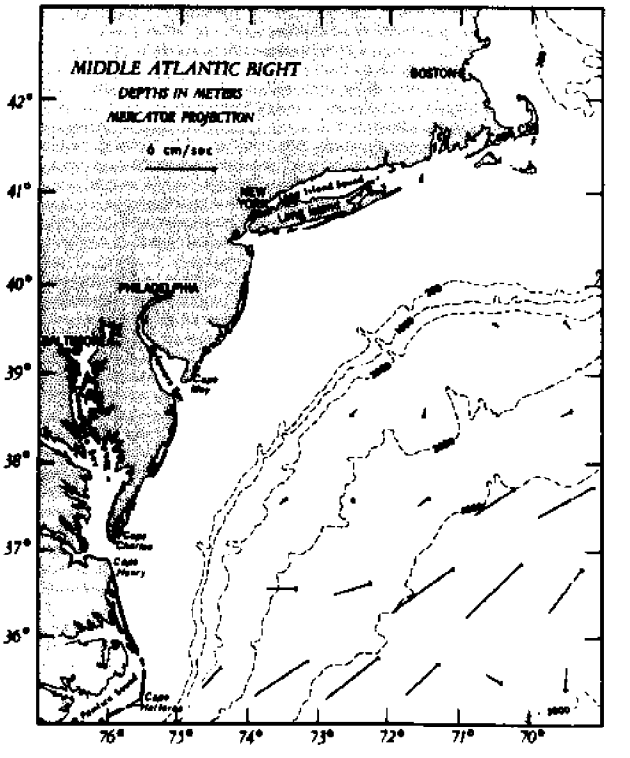

1000m Distribution, September

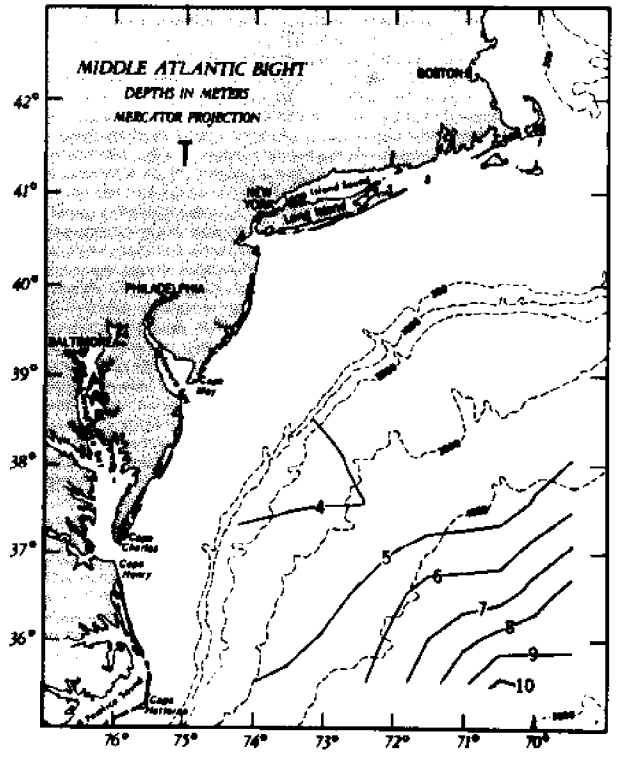

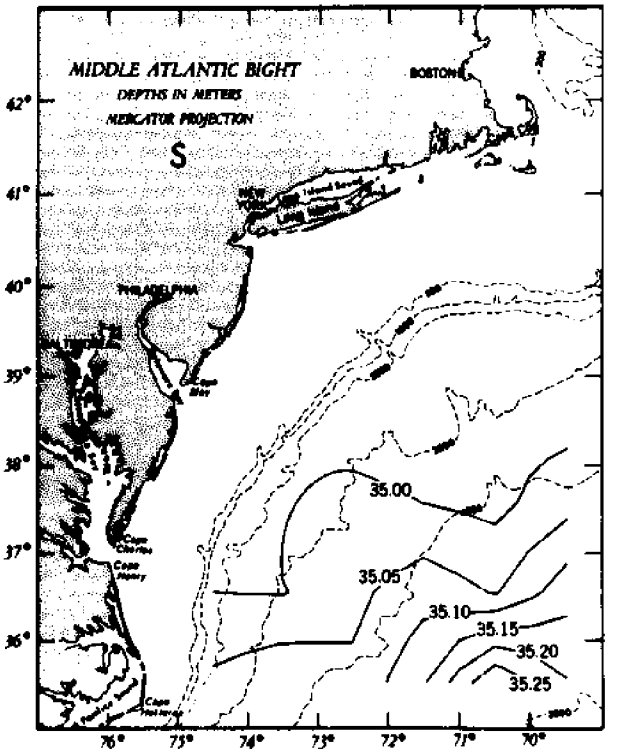

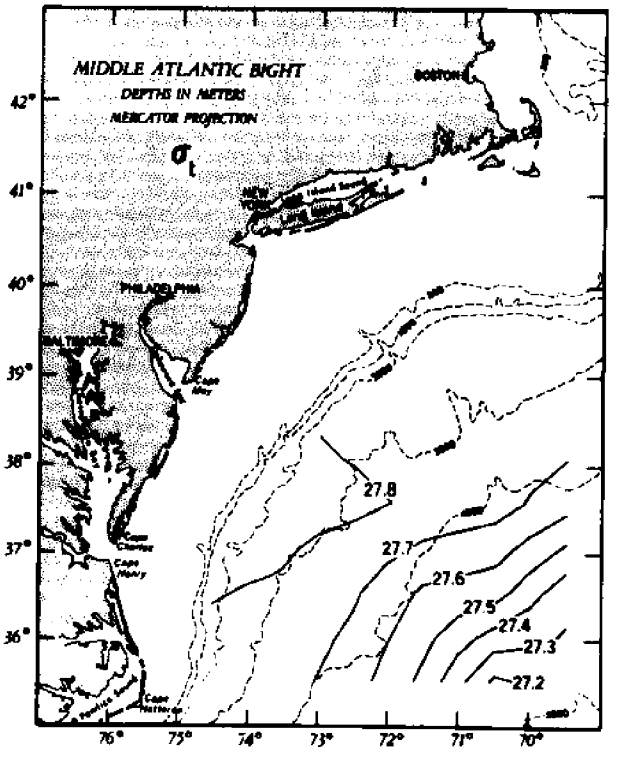

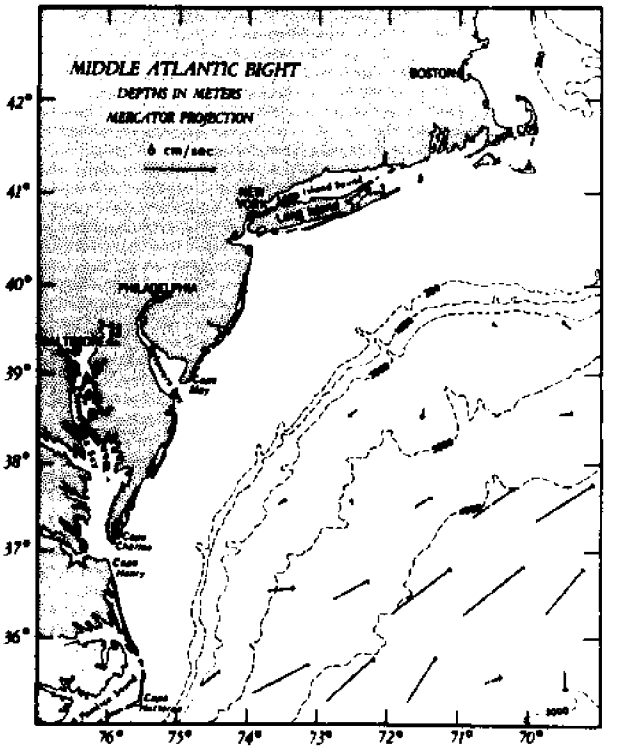

1000m Distribution, October

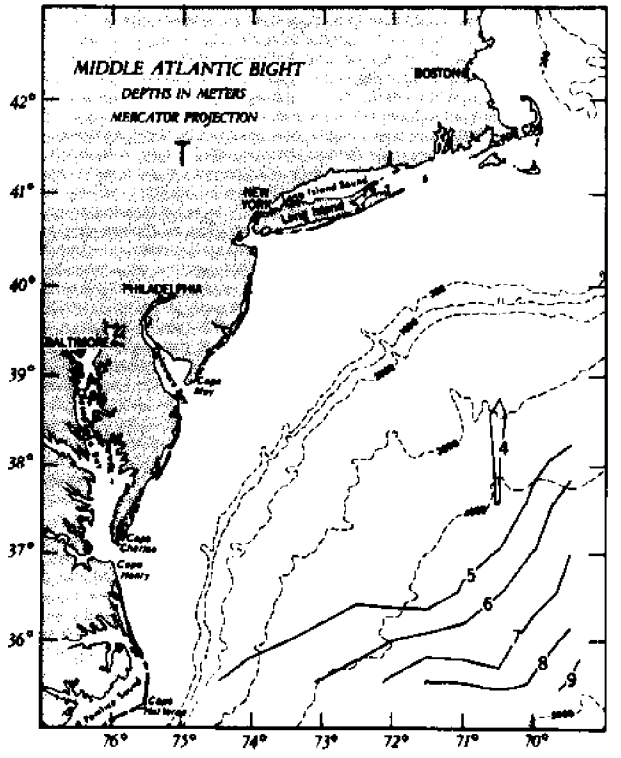

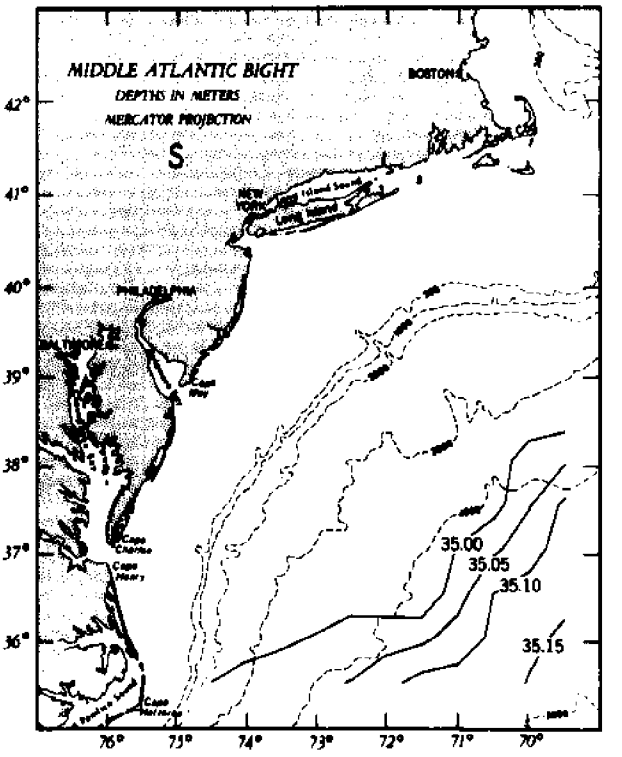

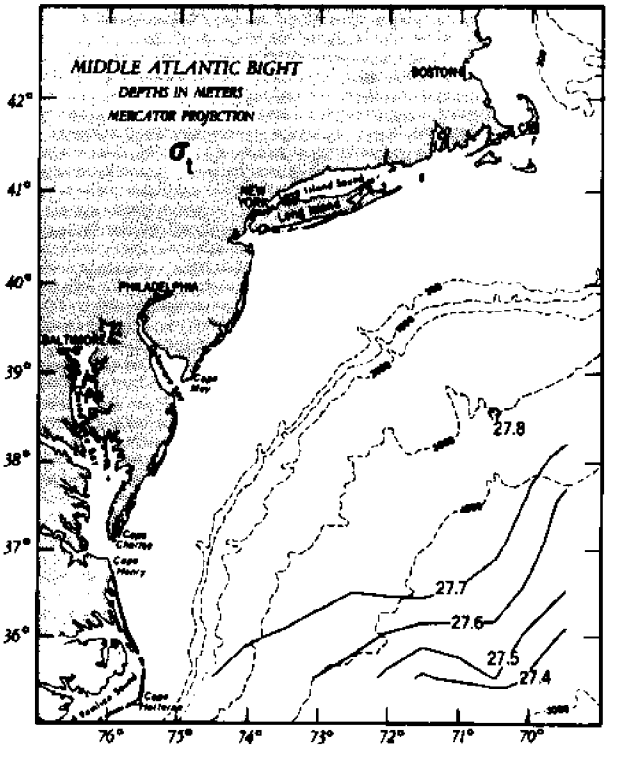

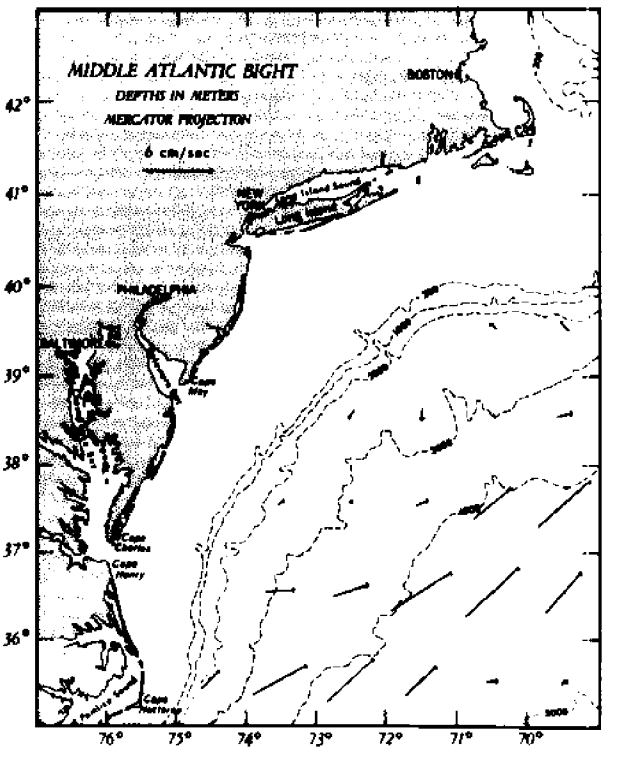

1000m Distribution, November

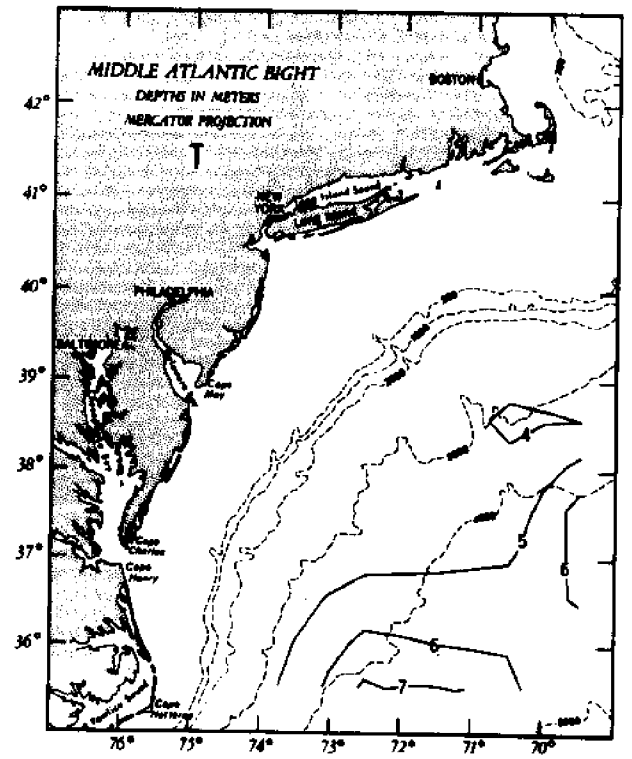

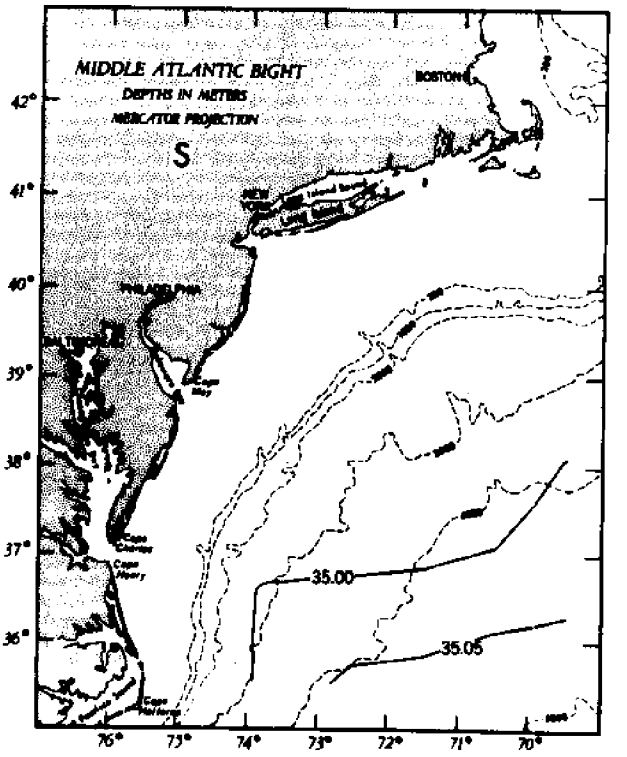

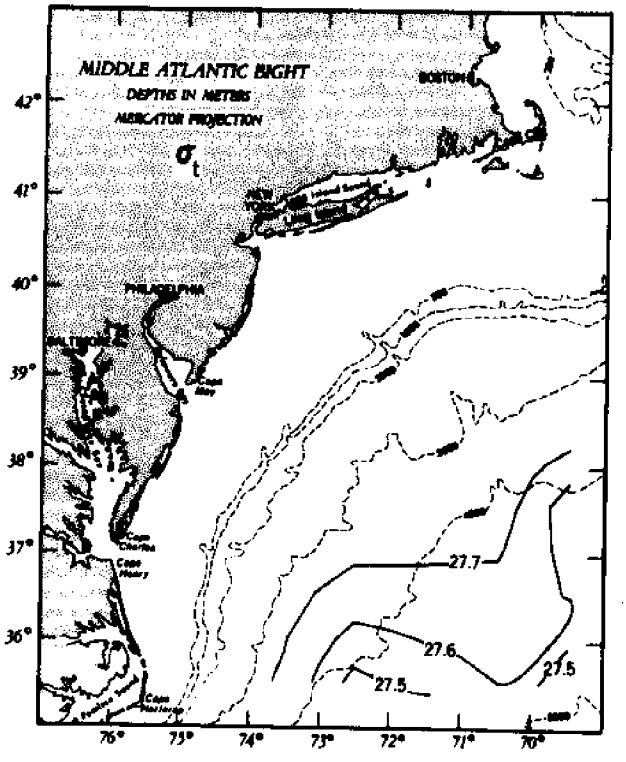

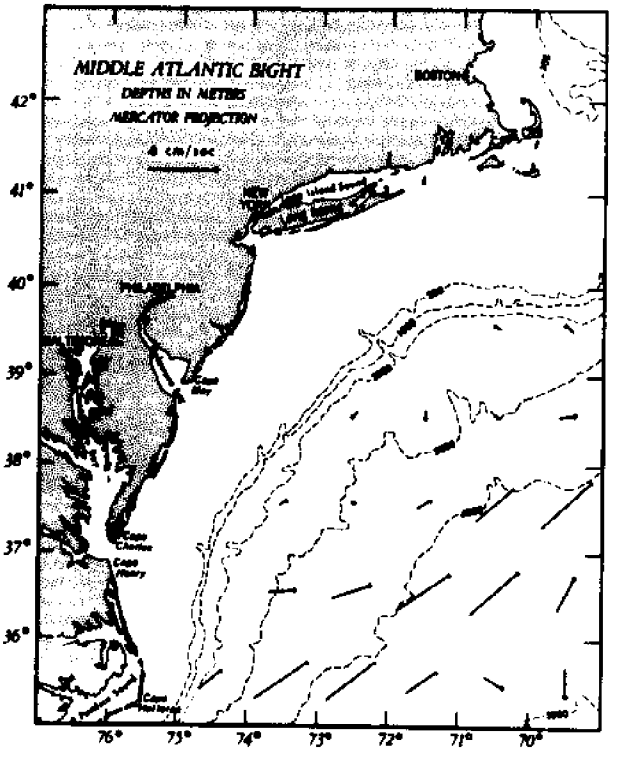

1000m Distribution, December

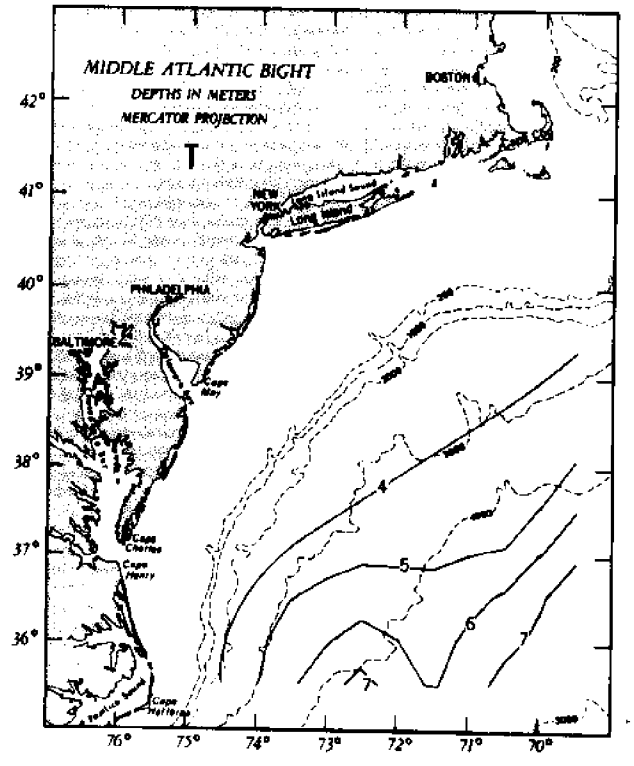

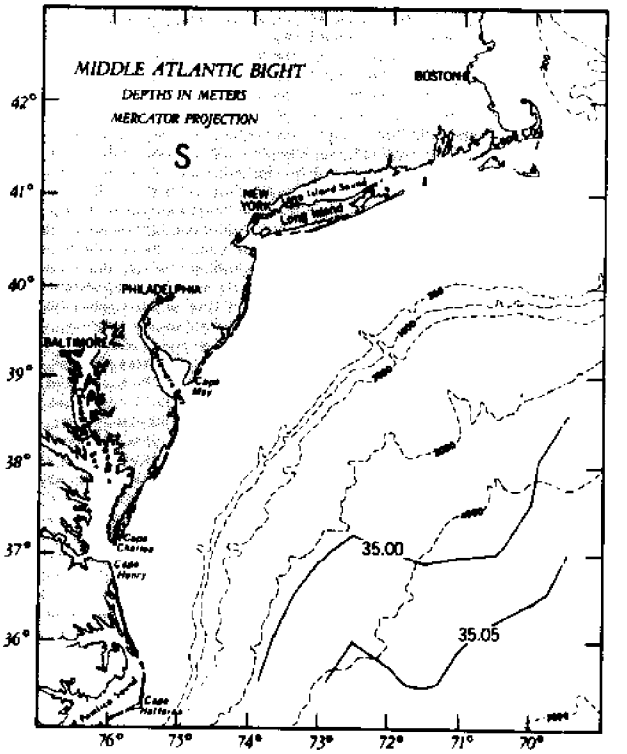

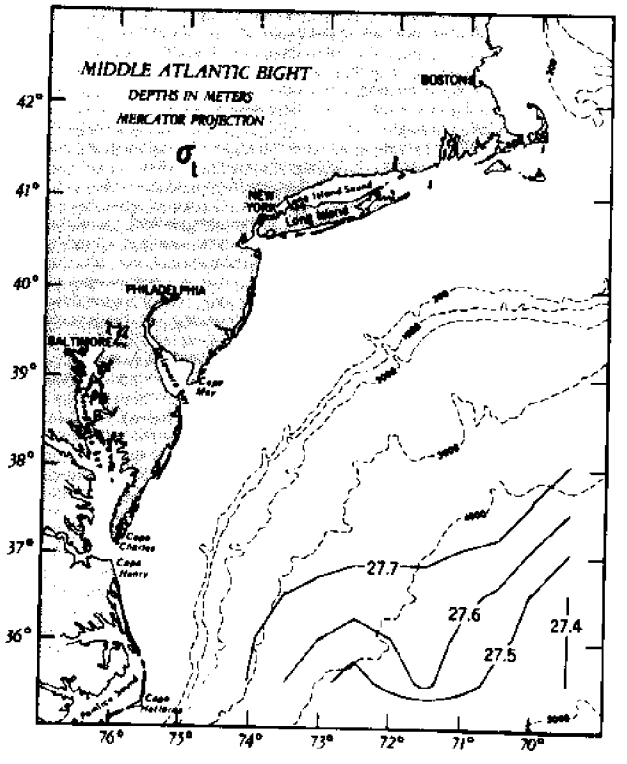

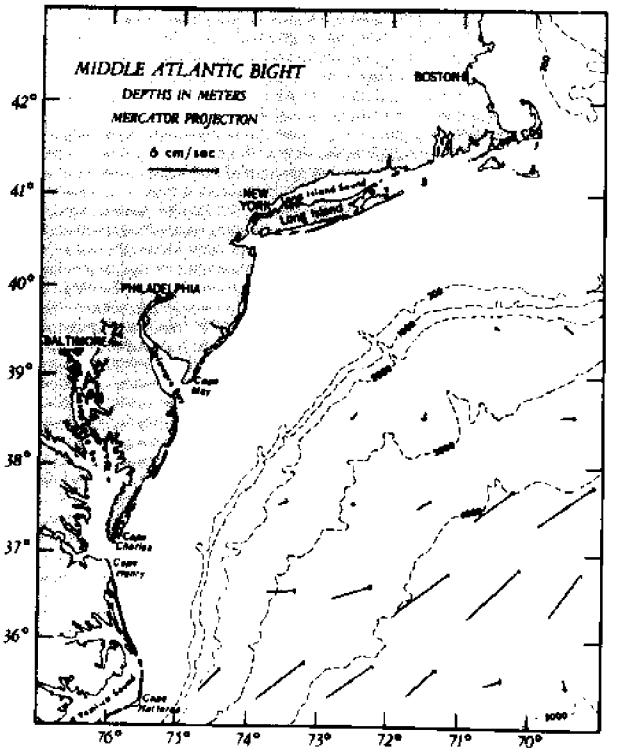

2000m Distribution, Annual

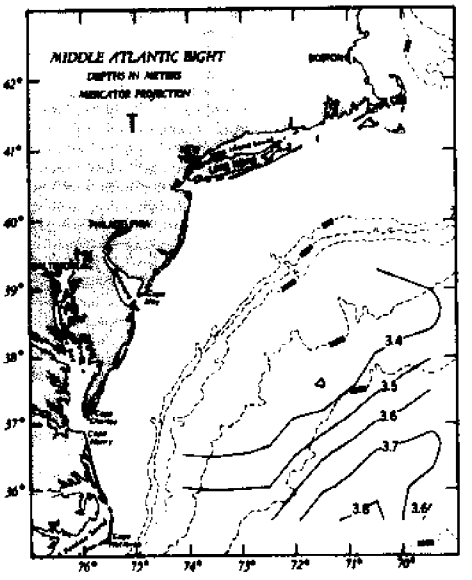

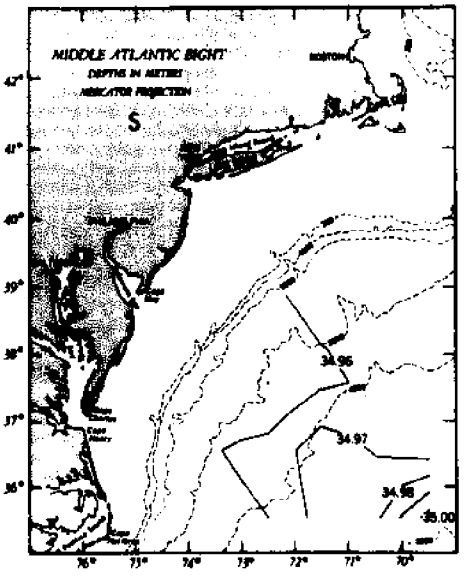

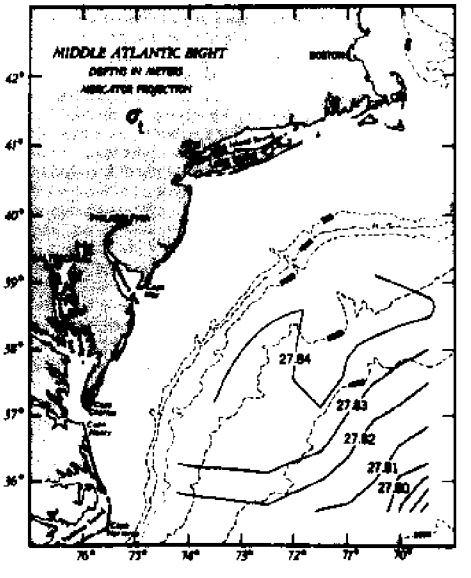

3000m Distribution, Annual

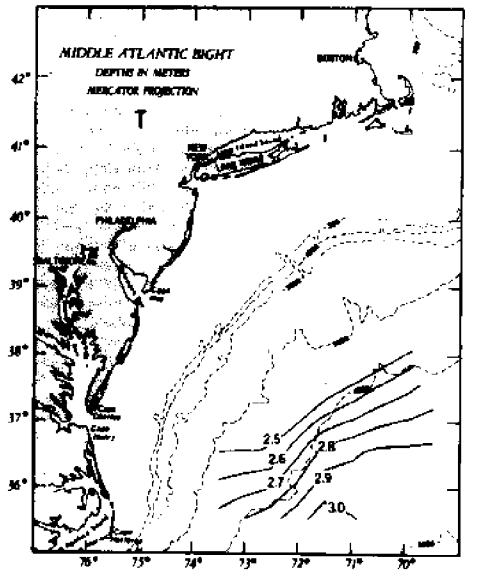

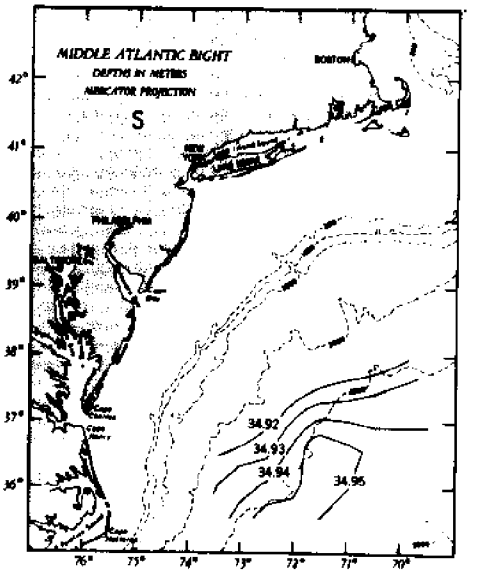

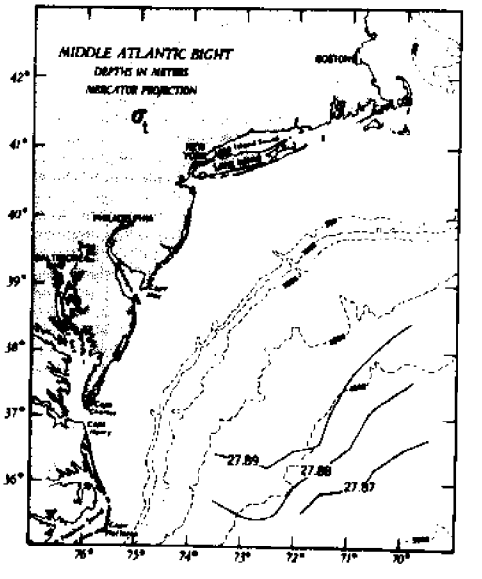

4000m Distribution, Annual

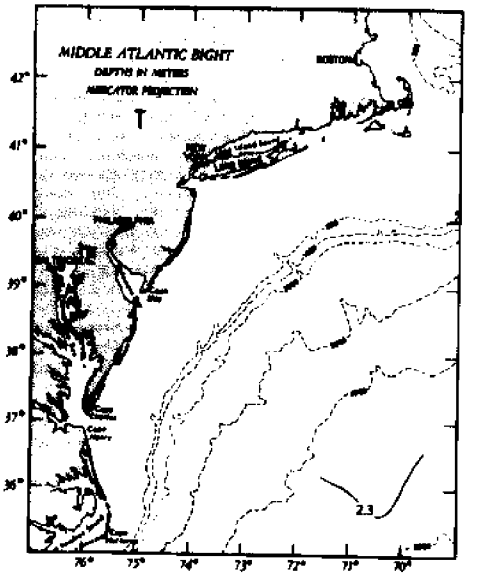

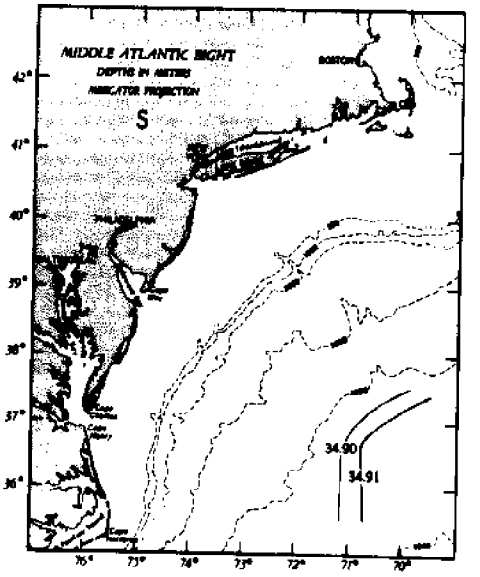

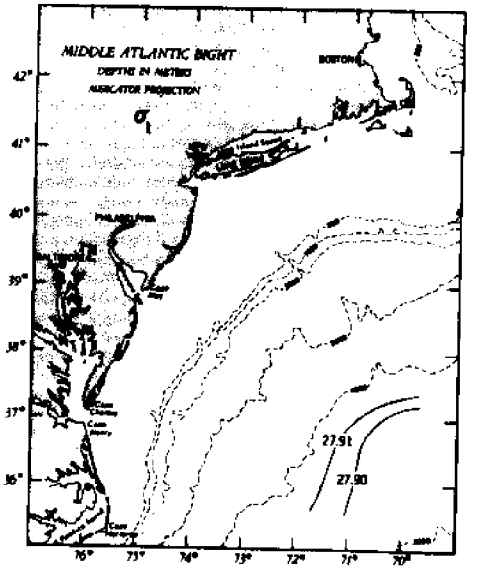

East—West Section along 35°30' N, January

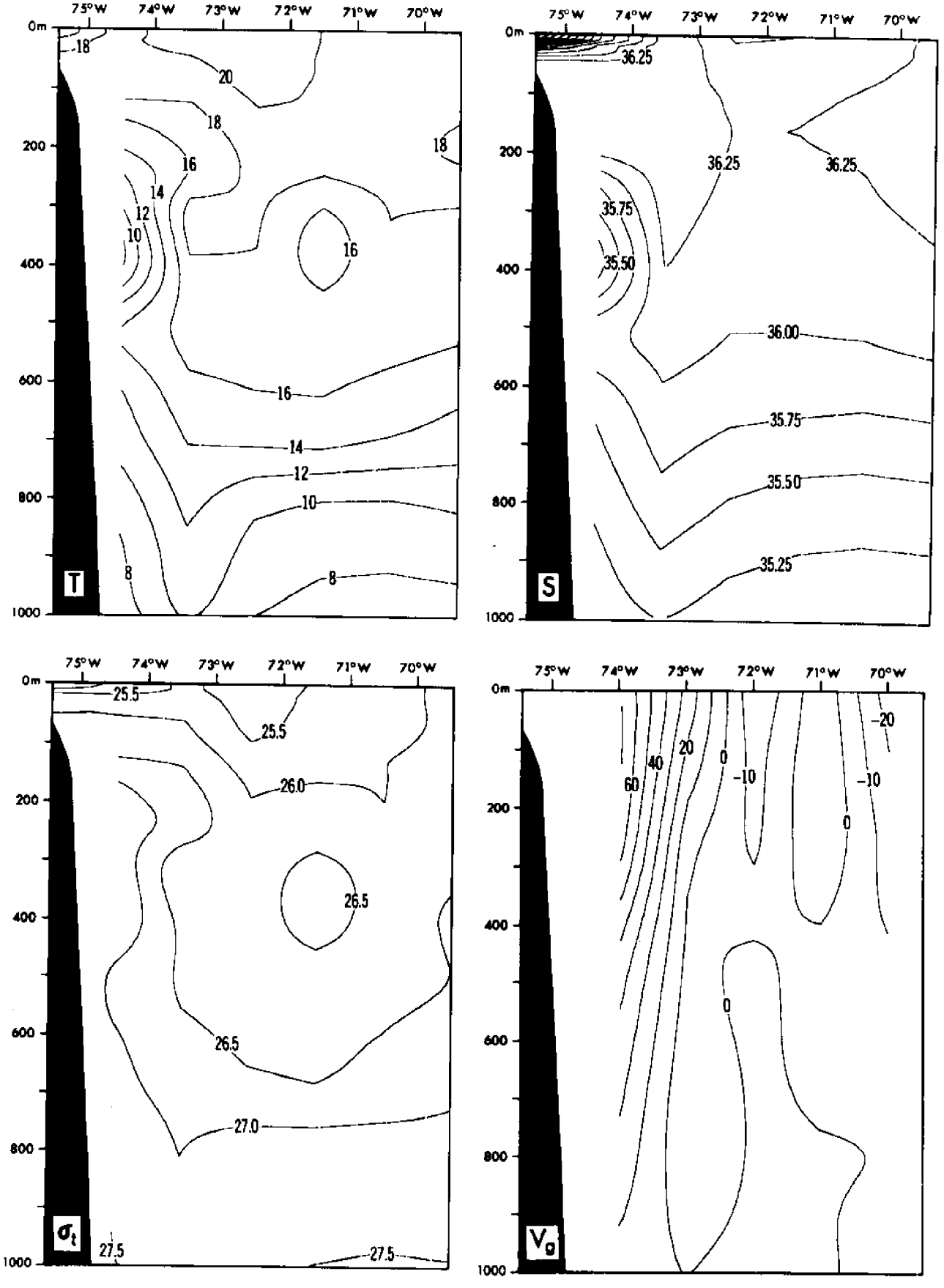

East—West Section along 35°30' N, February

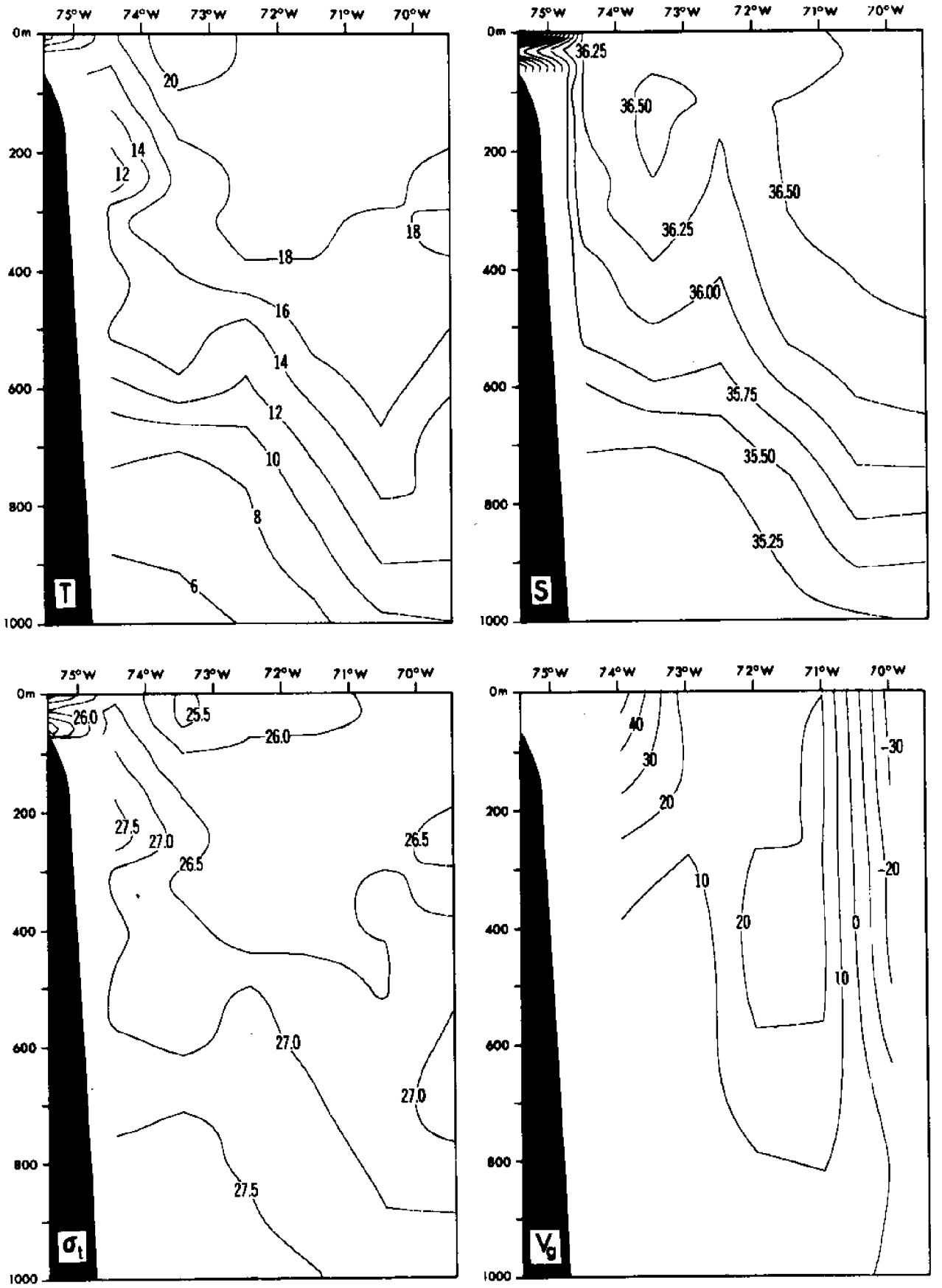

East—West section along 35°30' N, March

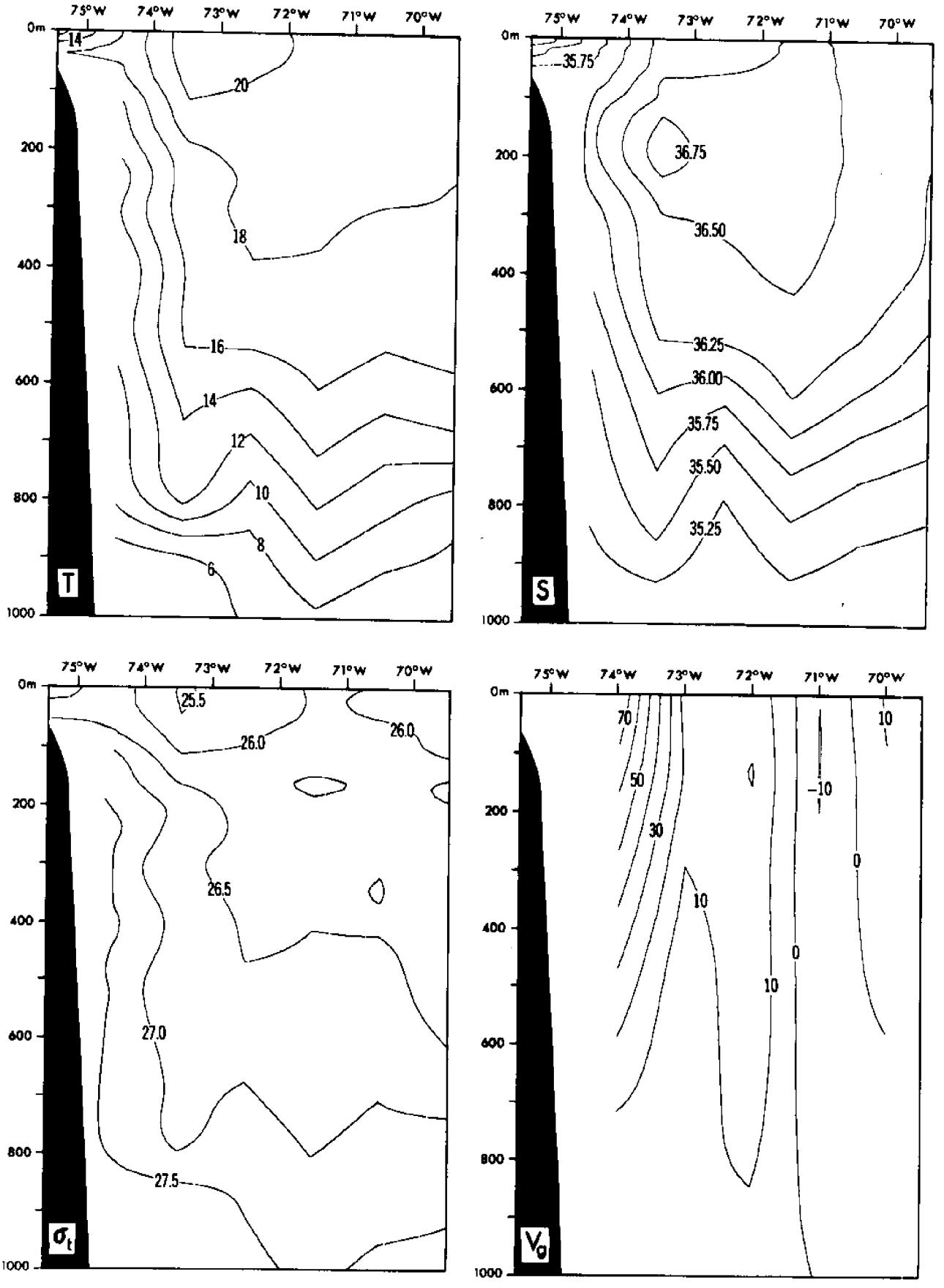

East—West Section along 35°30'N, April

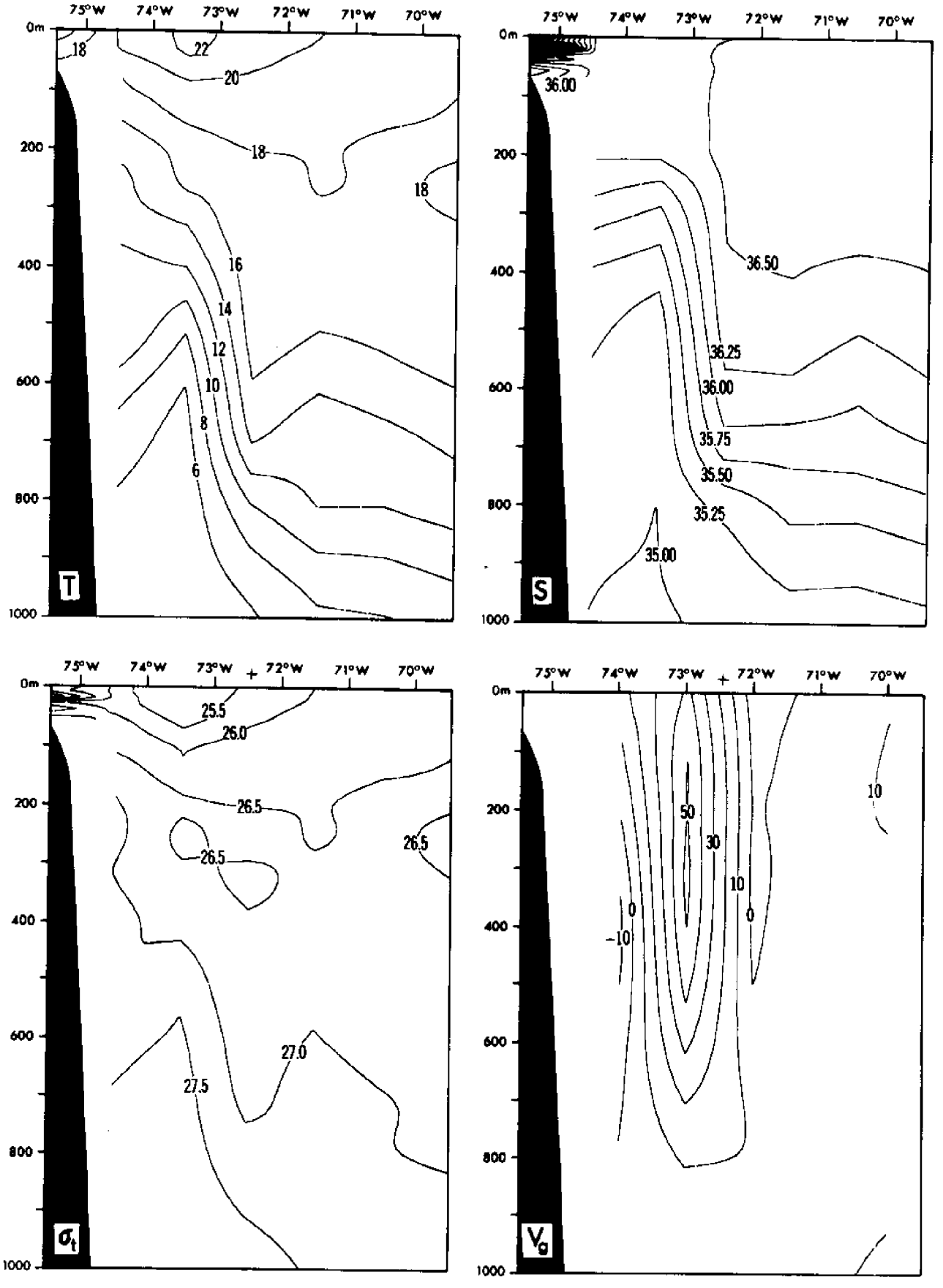

East—West Section along 35°30'N, May

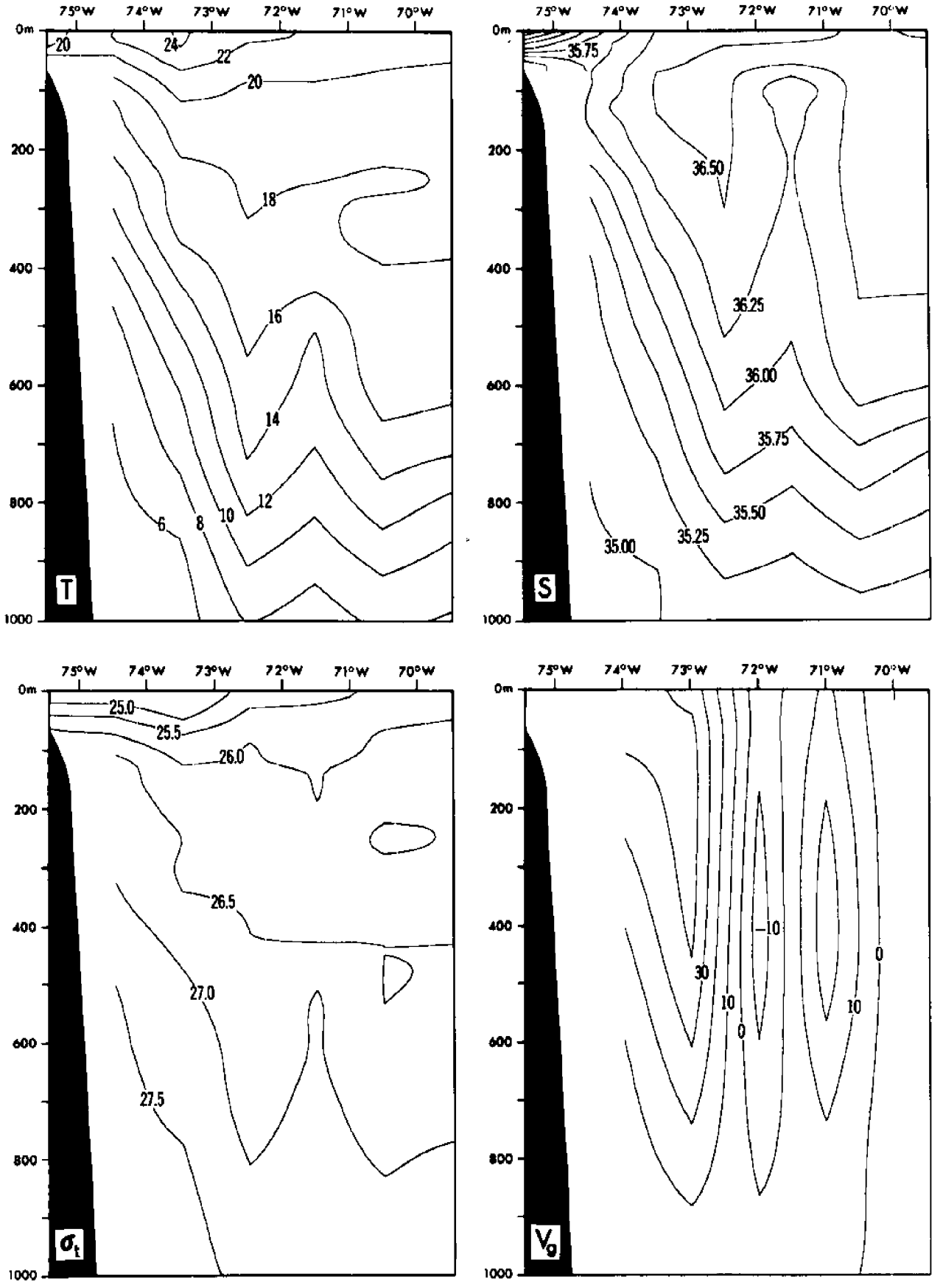

East—West Section along 35°30'N, June

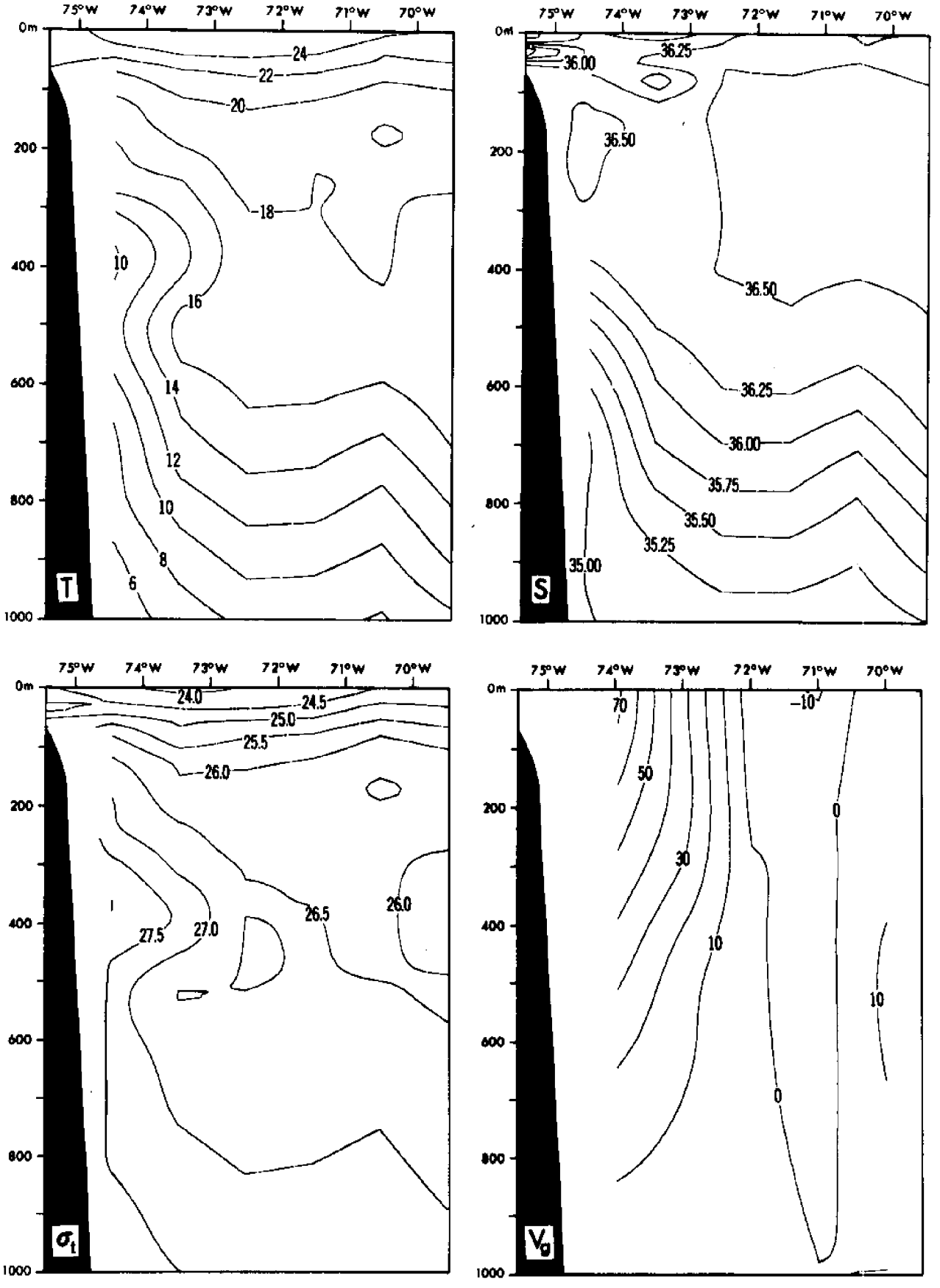

East—West Section along 35°30' N, July

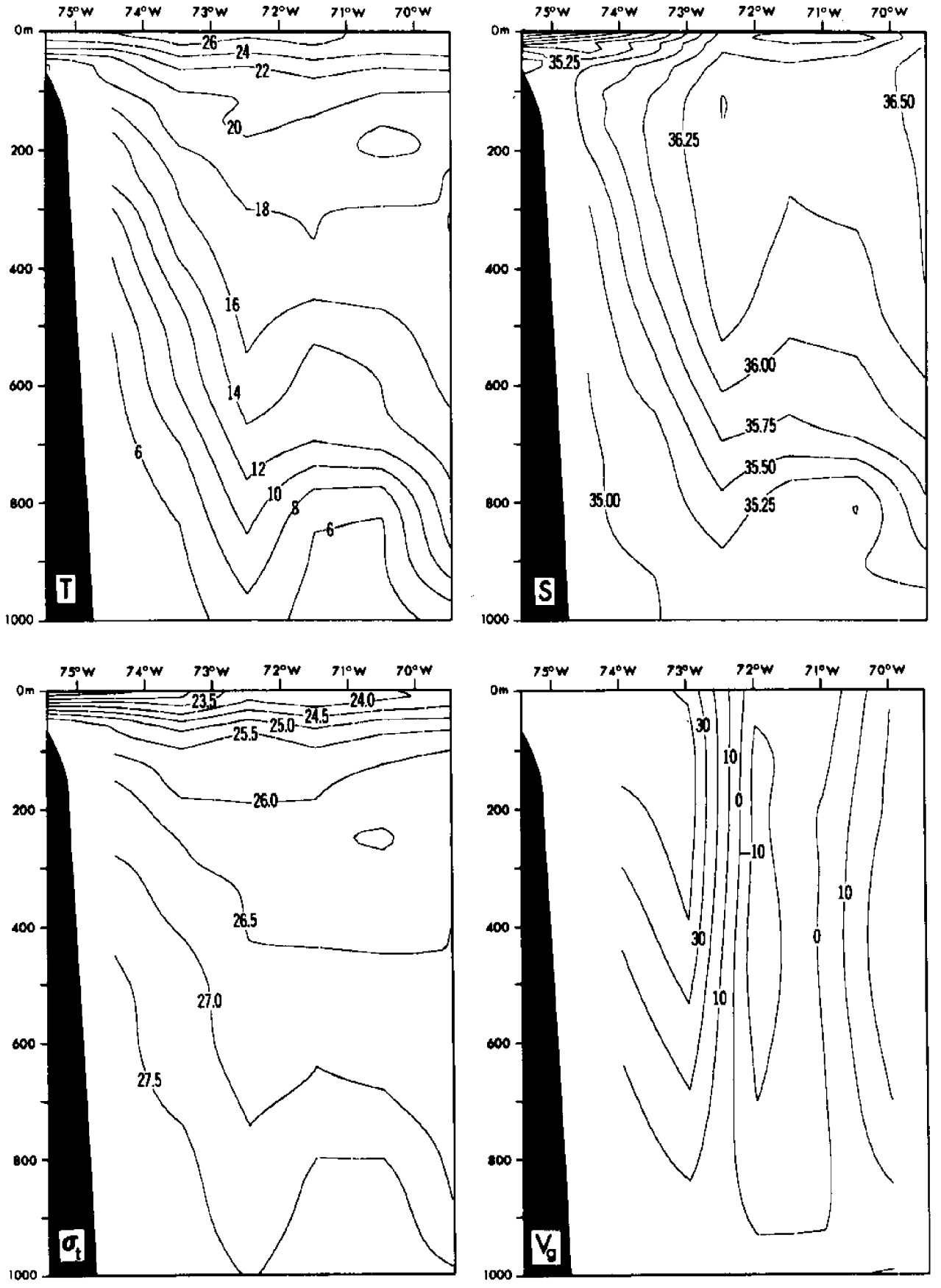

East—West Section along 35°30'N, August

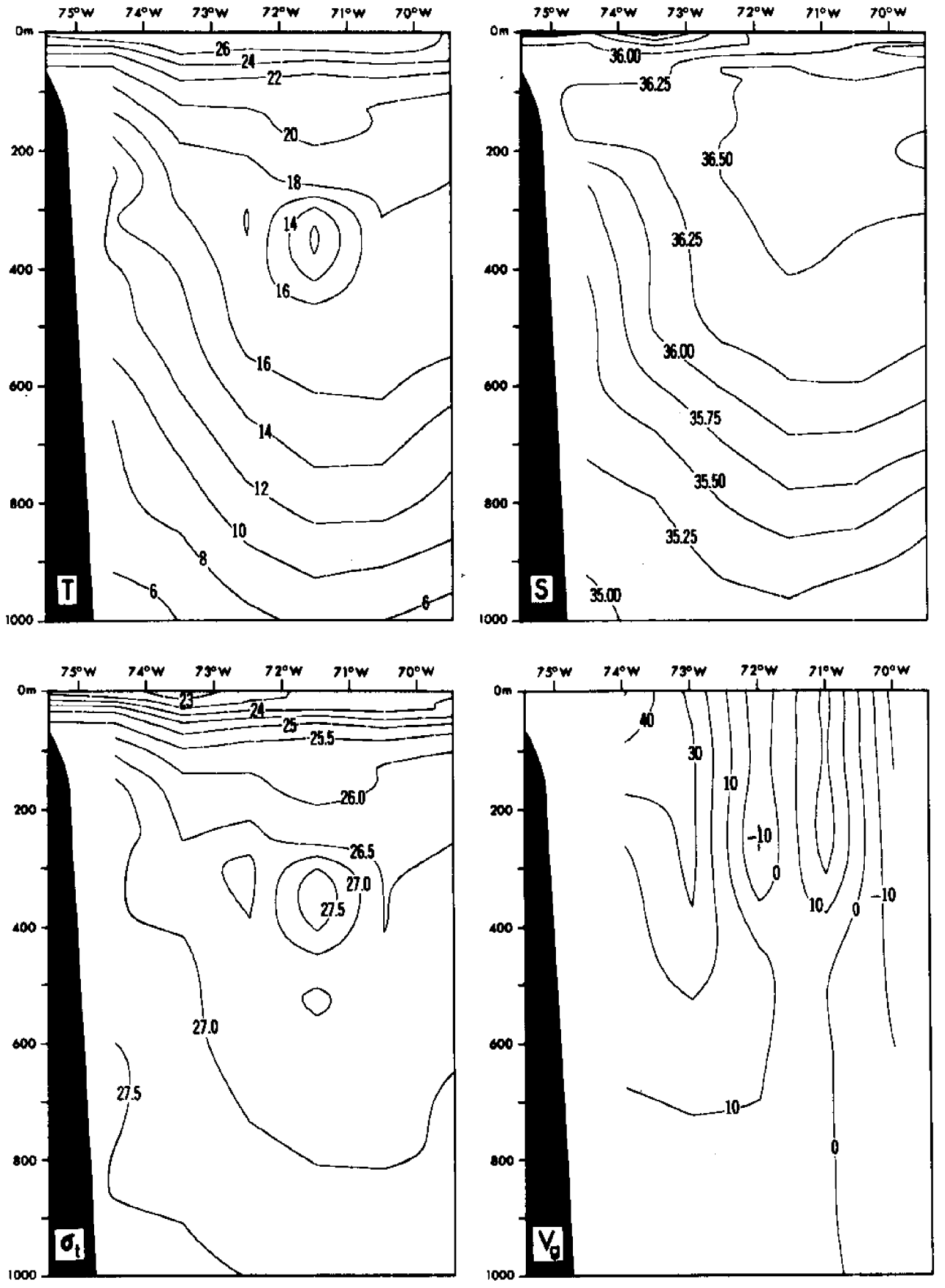

East—West Section along 35°30' N, September

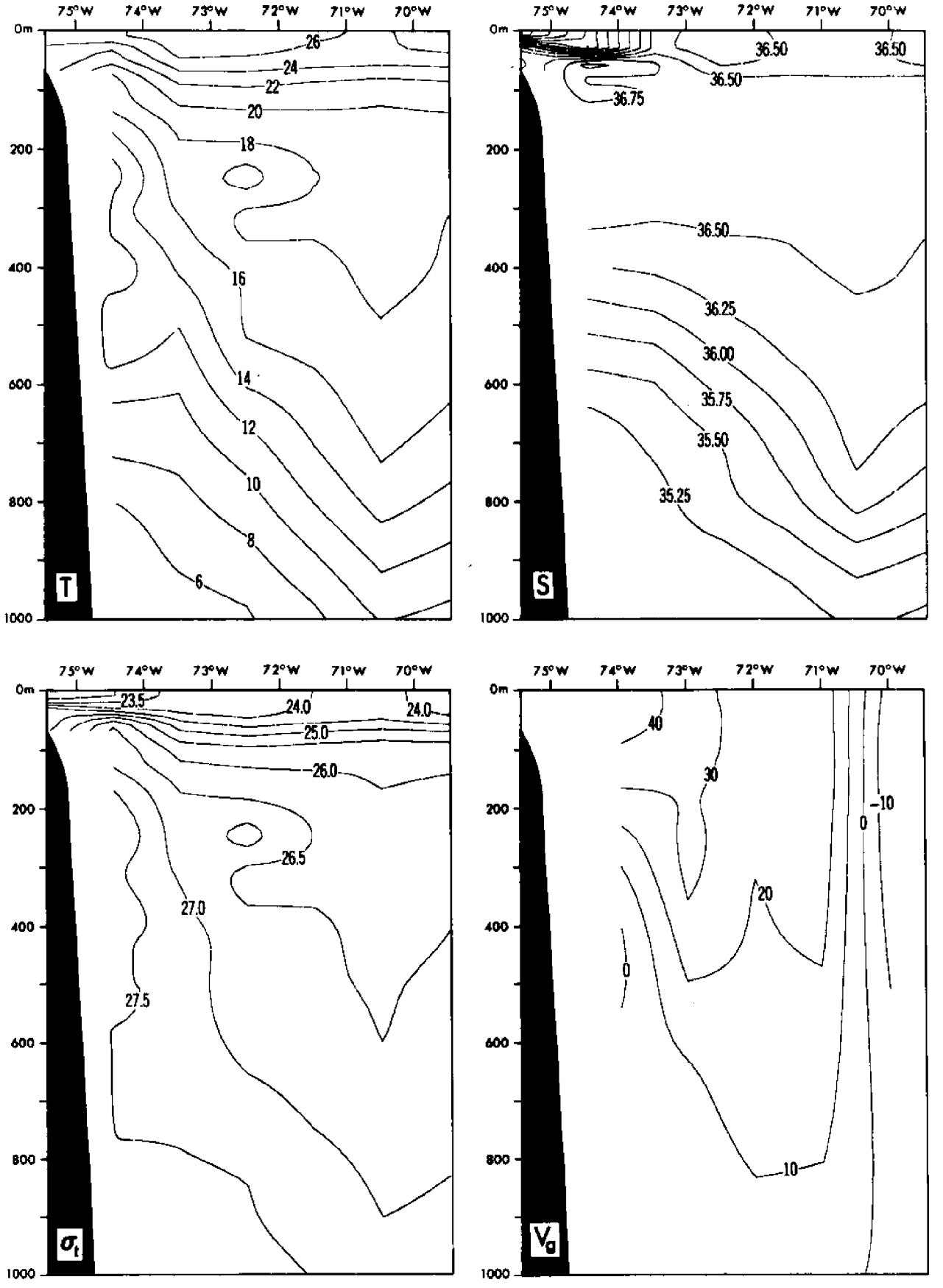

East—West Section along 35°30' N, October

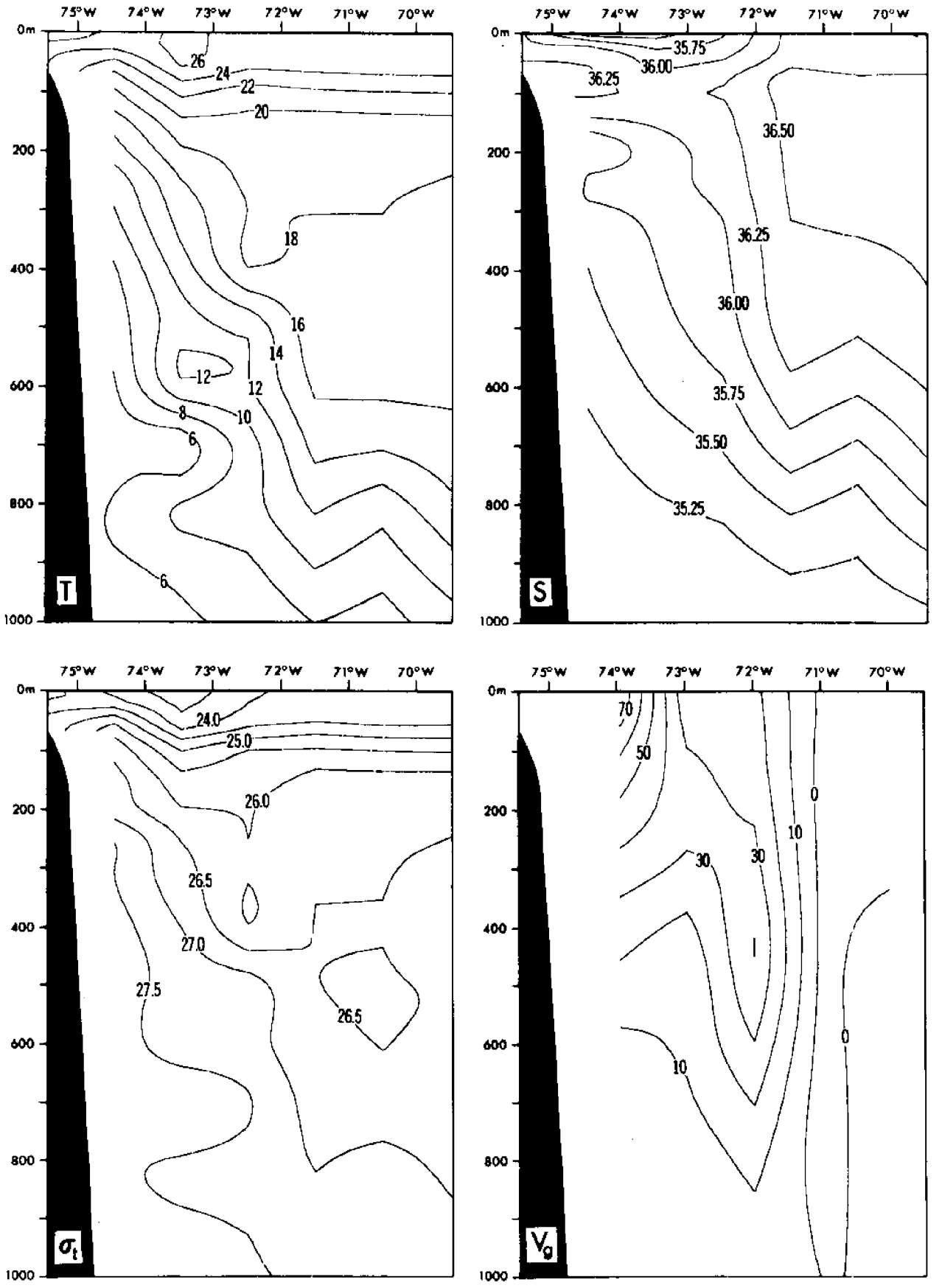

East—West Section along 35°30' N, November

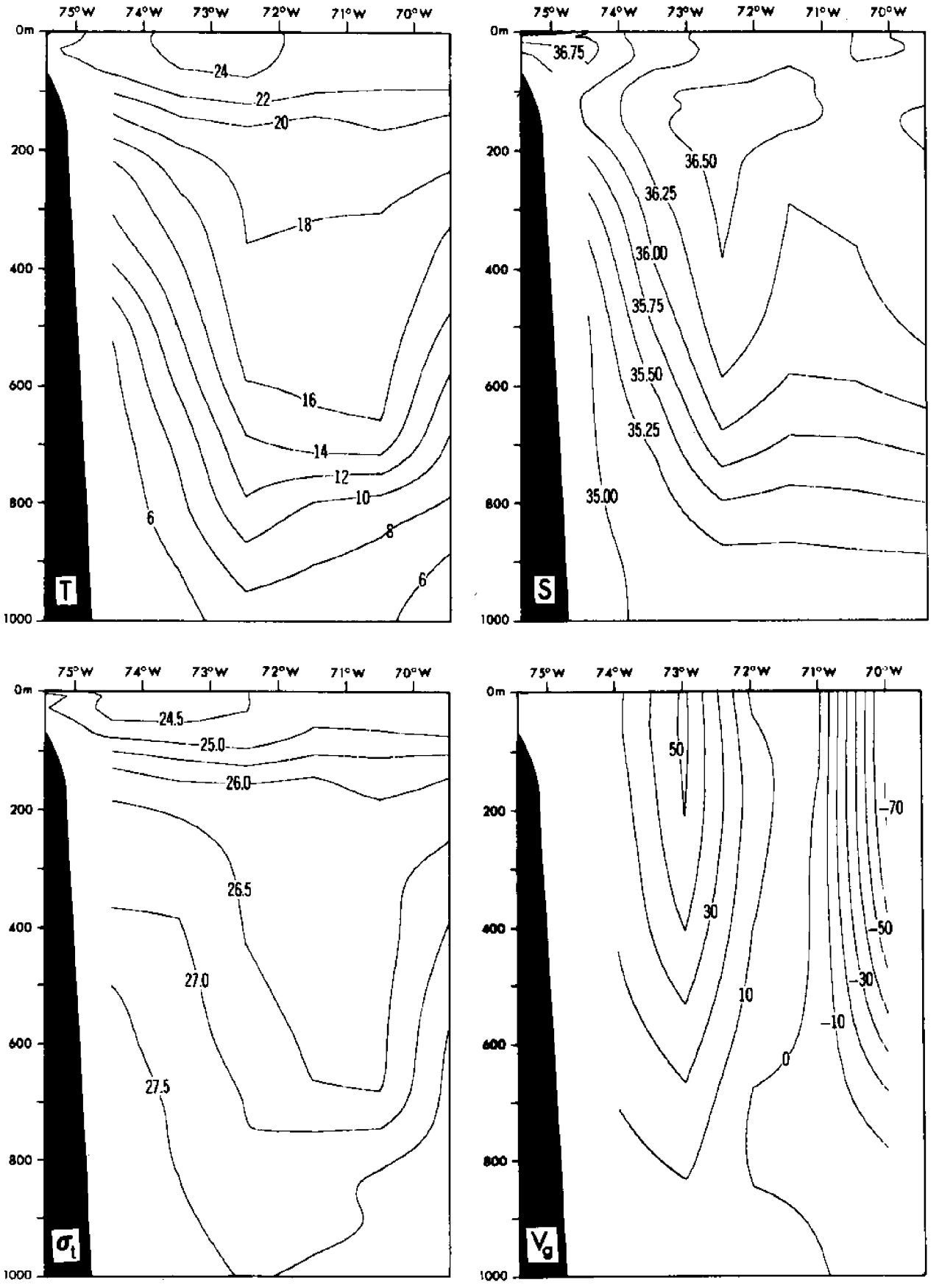

East—West Section along 35°30' N, December

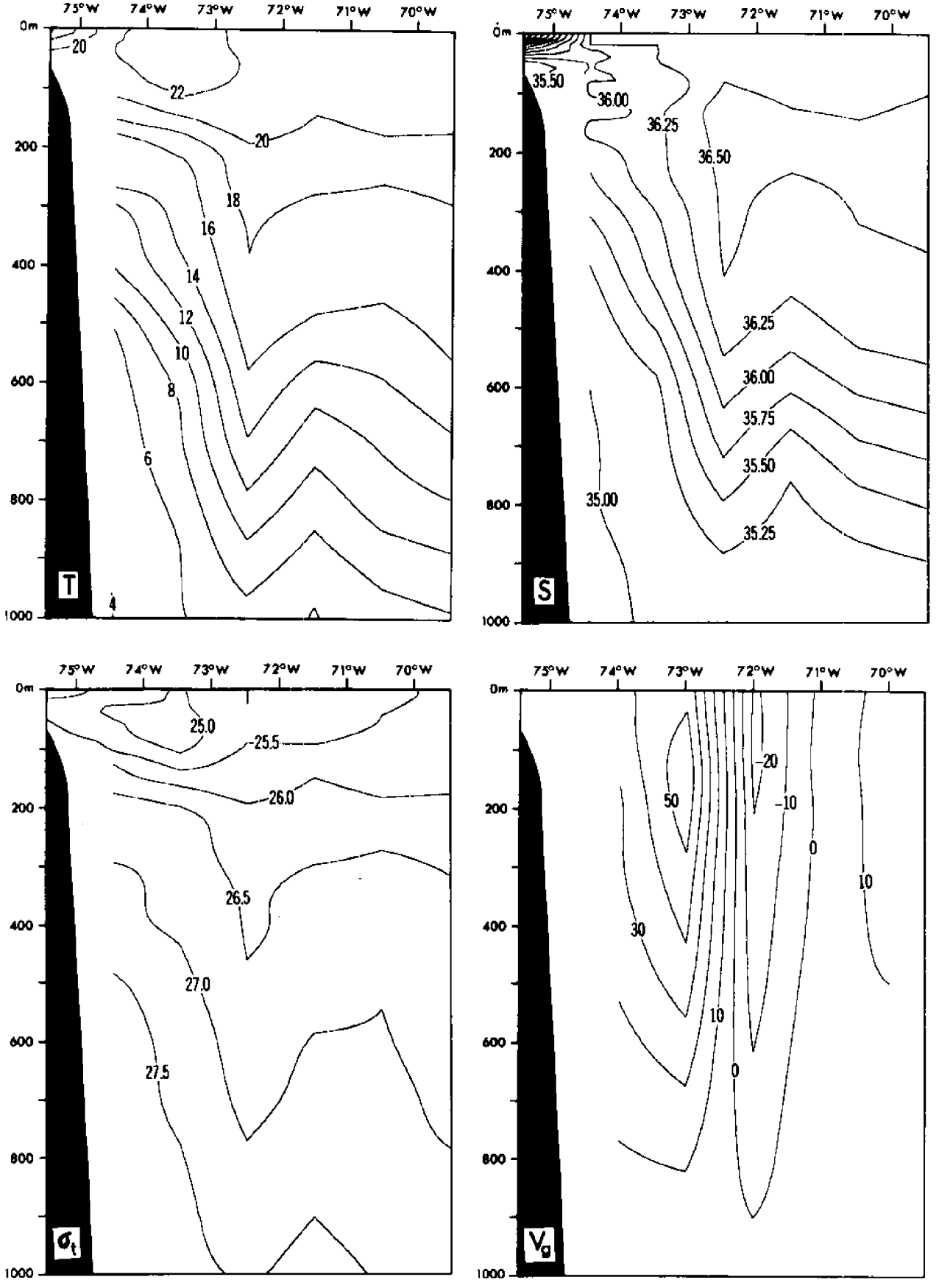

East – West Section along 35°30' N
Annual

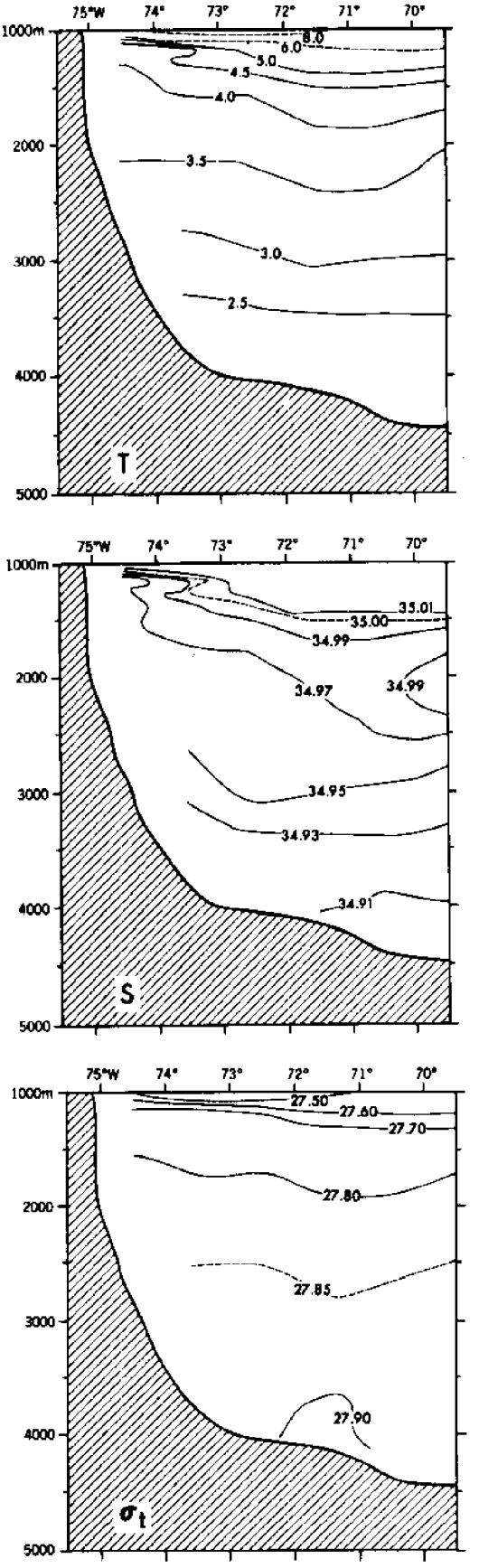

Diagonal Section, January

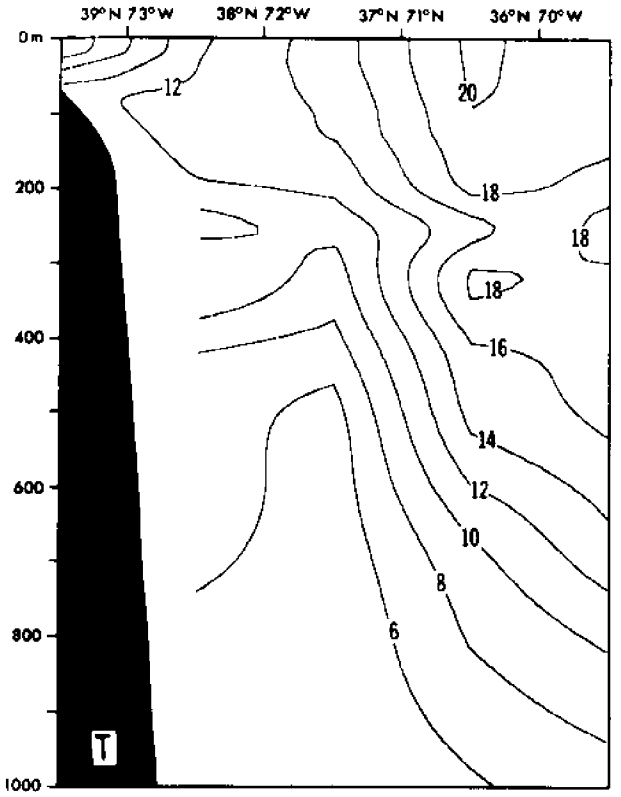

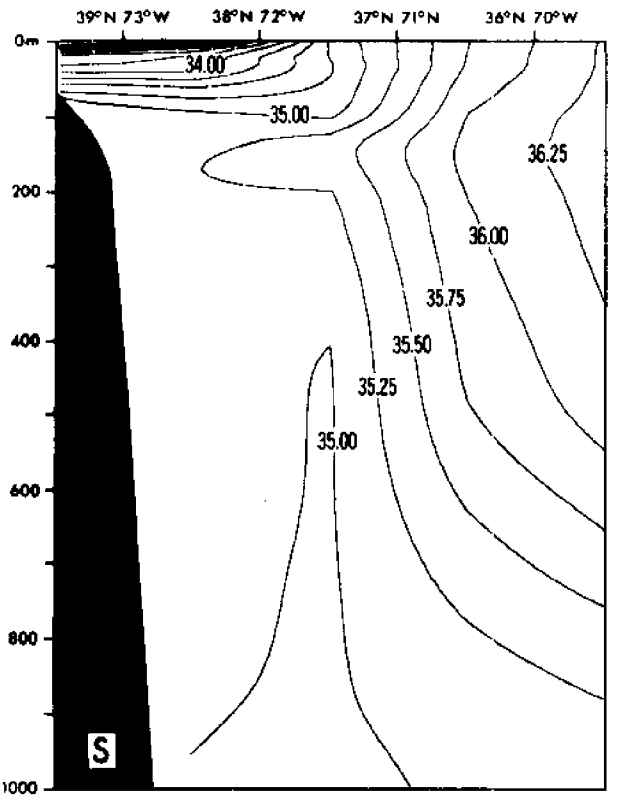

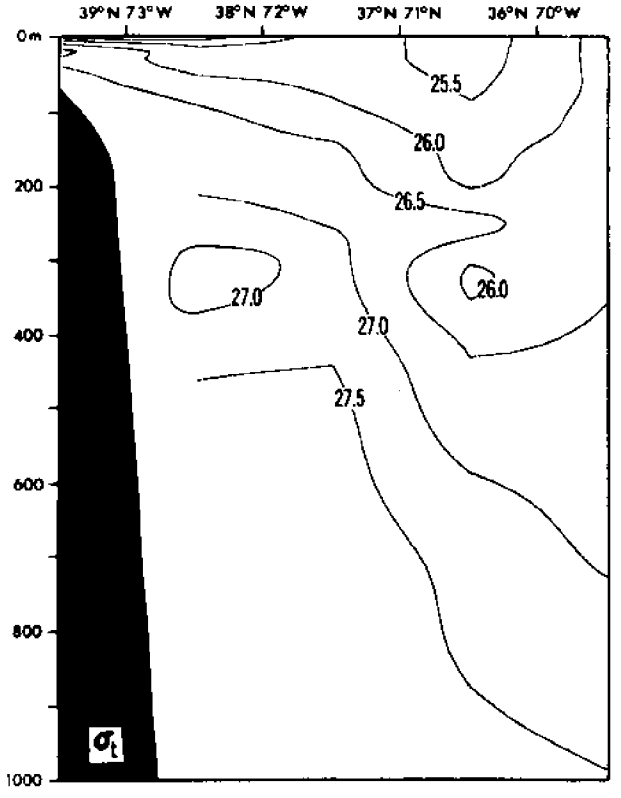

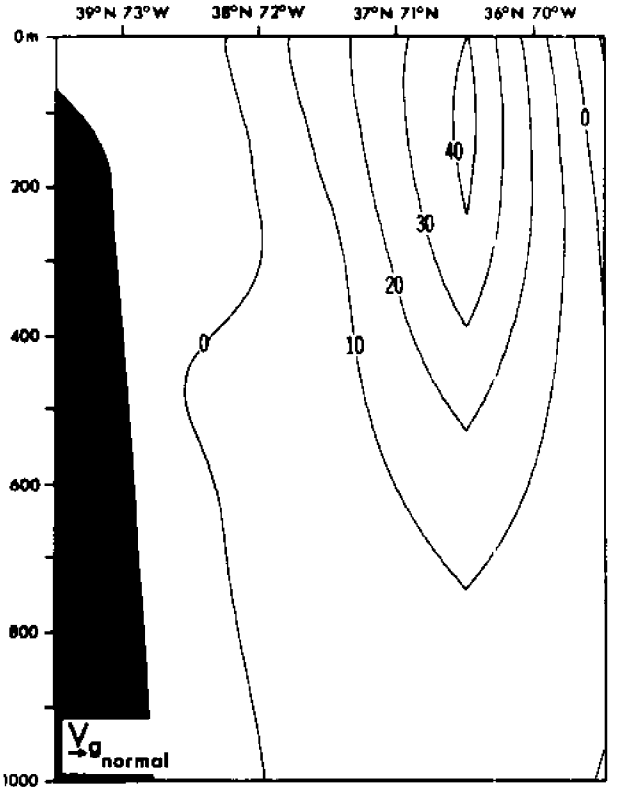

Diagonal Section, February

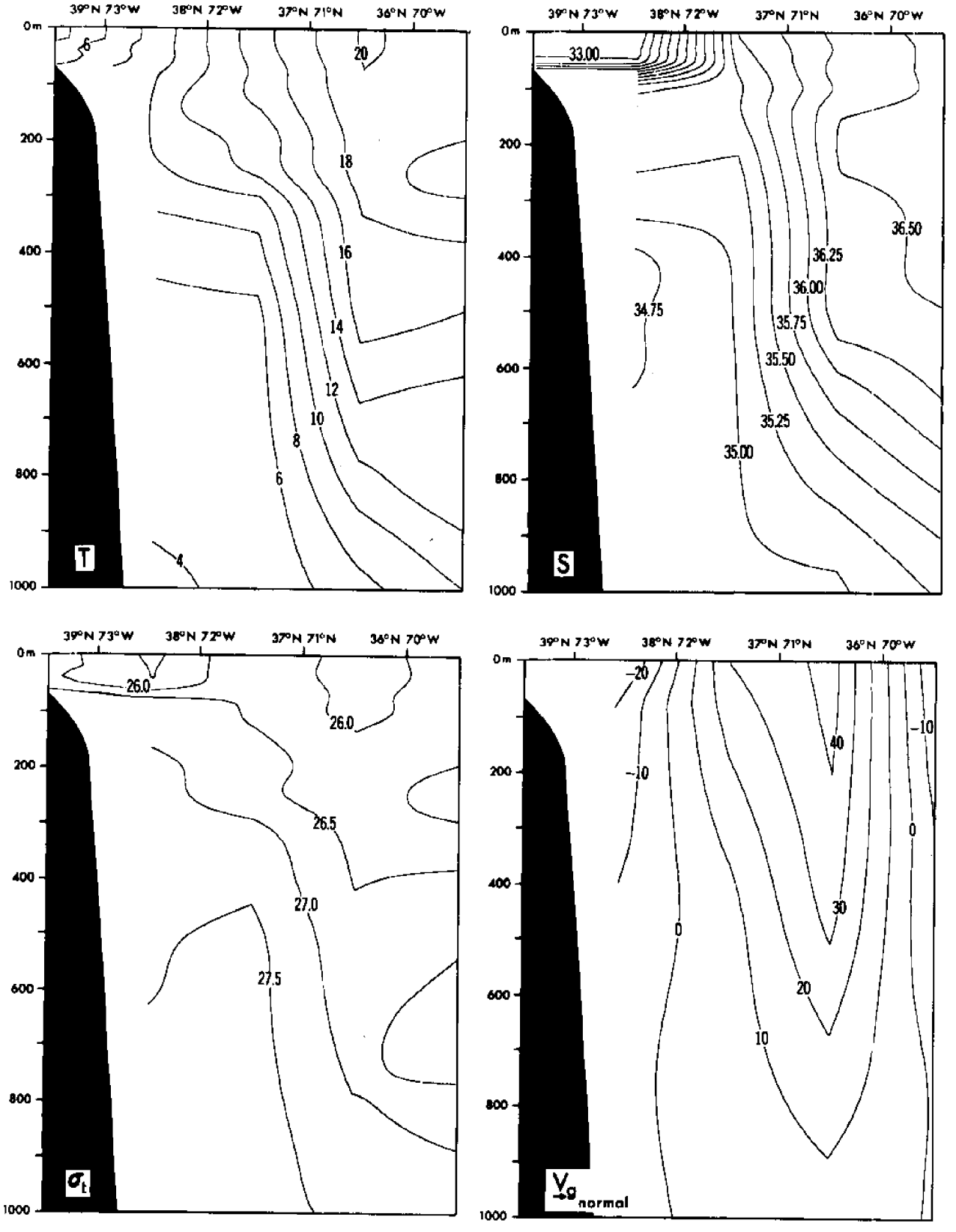

Diagonal Section, March

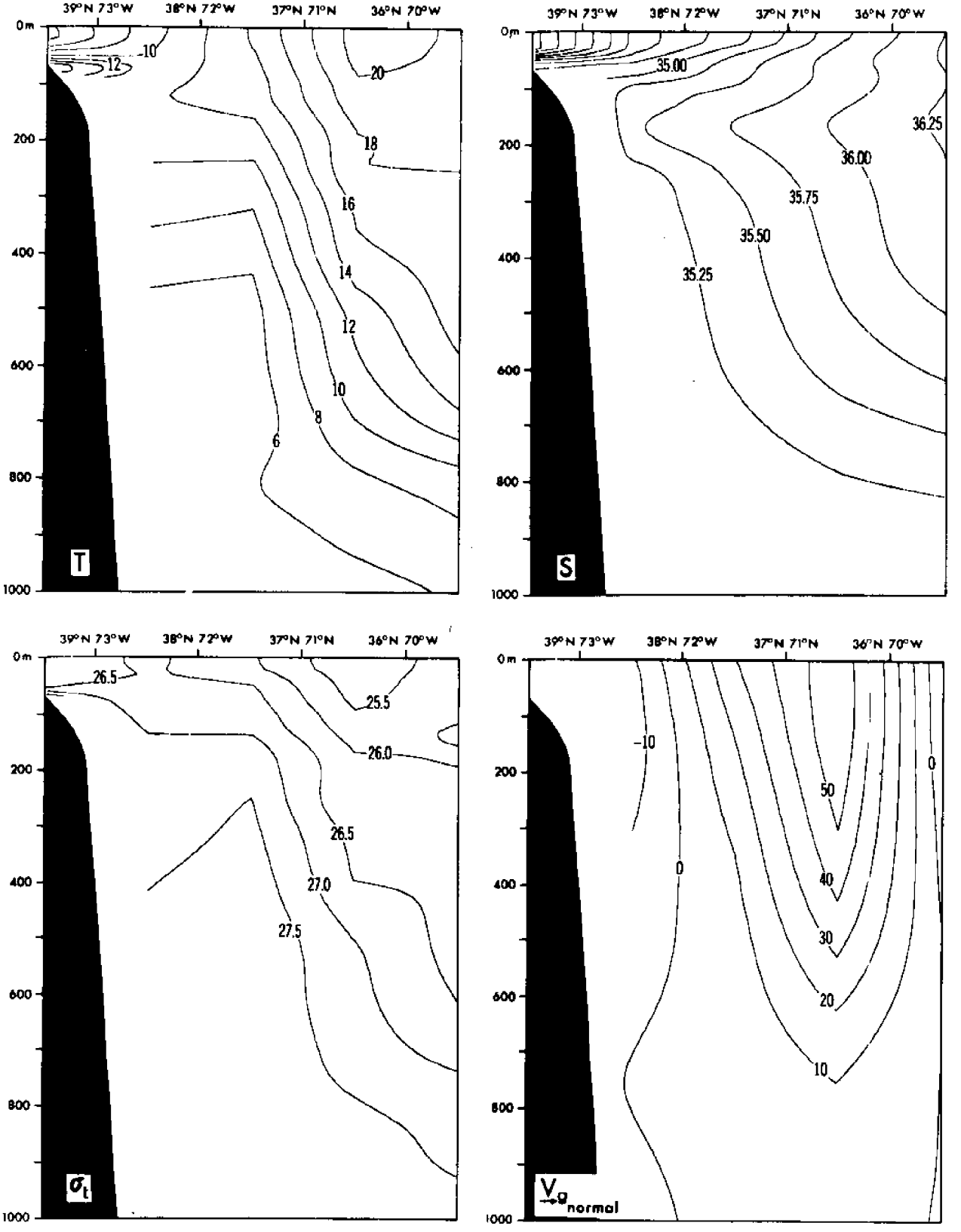

Diagonal Section, April

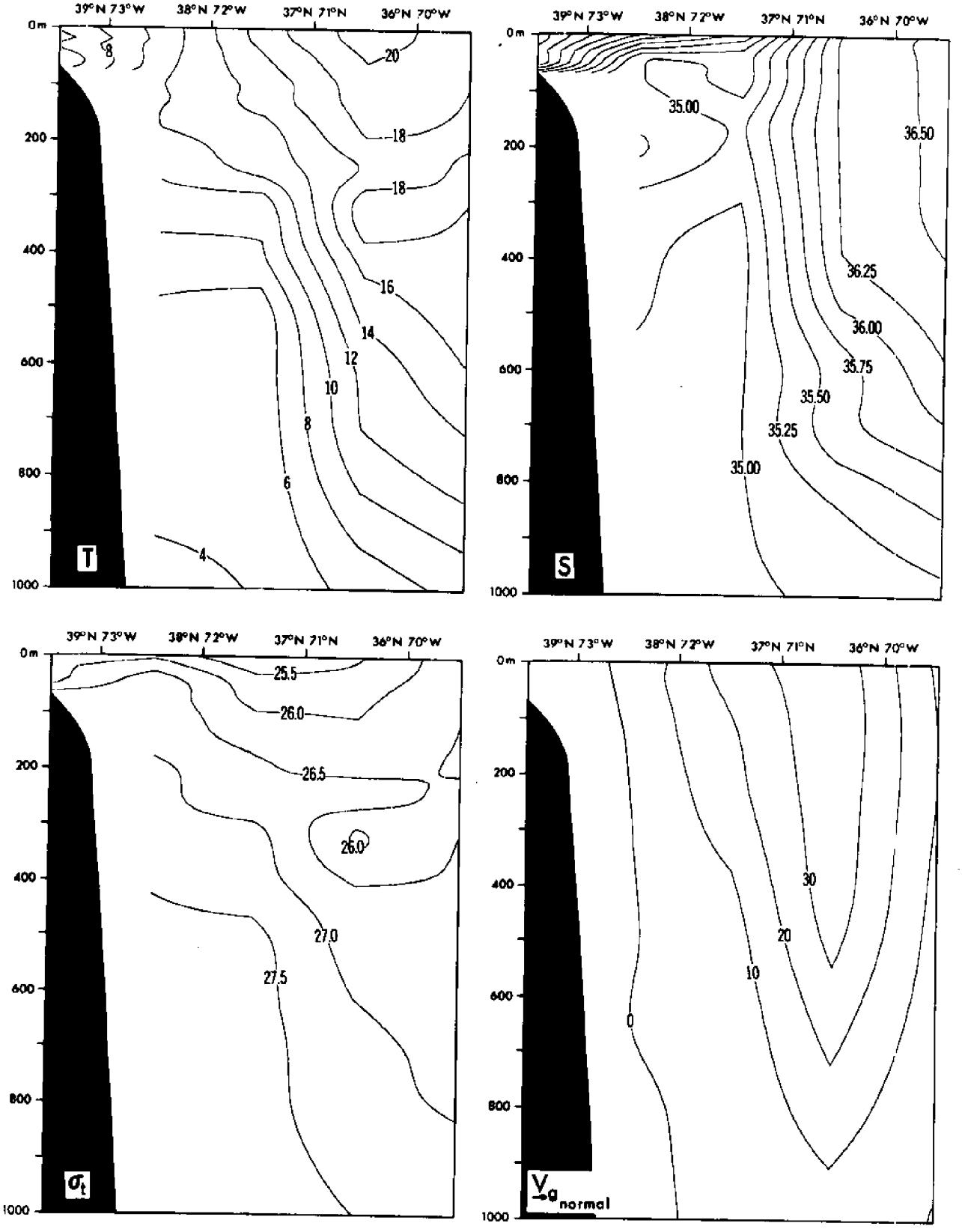

Diagonal Section, May

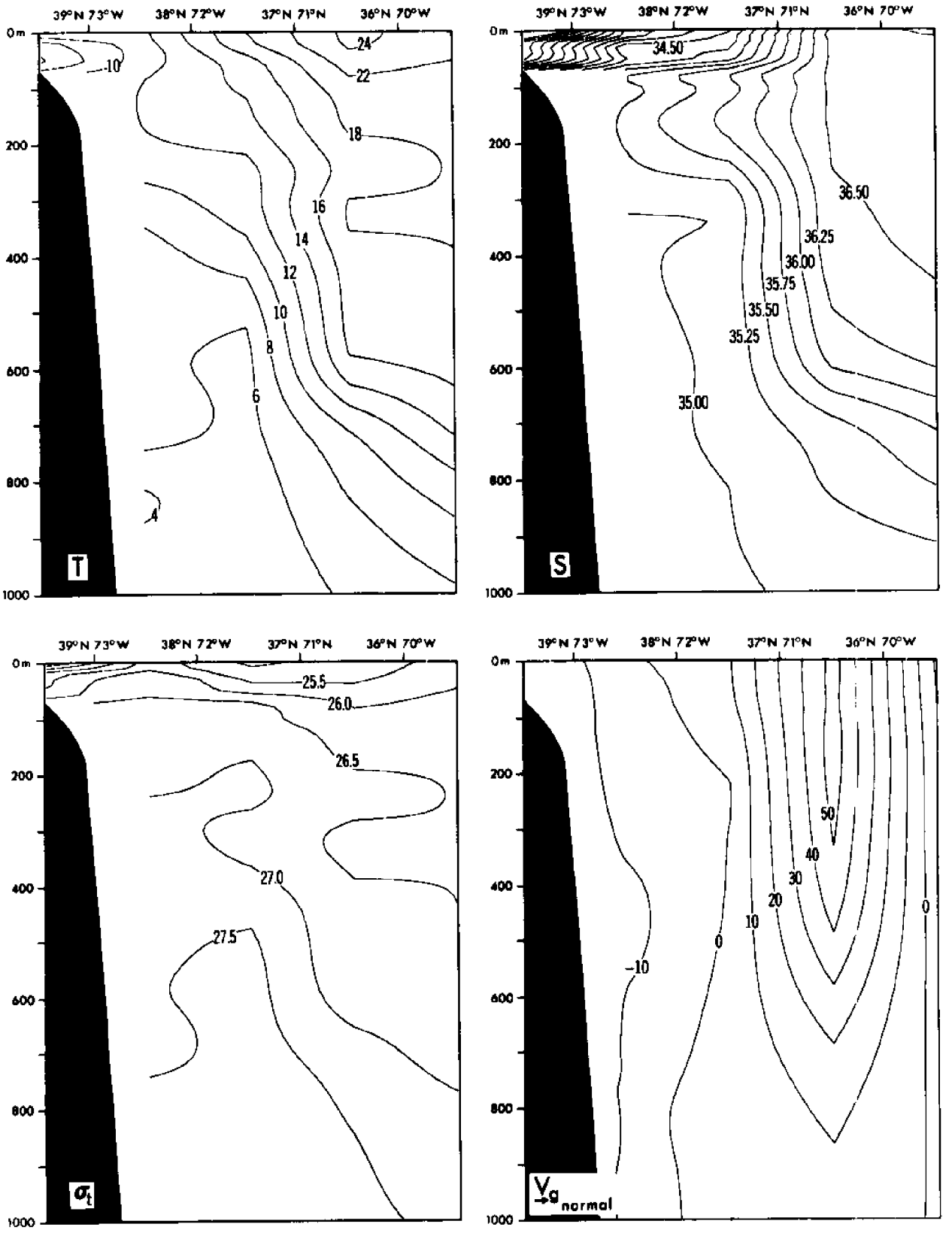

Diagonal Section, June

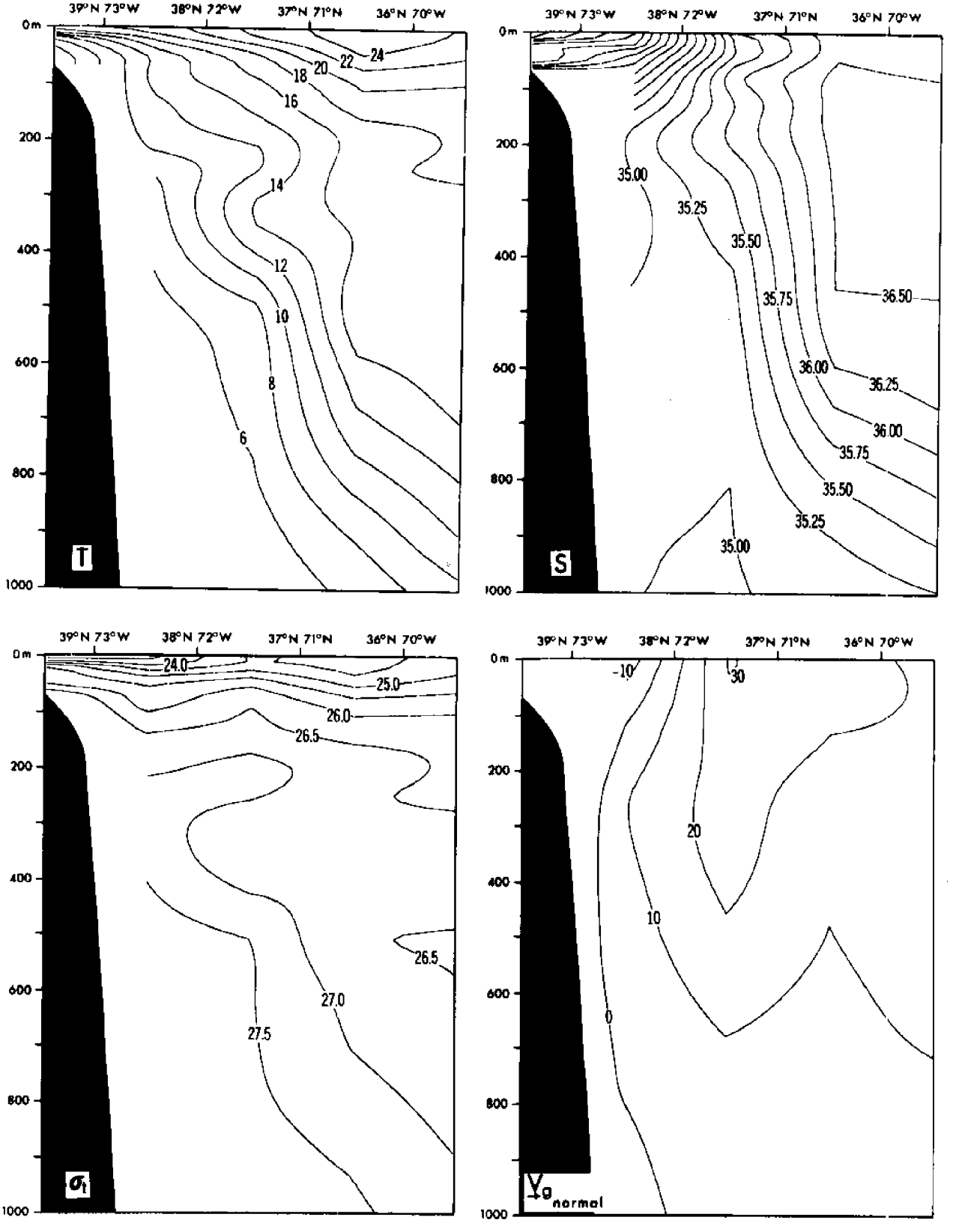

Diagonal Section, July

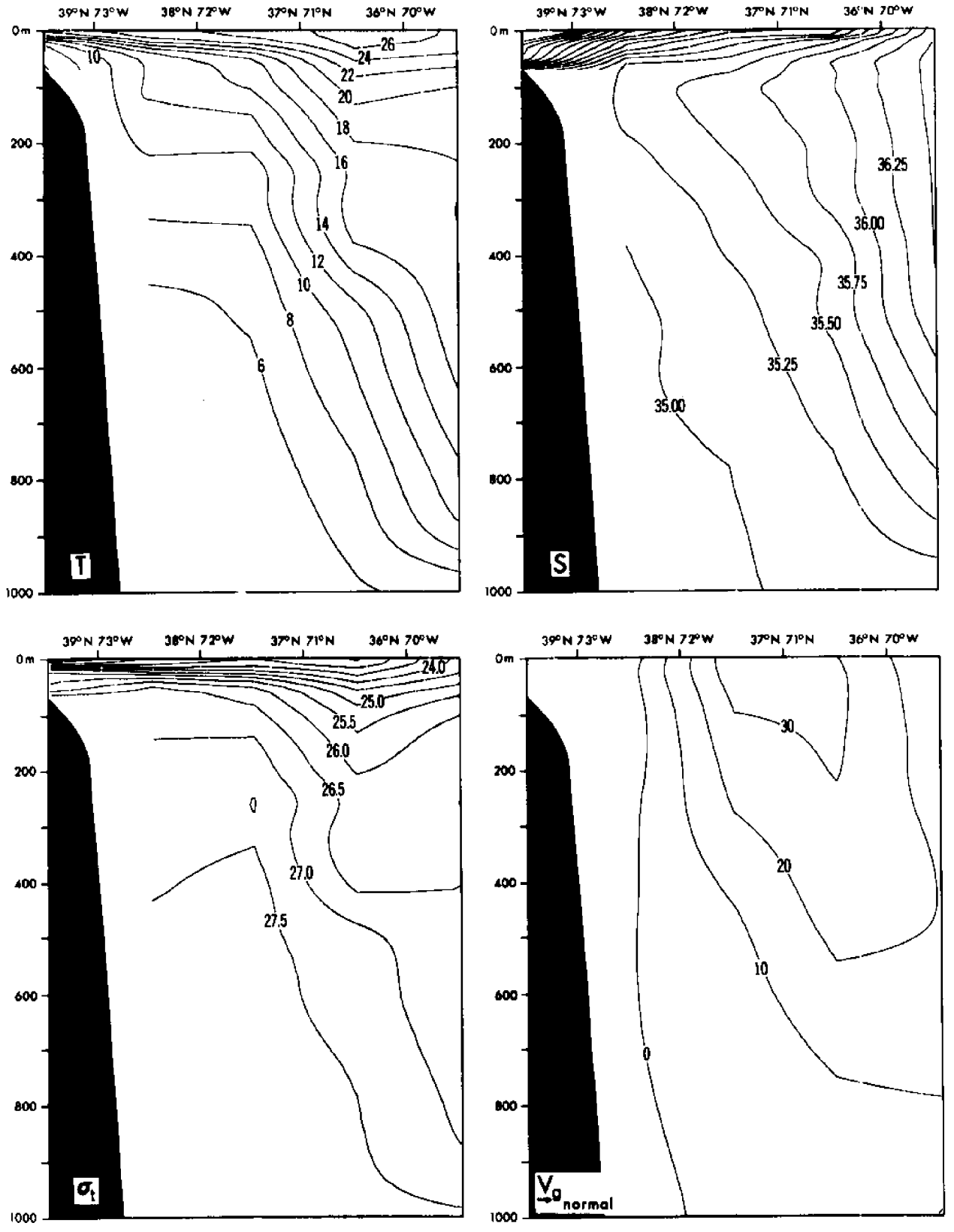

Diagonal Section, August

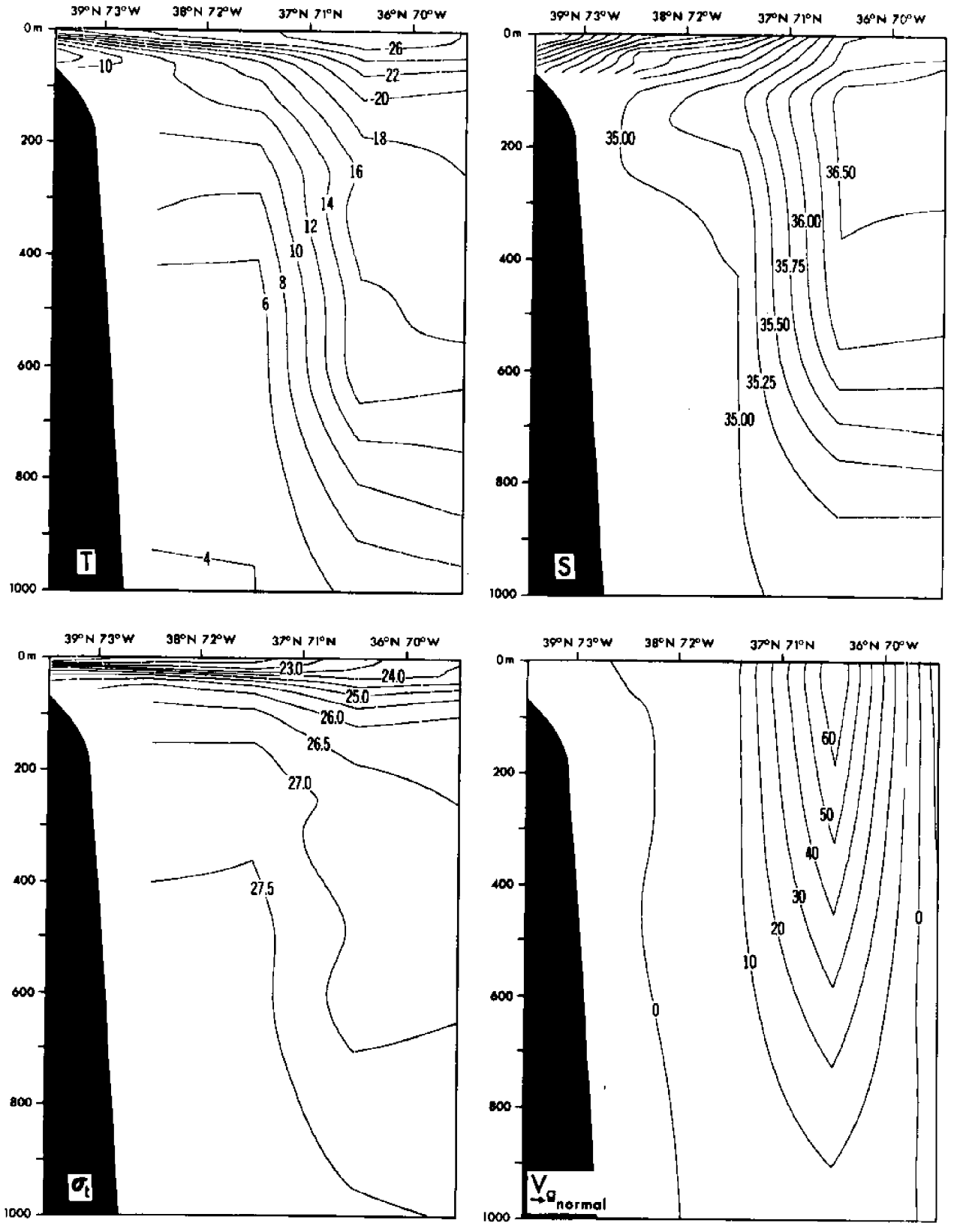

Diagonal Section, September

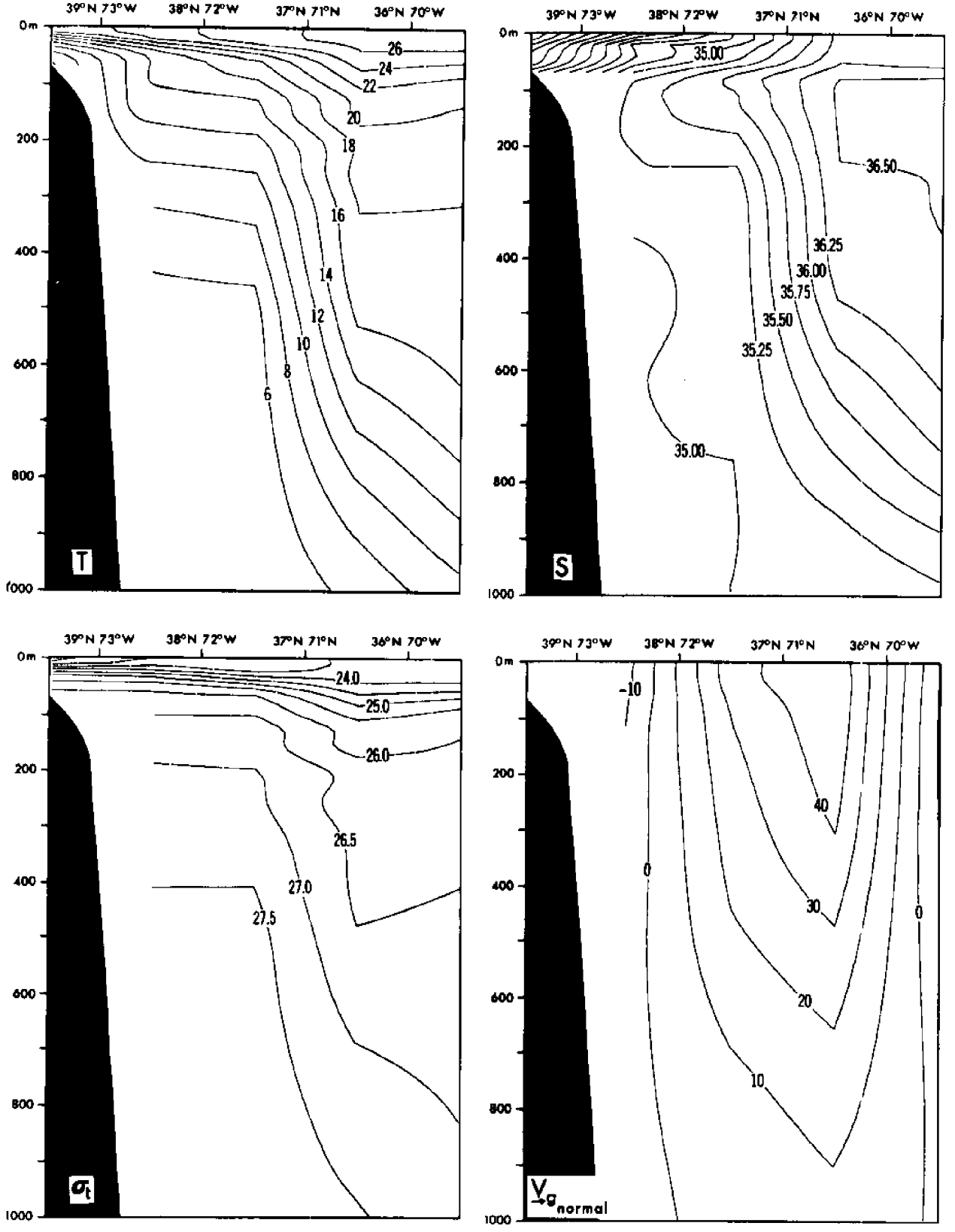

Diagonal Section, October

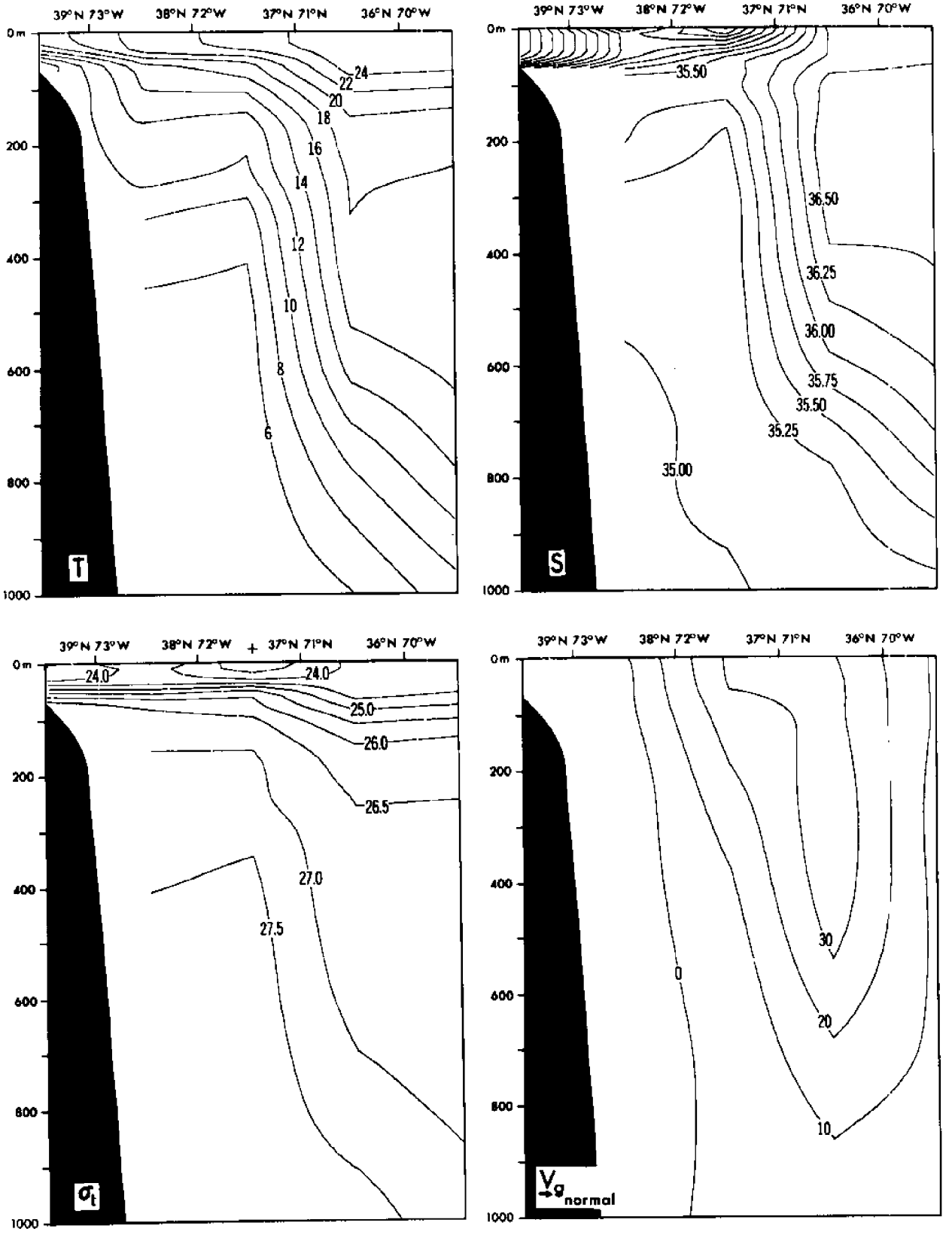

Diagonal Section, November

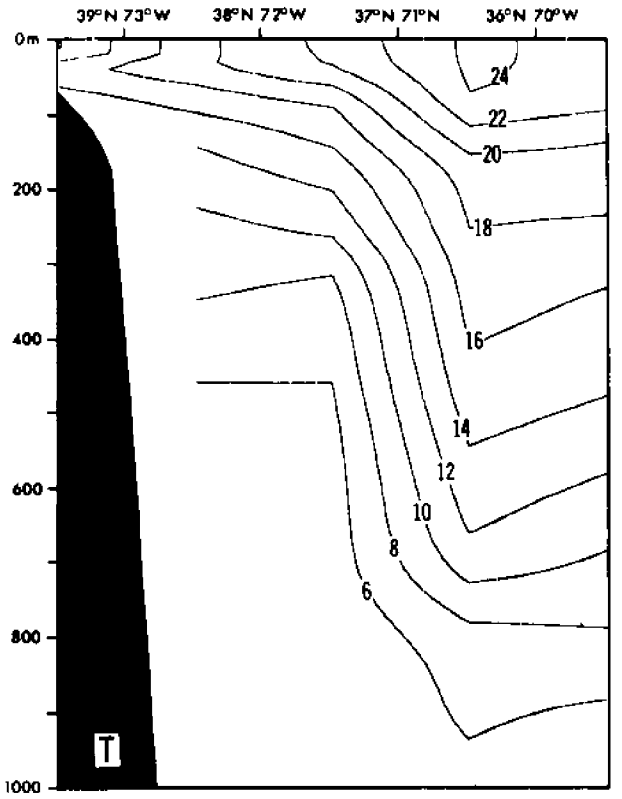

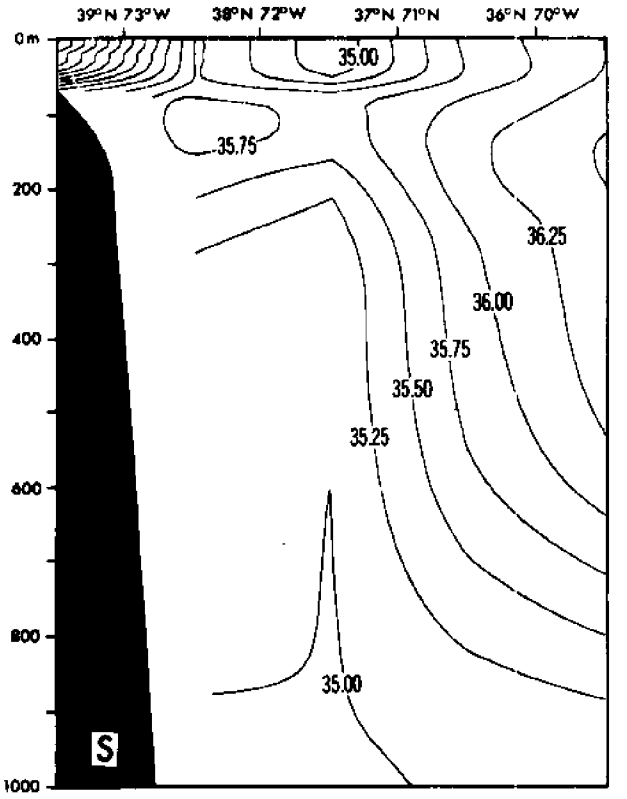

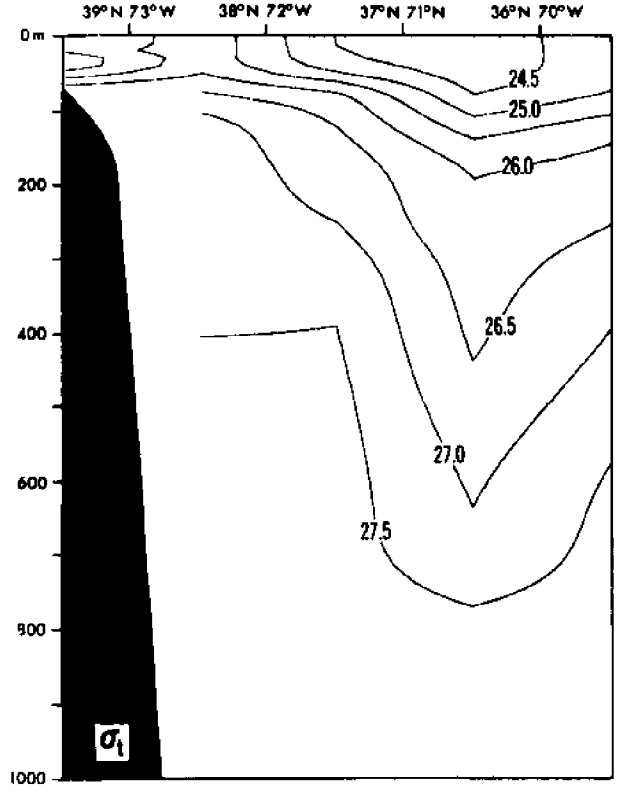

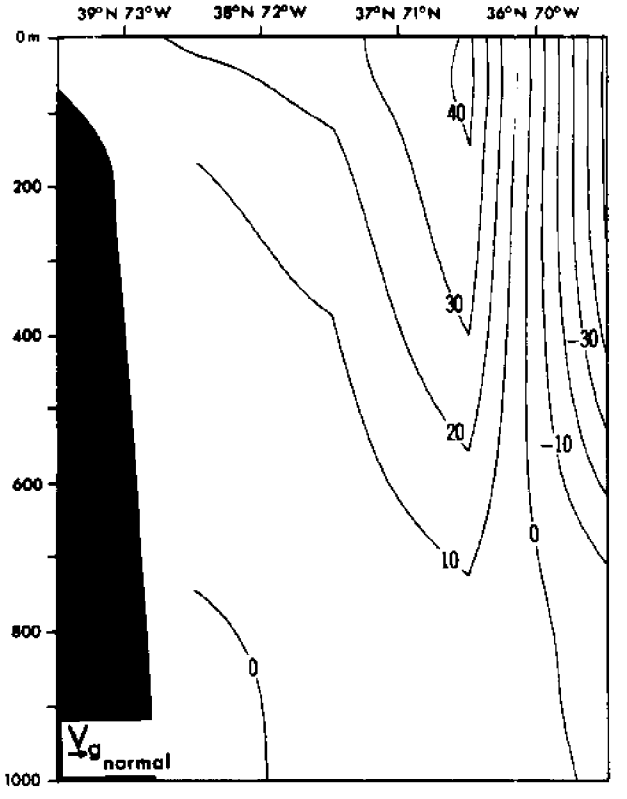

Diagonal Section, December

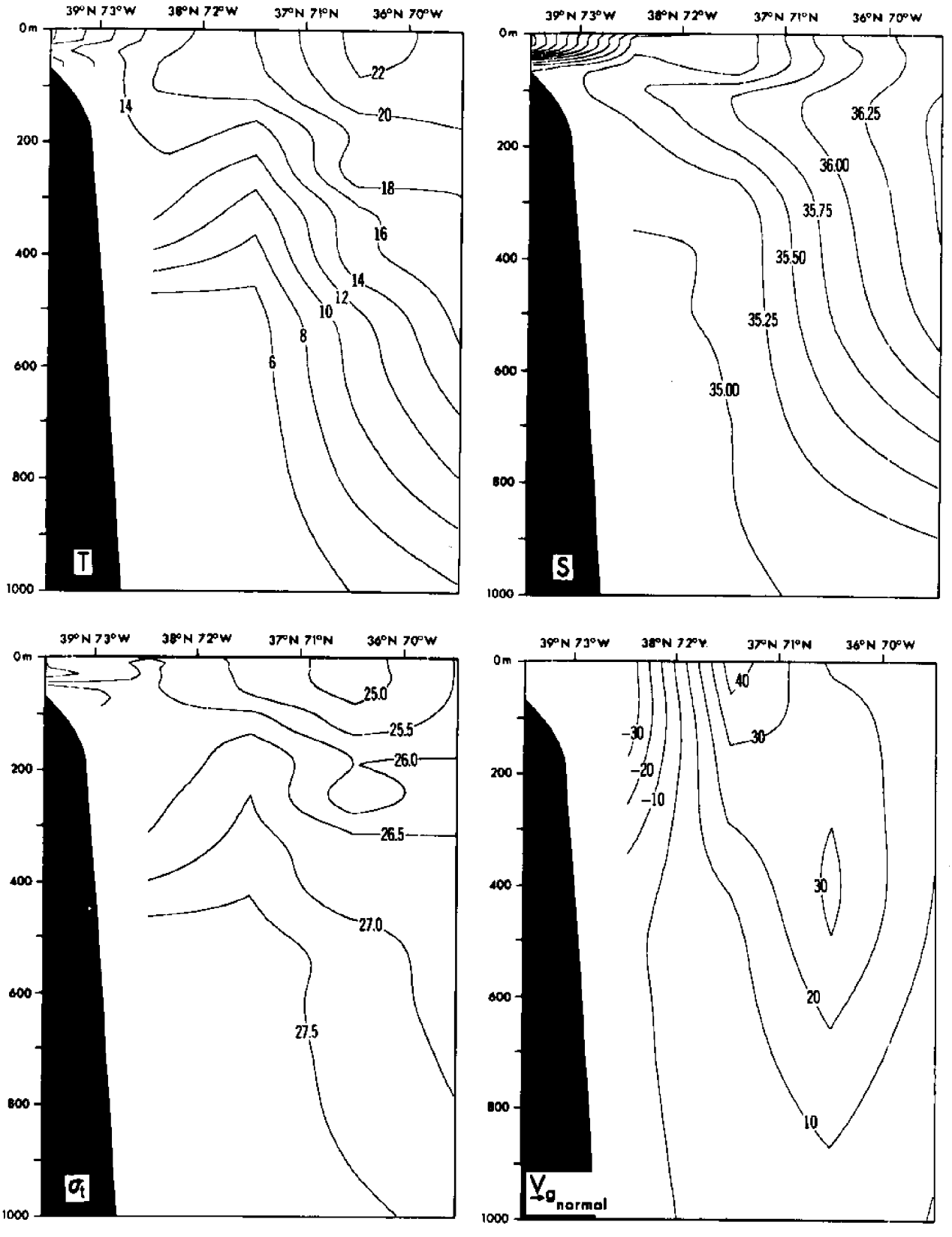

Diagonal Section, Annual

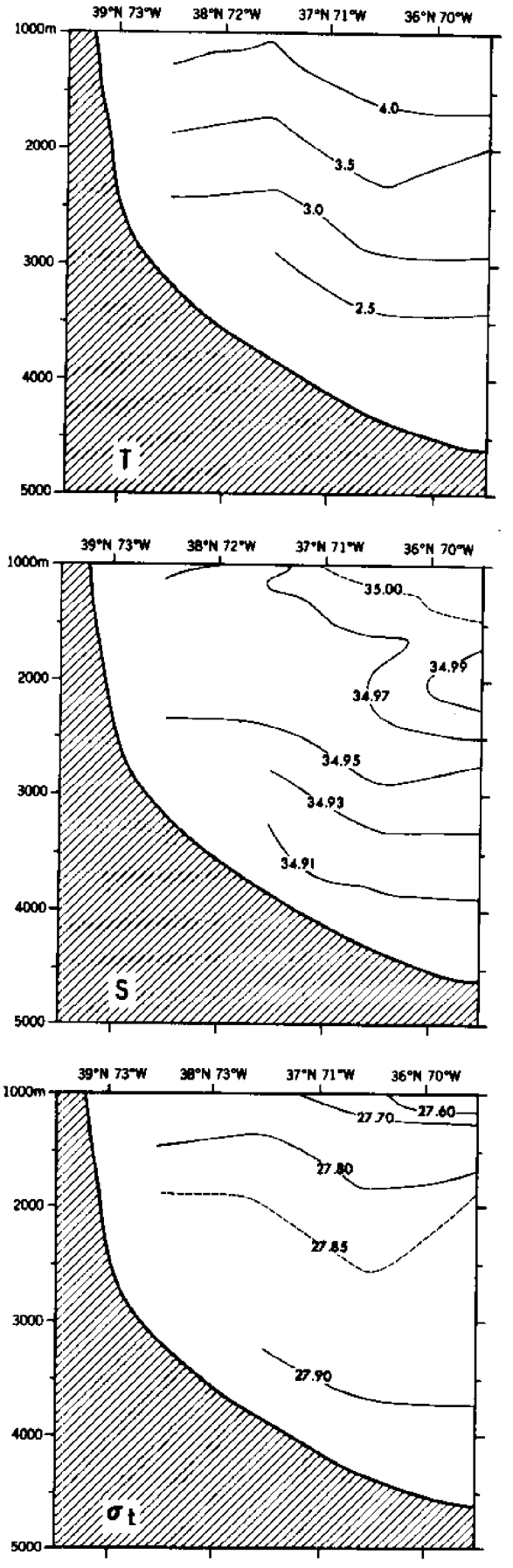

North—South Section along 69°30' W, January

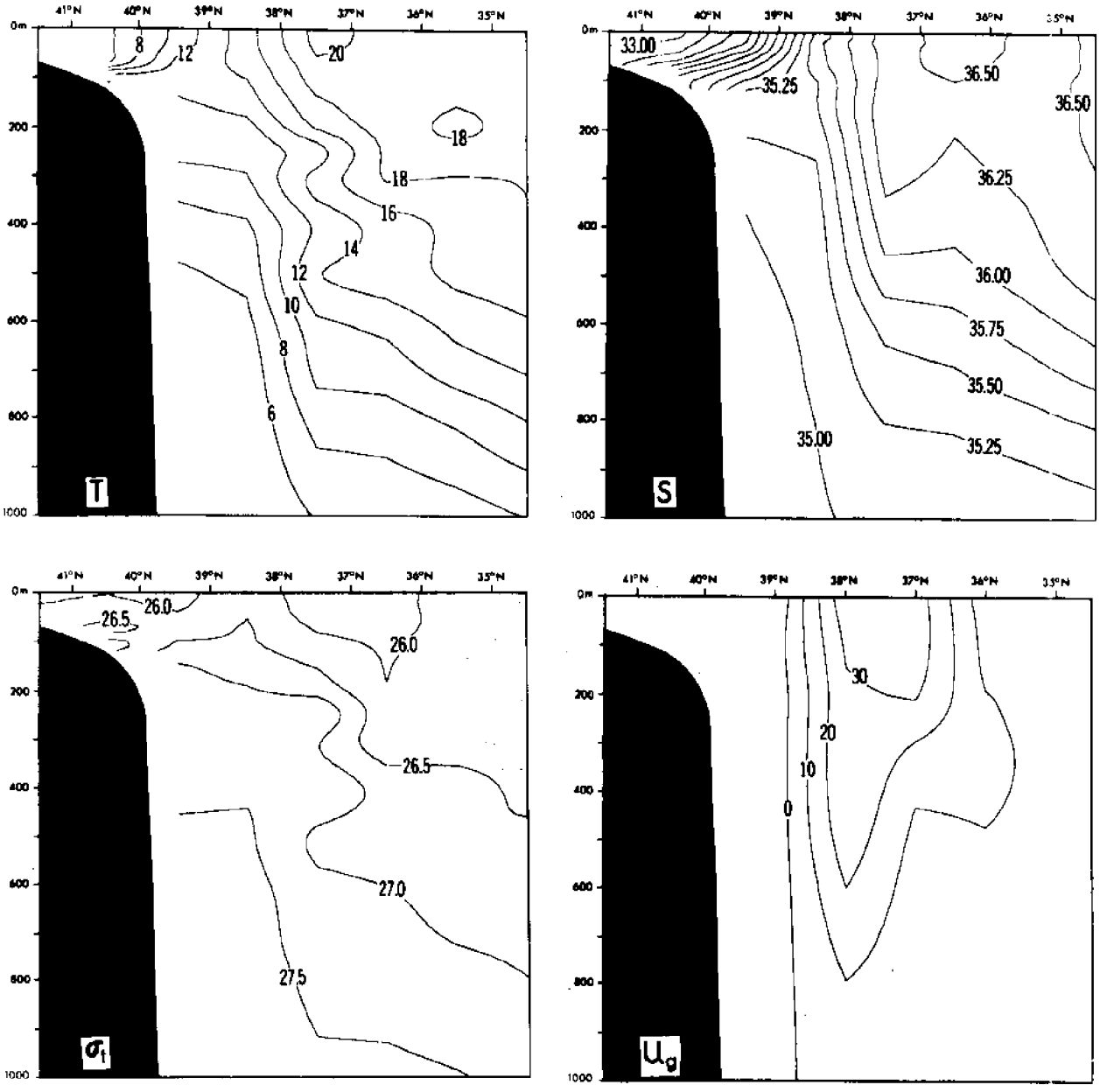

North—South Section along 69°30' W, February

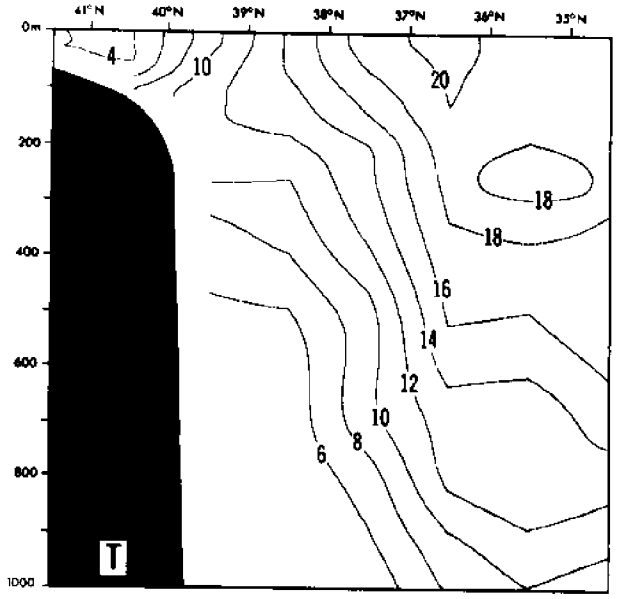

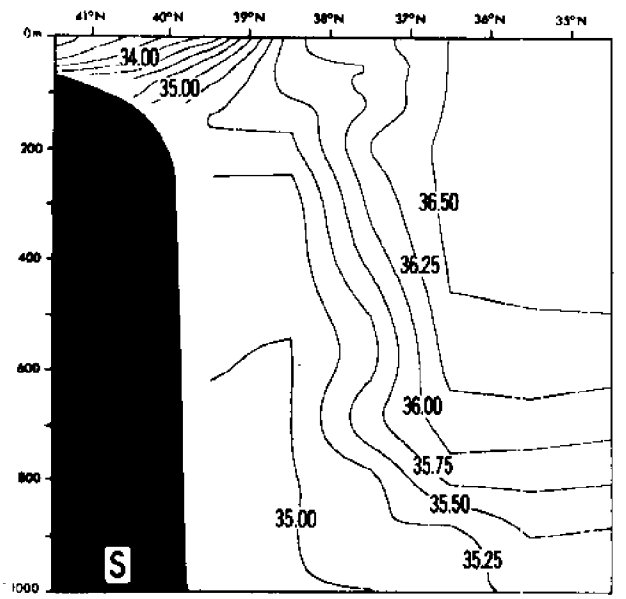

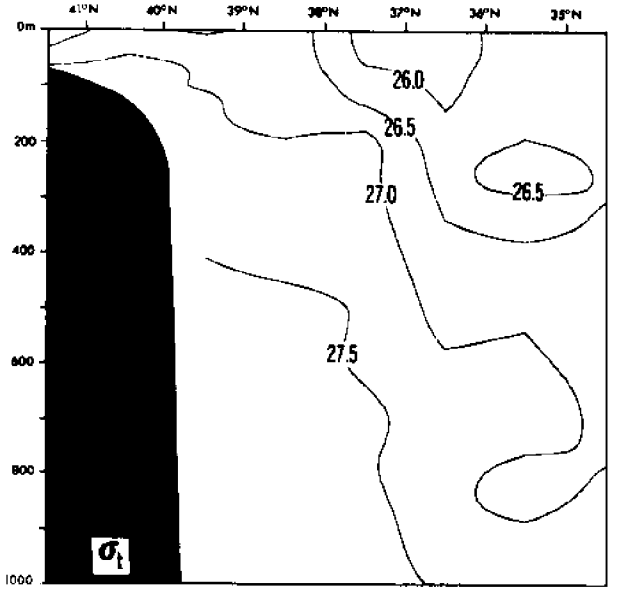

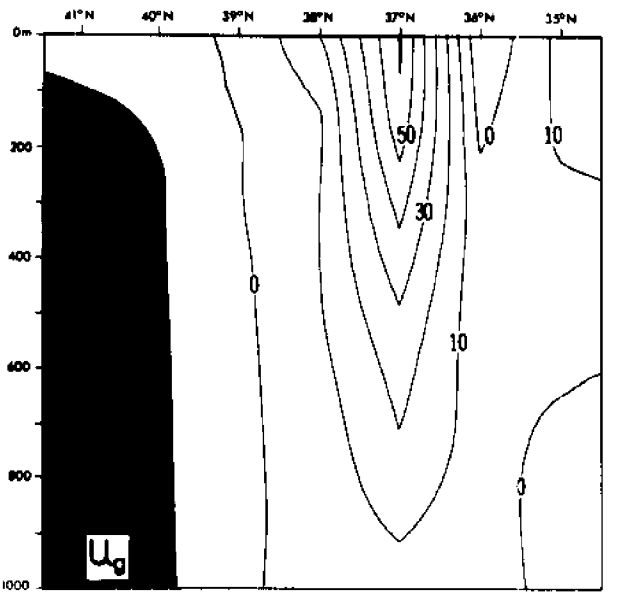

North—South Section along 69°30' W, March

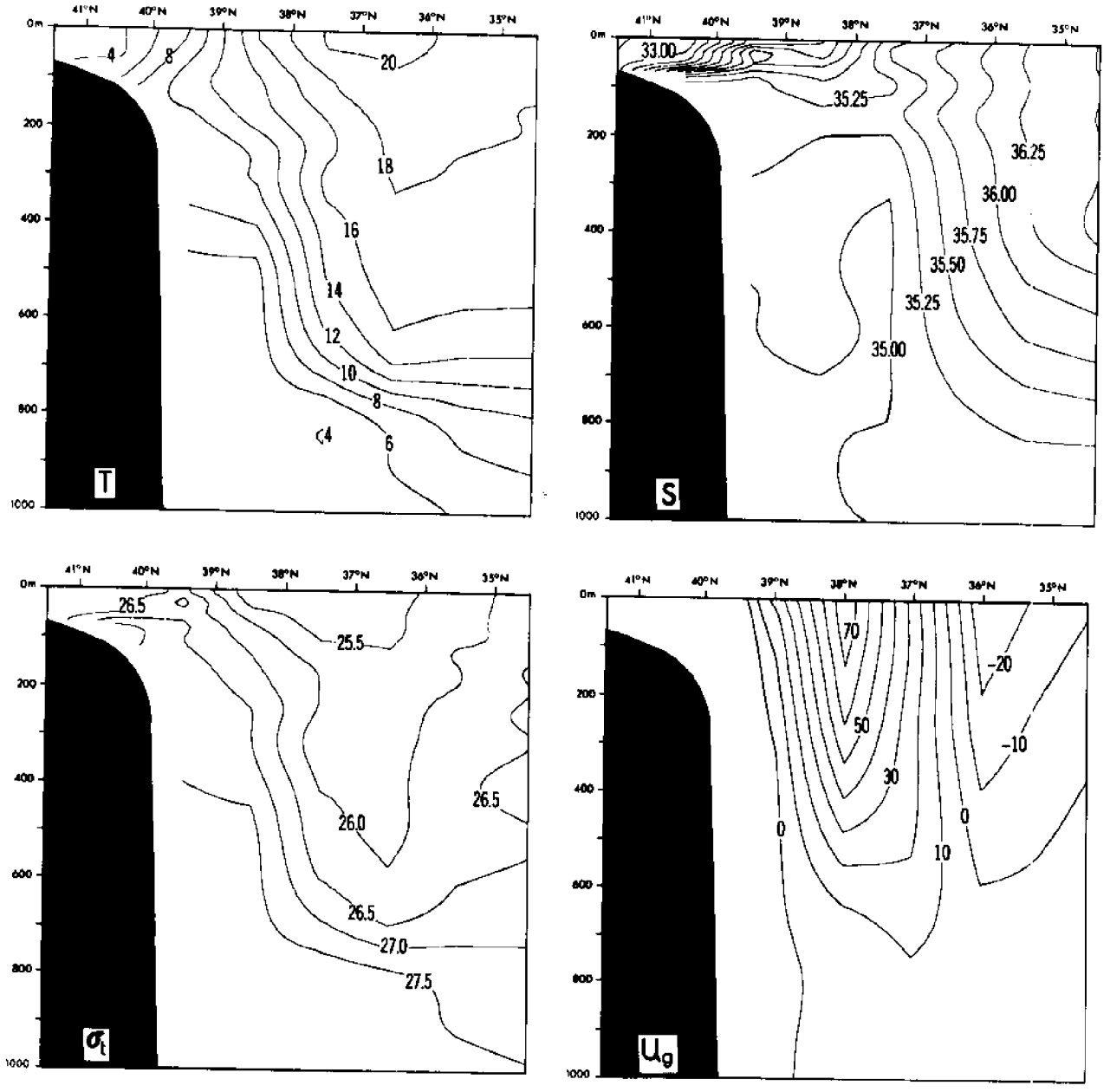

North—South Section along 69°30' W, April

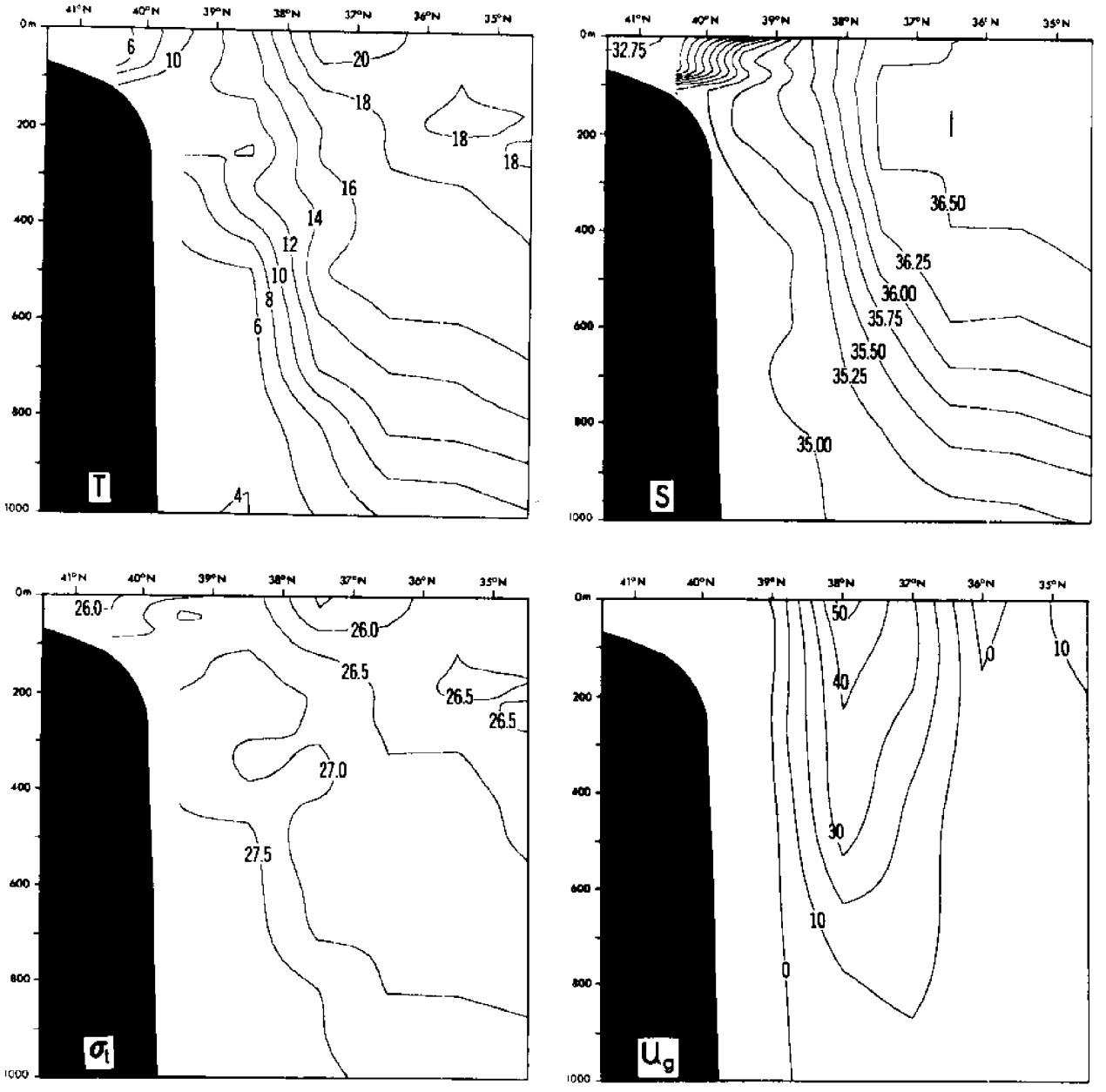

North—South Section along 69°30' W, May

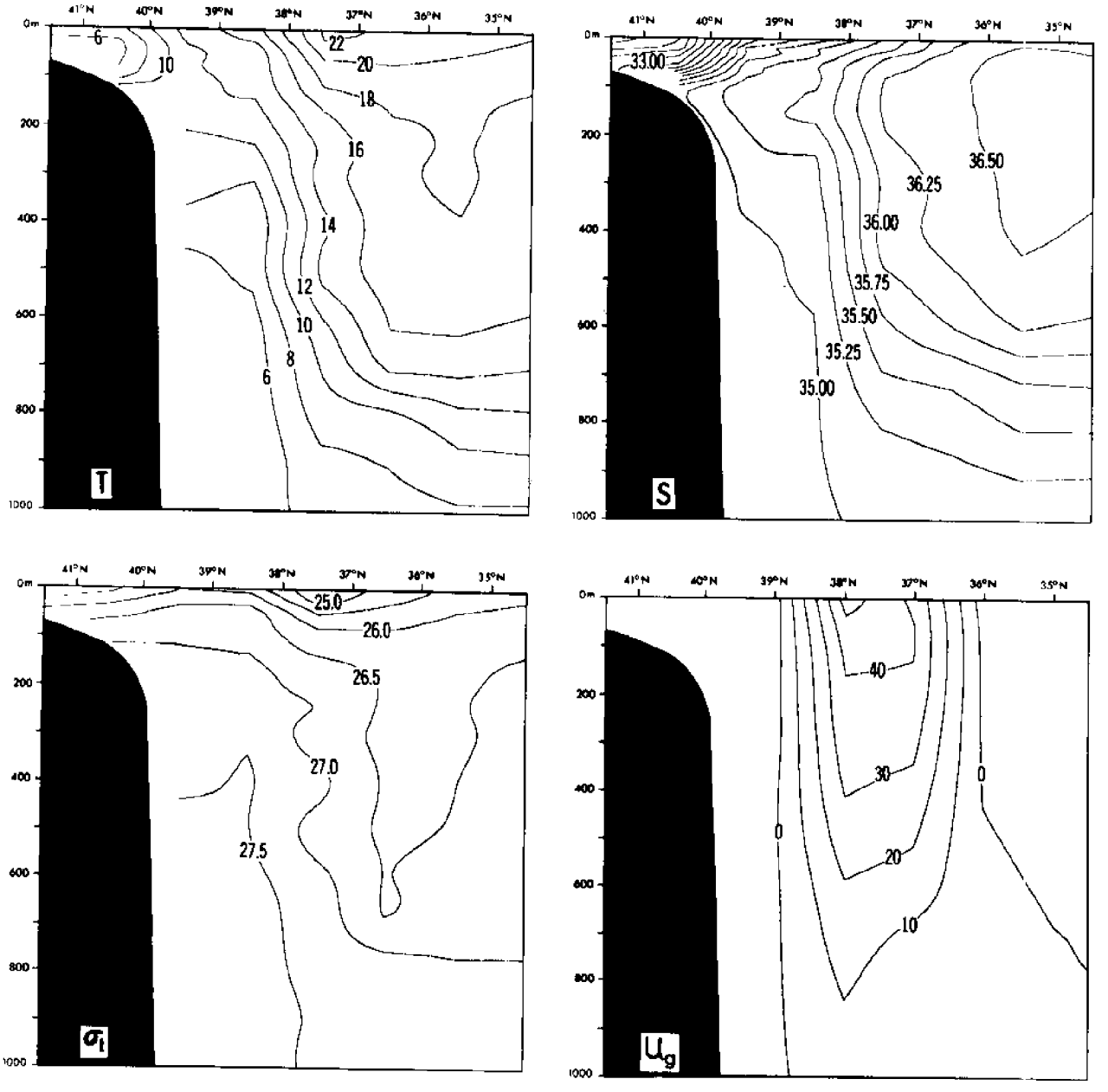

North—South Section along 69°30' W, June

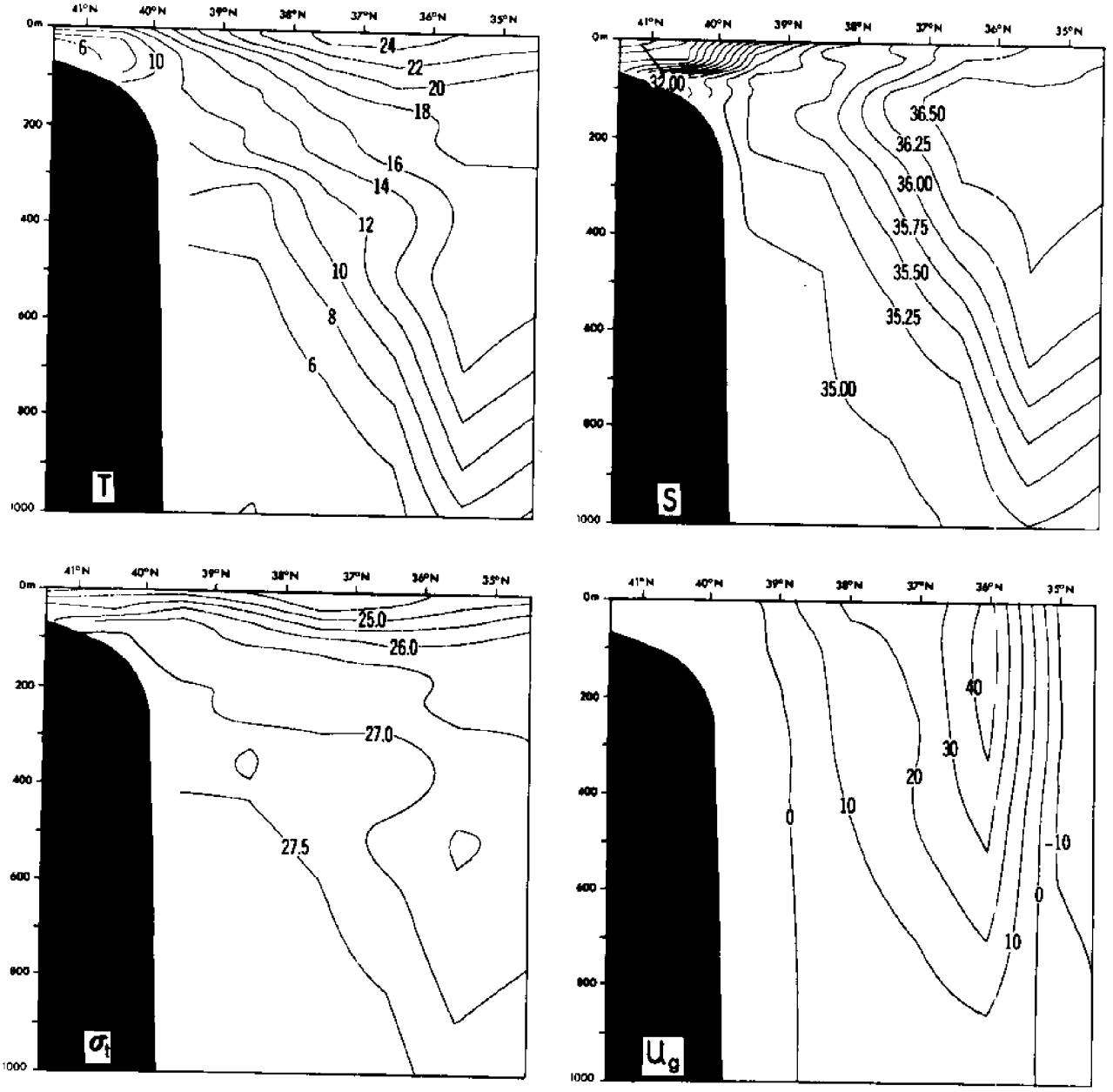

North—South Section along 69°30' W, July

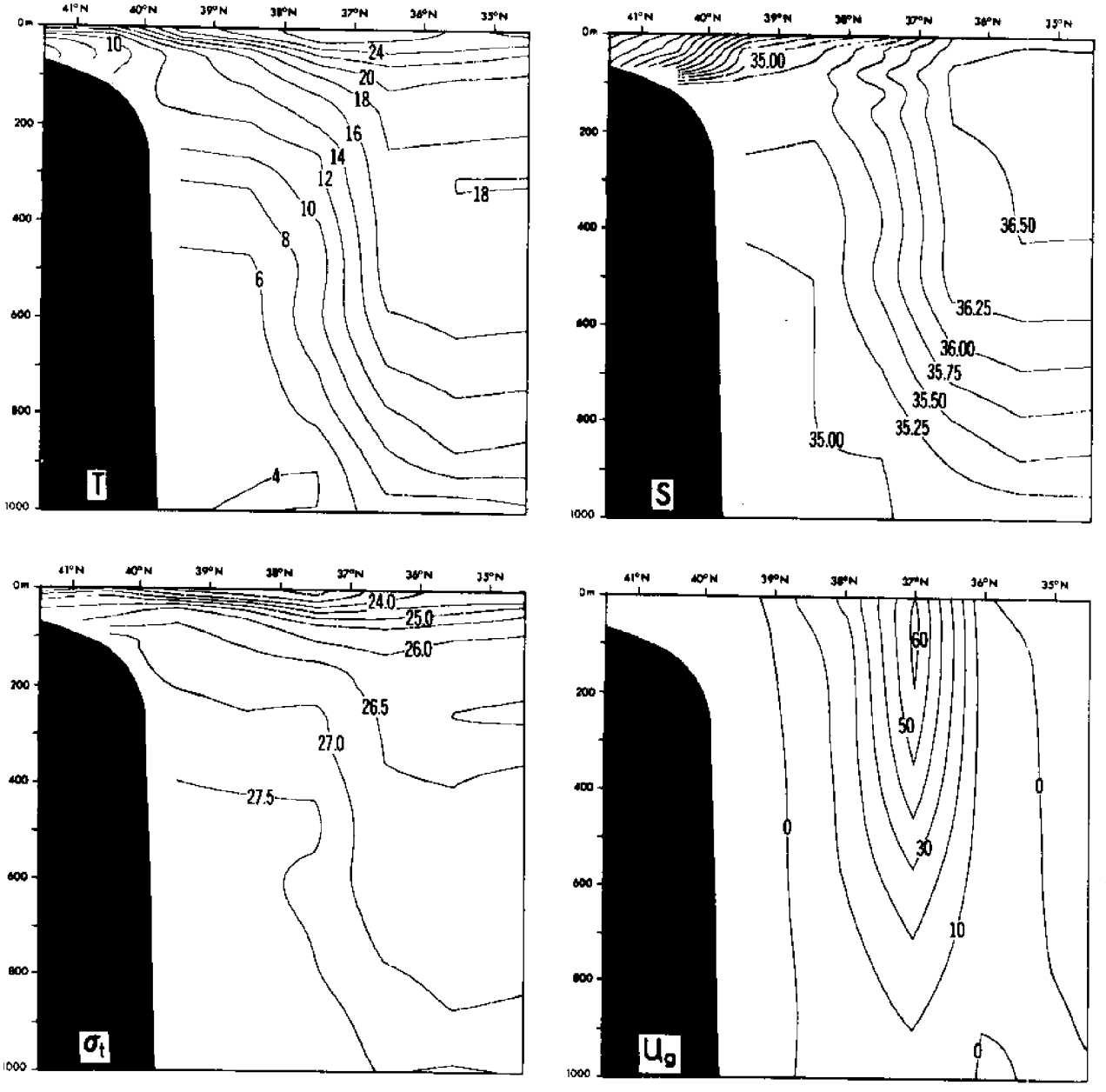

North—South Section along 69°30' W, August

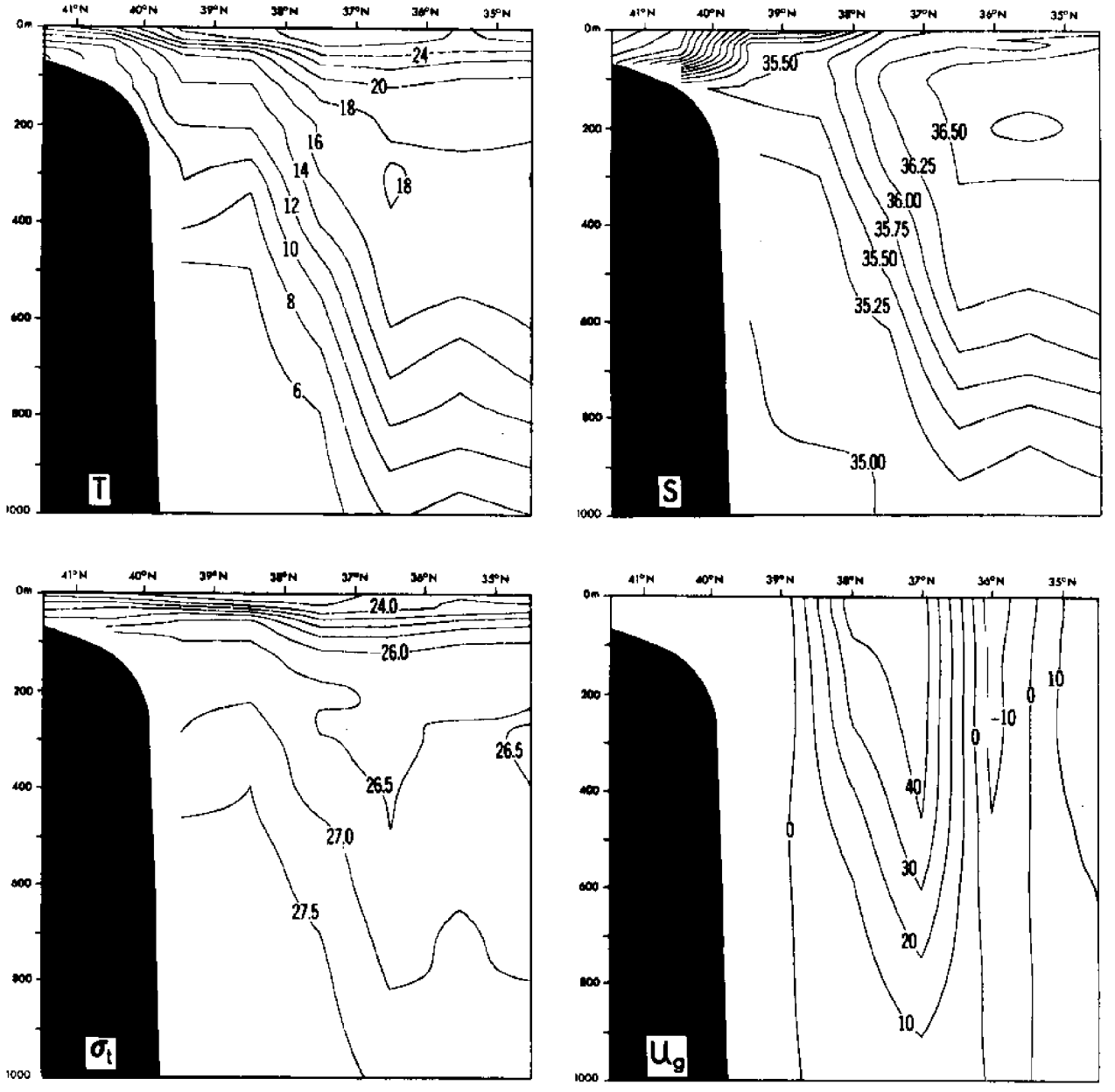

North—South Section along 69°30' W, September

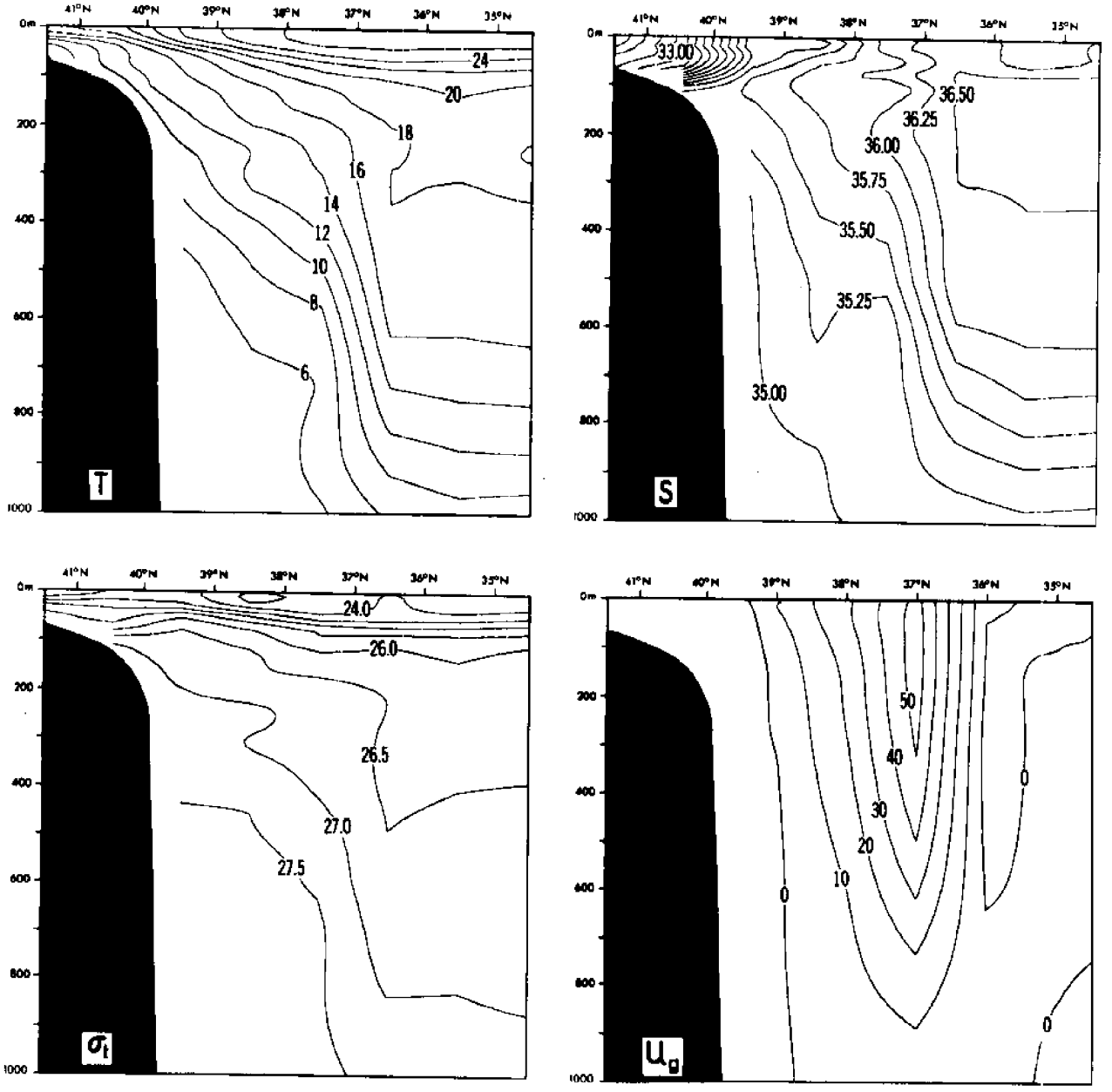

North—South Section along 69°30' W, October

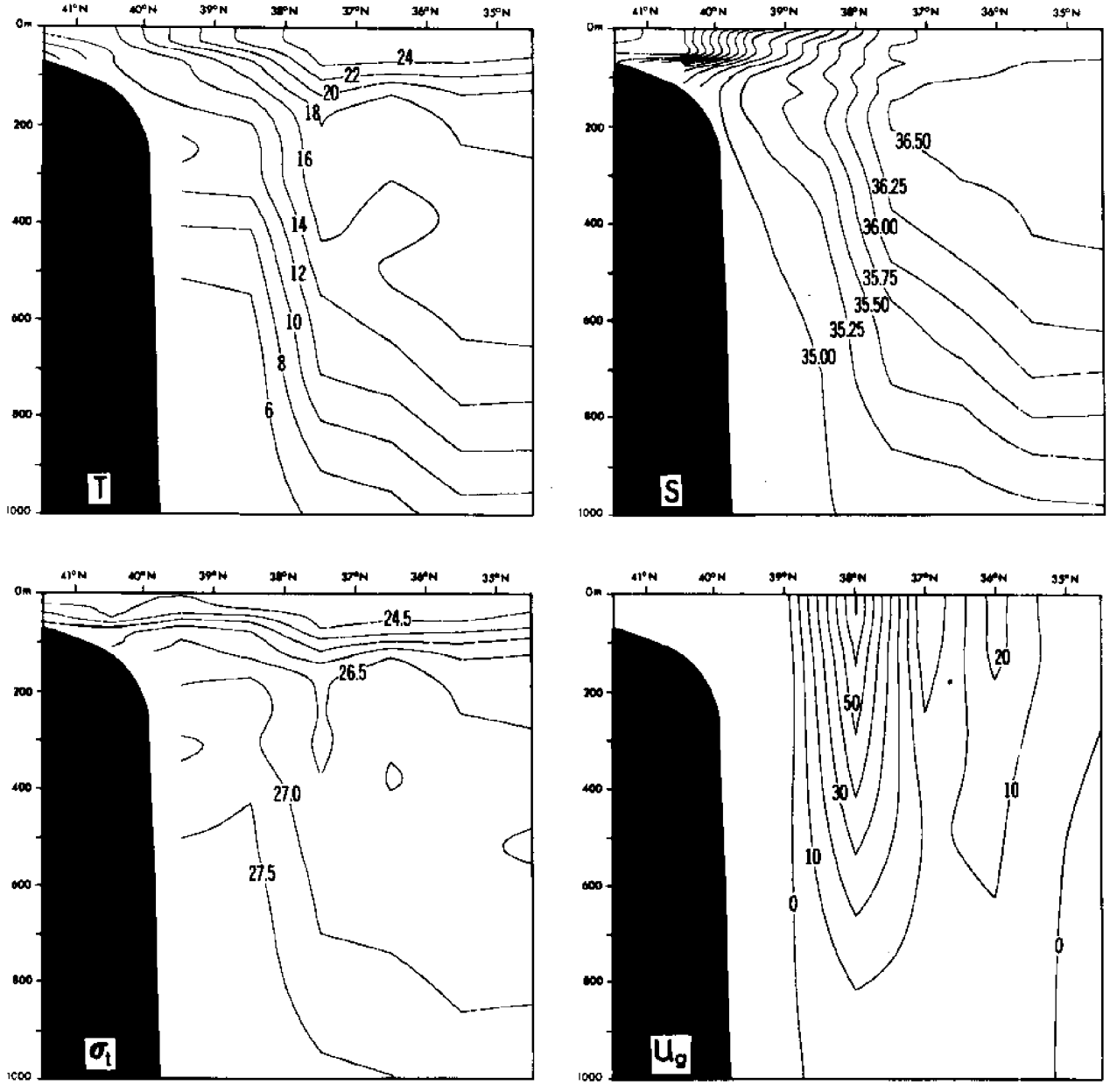

North—South Section along 69°30' W, November

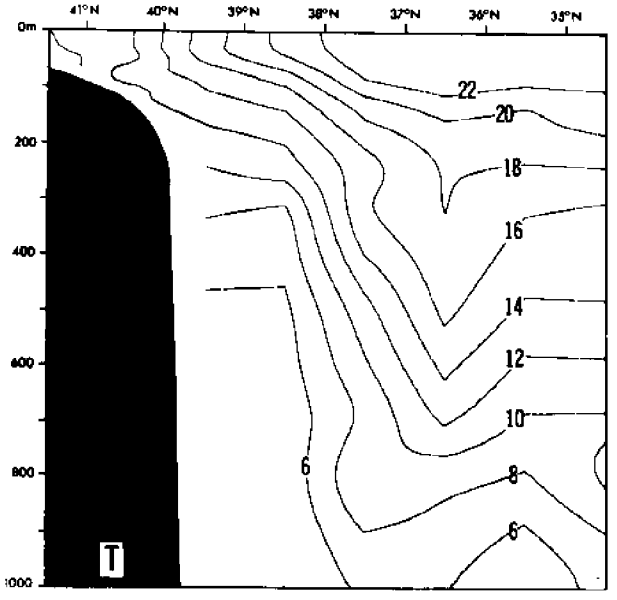

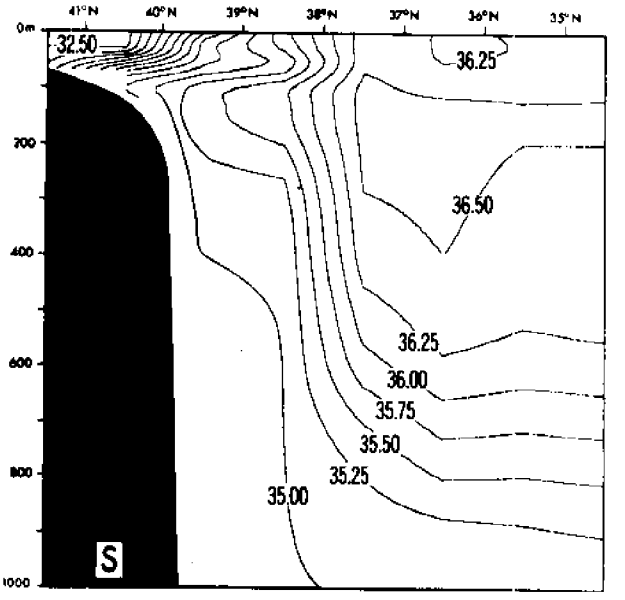

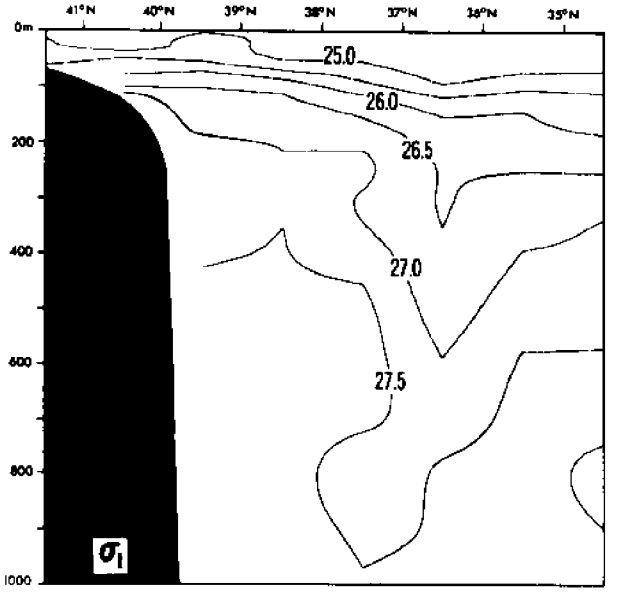

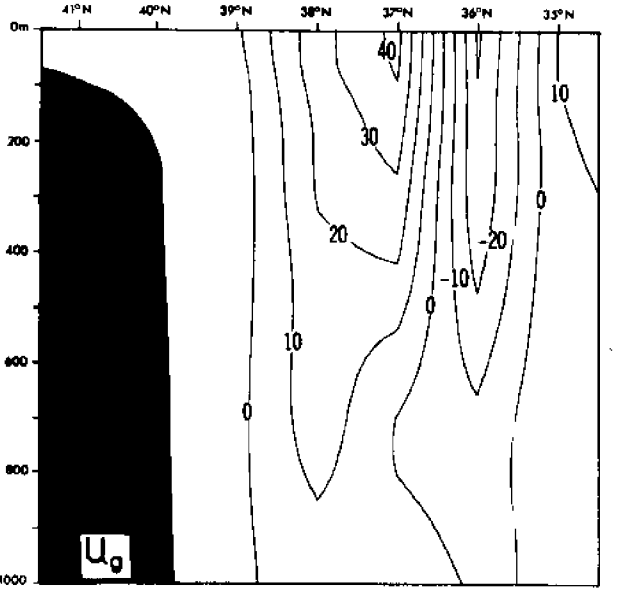

North—South Section along 69°30' W, December

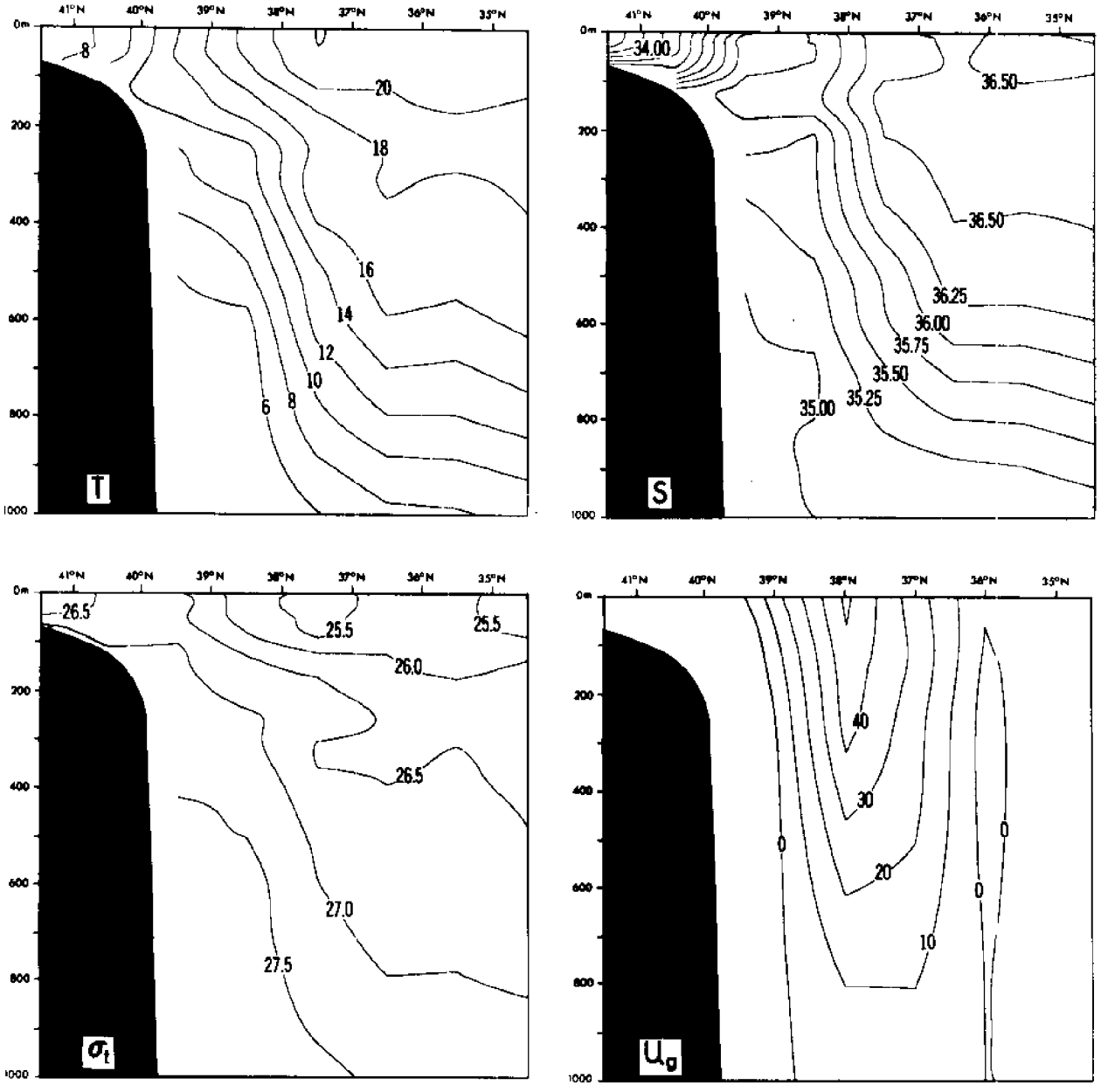

North – South Section along 69°30' W, Annual

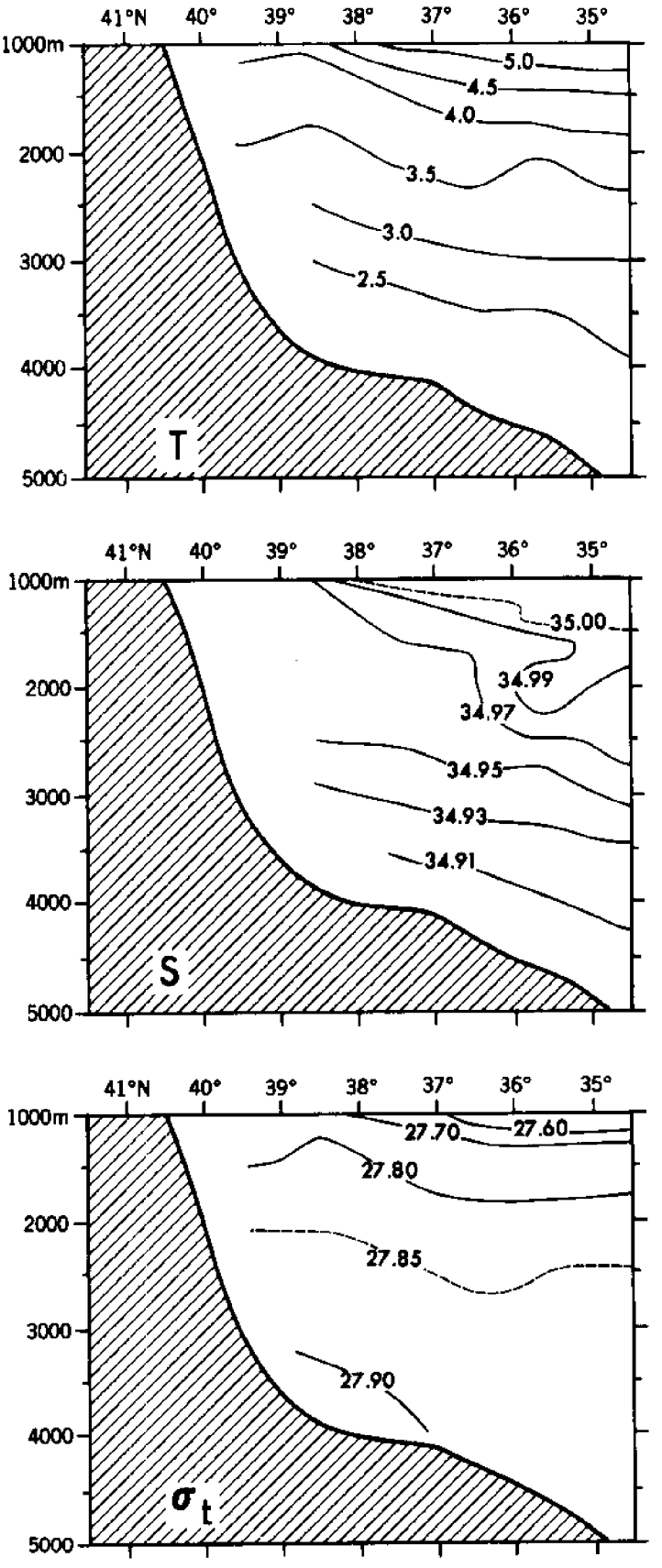

Distribution of Oxygen

Oxygen Distribution at Various Depths: *I*, Annual

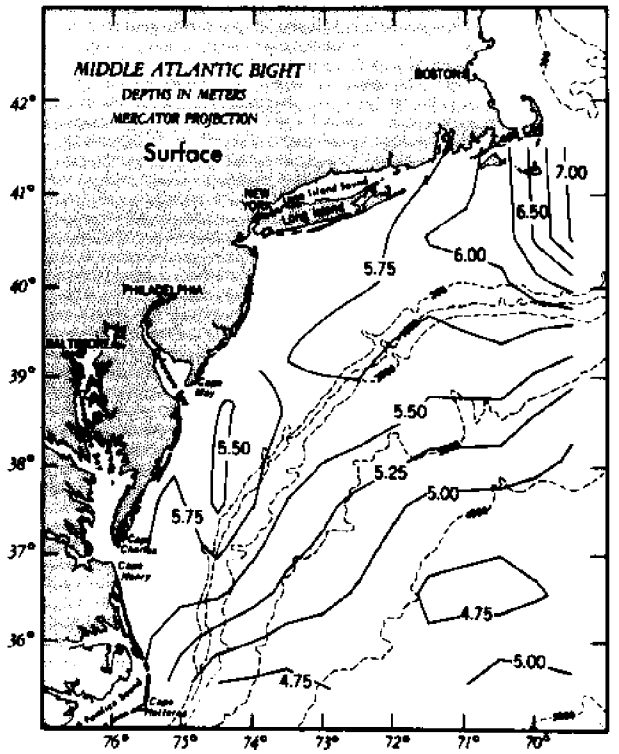

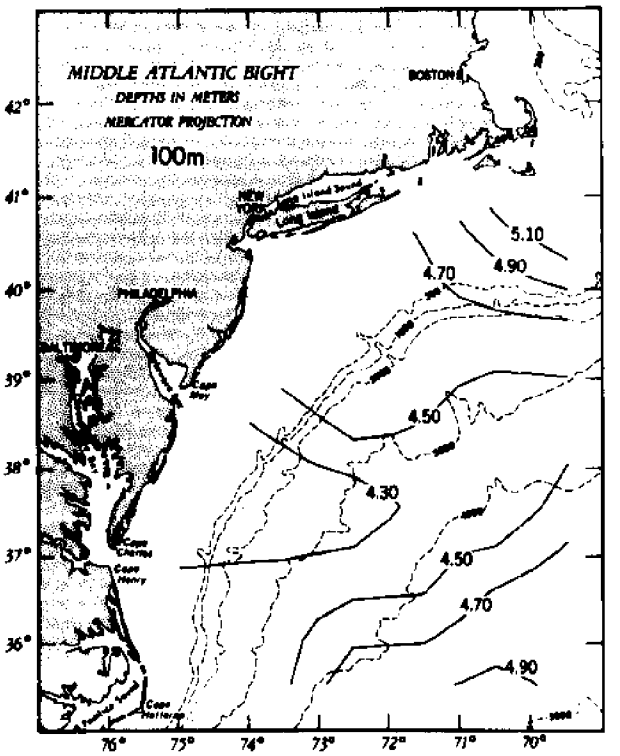

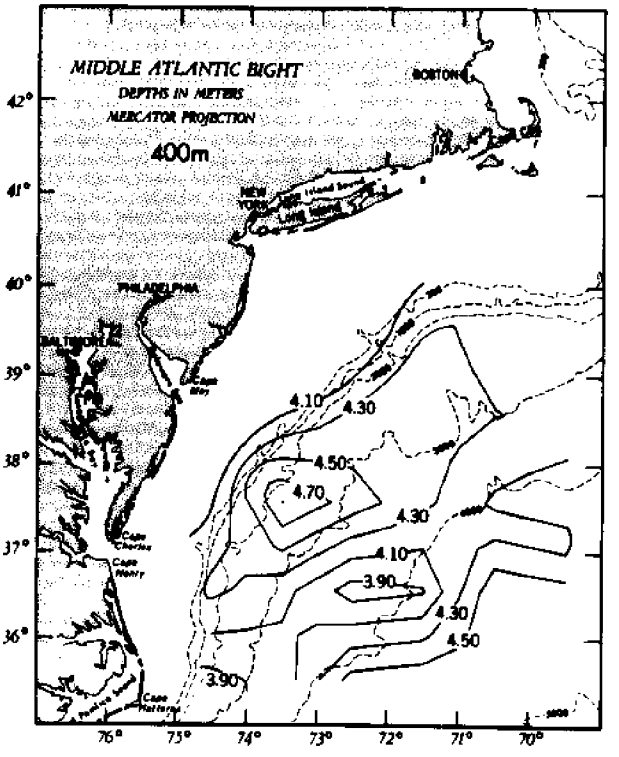

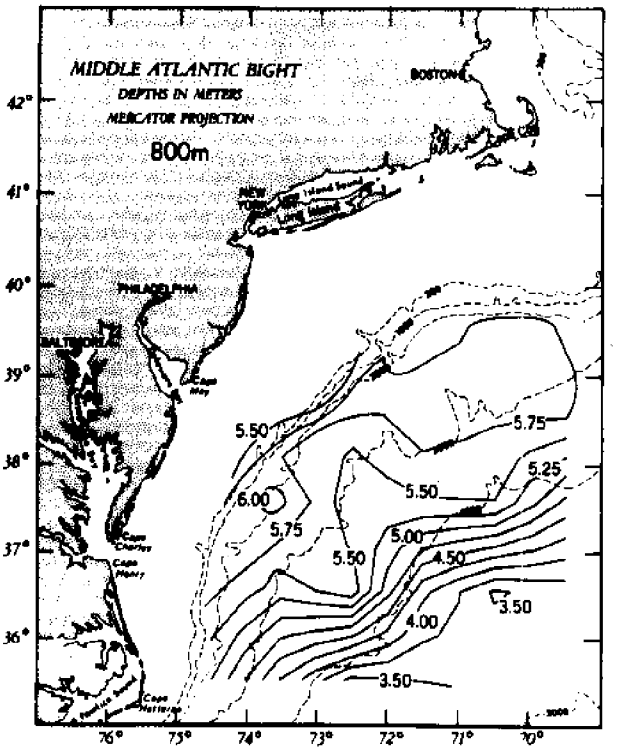

Oxygen Distribution at Various Depths: *II*, Annual

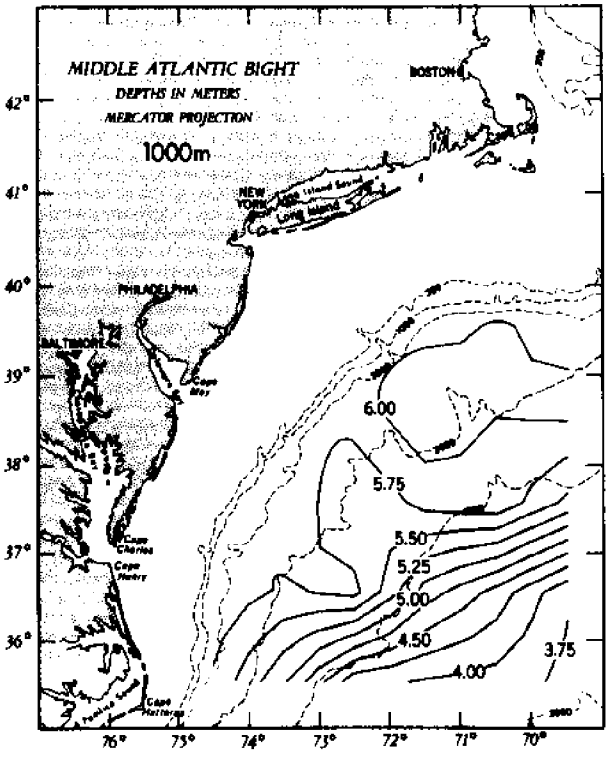

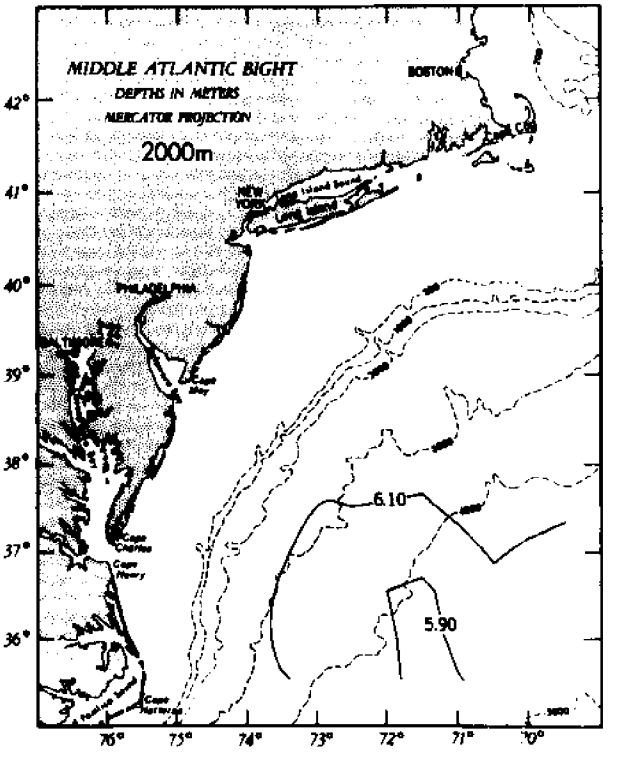

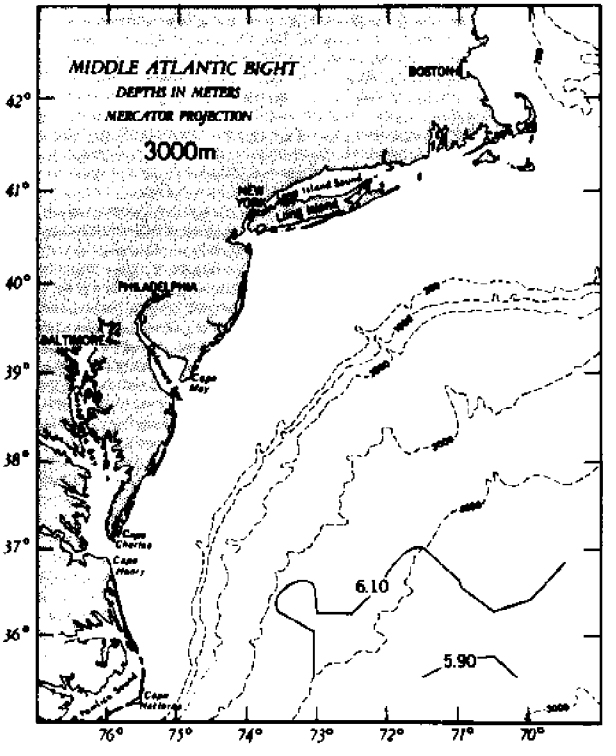

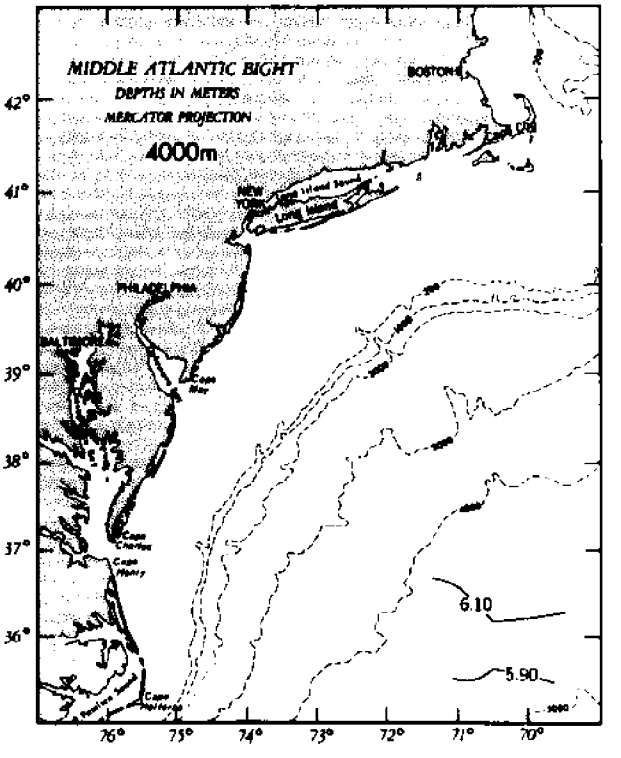

East—West Section along 35°30' N, Annual

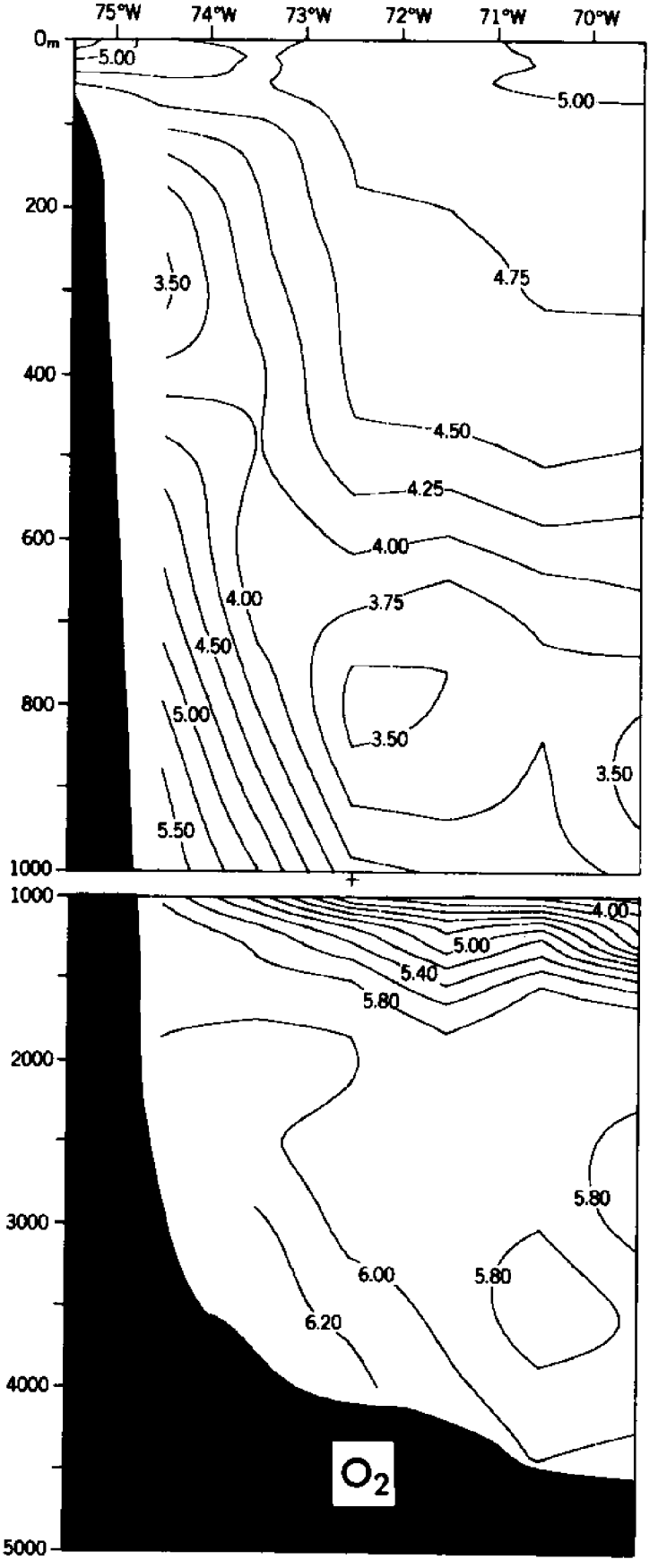

Diagonal Section, Annual

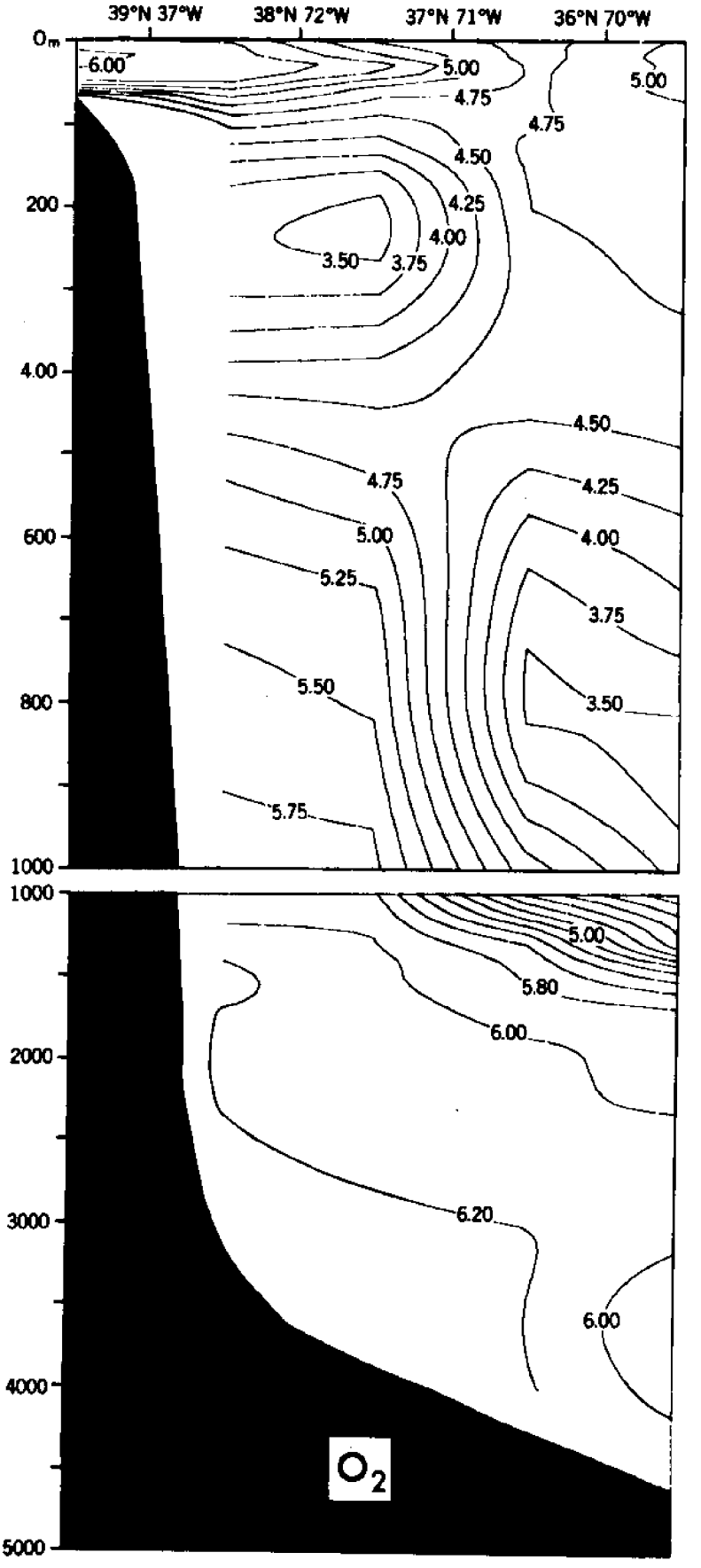

North—South Section along 69°30' W, Annual